POLITECNICO DI MILANO
School of Civil, Environmental and Land Management Engineering
M. Sc. Civil Engineering for Risk Mitigation

ASSESSMENT OF LIQUEFACTION TRIGGERING THROUGH IN-SITU METHODS: CPT, SPT, AND VS

Supervisor: *Prof. Roberto Paolucci*
Co – Supervisors: *Prof. Carlo G. Lai & Dr. Ali Güney Özcebe*

Submitted by: *Raúl Hernán Moreno Montoya*
Matr. *865275*

Academic year 2017/2018

Acknowledgements

First of all, I would like to thank my supervisor professor Dr. Roberto Paolucci and co-supervisor professor Carlo G. Lai and to express my gratitude to co-supervisor professor and researcher Dr. Ali Güney Özcebe for all their dedication and exceptional guidance during the development of this investigation. Special thanks to Università degli Studi di Pavia, Department of Civil Engineering and Architecture - DICAr for their help and provide information for the accomplishment of the case studies

Lovely and huge thanks go to my mother Dalila Montoya for all her support during this time and to my family and friends as well for all you best wish that have given to me.

A big thank you goes to all my colleagues and classmates with whom I have shared lectures, studies, and experiences, to all professors from who I have learned many things that have made me a better person and professional as well.

…and thanks to all my special persons in the past, the present… and the future.

Abstract (English)

In soil dynamics, it is well known that liquefaction is one of the most important and complex problems. Its simplest definition is; "the process of temporary or permanent loss of shear in saturated cohesionless soil under the influence of vibrations caused by mostly earthquakes".

Due to the large number of loss of lives and infrastructure system like bridges, highways, buildings etc. caused by liquefaction during more than three recent decades emphasize the need for strong and reliable methods for evaluating the liquefaction potential of sites. As a result of its low cost compared to rigorous laboratory tests, simplified techniques based on in situ testing methods such as Standard Penetration Test (SPT), Cone Penetration Test (CPT) and Shear Wave Velocity (Vs) are commonly used to measure seismic liquefaction potential at least for preliminary purposes. Regarding its evaluation, researchers have developed various routines and techniques.

This thesis is proposed to focus on comparing most recent simplified methods for assessing the resistance of the soil to liquefaction expressed as Cyclic Resistance Ratio (CRR) and the level of cyclic loading on the soil caused by the earthquake, expressed as a Cyclic Stress Ratio (CSR), based on the field test CPT, SPT and Vs. A case study for the Pieve di Cento response during 2012 Emilia Earthquake is studied as the benchmark case, where further extensive research work has been ongoing within the confines of LIQUEFACT project.

Further, most up-to-date methods are coded in MATLAB platform with a graphical interface, where the user is able to select the preferred method for assessing liquefaction, analyze and see the results. Moreover, the user can use their own CSR values if they have obtained them through local response studies.

It is important to mention that this thesis work not only makes a revision and comparison of the main simplified methods to evaluate liquefaction in soils but also makes a contribution in the development of set of routines developed in MATLAB that can be used in the future as line of research. Therefore, both the code package in MATLAB of the analysis methods used and the graphics interface and a user manual are attached as annexes to this thesis.

Abstract (Italian)

In dinamica dei terreni è noto che la liquefazione è uno dei problemi più importanti e complessi. La sua definizione più semplice è; "Il processo di perdita temporanea o permanente di taglio in terreno saturo privo di coesione sotto l'influenza di vibrazioni causate principalmente da terremoti".

A causa del gran numero di perdite di vite umane e il sistema di infrastrutture come ponti, autostrade, edifici, ecc, causati dalla liquefazione durante più di tre ultimi decenni sottolineare la necessità di metodi forti e affidabili per valutare il potenziale di liquefazione dei siti. Come risultato del suo basso costo rispetto ai test di laboratorio rigorosi, tecniche semplificate basate su metodi di prova situ come Standard Penetration Test (SPT), Cone Penetration Test (CPT) e Shear velocità dell'onda (Vs) sono comunemente utilizzati per misurare liquefazione sismica potenziale almeno ai fini preliminari. Per quanto riguarda la sua valutazione, i ricercatori hanno sviluppato varie routine e tecniche.

Questa tesi si propone di concentrarsi sul confronto dei più recenti metodi semplificati per valutare la resistenza del terreno alla liquefazione espressa come CRC (Cyclic Resistance Ratio) e il livello di carico ciclico sul suolo causato dal terremoto, espresso come CSR (Cyclic Stress Ratio), basato sul test sul campo CPT, SPT e Vs. Un caso di studio per la risposta di Pieve di Cento nel corso del 2012 in Emilia Earthquake è stato studiato come caso di riferimento, dove sono proseguiti ulteriori approfonditi lavori di ricerca all'interno dei confini del progetto LIQUEFACT.

Inoltre, i metodi più aggiornati sono codificati nella piattaforma MATLAB con un'interfaccia grafica, in cui l'utente è in grado di selezionare il metodo preferito per valutare la liquefazione, analizzare e vedere i risultati. Inoltre, l'utente può utilizzare i propri valori CSR se li ha ottenuti tramite studi di risposta locali.

È importante ricordare che questo lavoro di tesi non solo effettua una revisione e un confronto dei principali metodi semplificati per valutare la liquefazione nei terreni, ma contribuisce anche allo sviluppo di una serie di routine sviluppate in MATLAB che possono essere utilizzate in futuro come linea della ricerca. Pertanto, sia il pacchetto di codice in MATLAB dei metodi di analisi utilizzati che l'interfaccia grafica e un manuale utente sono allegati come allegati a questa tesi.

Contents

Figures

CHAPTER 1
INTRODUCTION

One of the most important causes of damage to structures and infrastructures in general through earthquakes is due to soil liquefaction. For that reason, during the recent years it have been an important and a controversial topic that have captured the attention of experts in soil dynamics.

The term liquefaction was used initially by Terzaghi, K. and Peck, R.B. (1948). and by Mogami, T., and Kubo, K. (1953) for describing the rapid loss of strength due to seismically-induced cyclic loading. During the past decades, particularly after the earthquakes in Alaska and in Niigata, Japan in 1964, a methodology named "simplified procedure" originally proposed by Seed HB. and Idriss IM (1971), has progressed as a standard of practice to evaluate the liquefaction resistance of soils, NCEER/NSF, Youd et al. (2001).

Evaluation of the liquefaction resistance of soils is an important step in many geotechnical investigations in earthquake prone regions owe to the impacts the is causes. One example of severe effects that of liquefaction produces is the excessive settlements and even collapse of residential buildings and even more important lifeline structures, such as bridges.

If one considers the case of bridges, because riverbeds often contain loose sand deposits, liquefaction also frequently causes damage on bridges that cross rivers or other bodies of water. Bridges are generally designated as essential facilities, because they provide necessary transportation routes for emergency response and rescue operations.

A bridge failure will also impede the transport of emergency supplies and can cause significant economic loss for businesses along the transportation corridor. There are several different ways that bridges can be impacted by liquefaction. For example, liquefaction beneath a bridge pier could cause collapse of a portion of the bridge. Likewise, liquefaction also reduces the lateral bearing, also known as the passive resistance.

With a reduced lateral bearing capacity, the bridge piers will be able to rock back and forth and allow for the collapse of the bridge superstructure. A final effect of liquefaction could be induced down-drag loads upon the bridge piers as the pore water pressures from the liquefied soil dissipate and the soil settles. Figure 1-1 shows the collapse of the superstructure of the Showa Bridge caused by the 1964 Niigata earthquake. The soil liquefaction apparently allowed the bridge piers to move laterally to the point where the simply supported bridge spans lost support and collapsed.

Figure 1-1 Collapse of the Showa Bridge during the Niigata earthquake on June 16, 1964. (Photograph from the Godden Collection, EERC, University of California, Berkeley.)

This example clearly illustrates the importance of accurate assessments of where liquefaction is likely and of what the consequences of liquefaction may be. Such assessments are needed to protect life and safety and to mitigate economic, environmental, and societal impacts of liquefaction in a cost-effective manner.

1.1 Liquefaction definition and related phenomena

According to the experience of engineers and researchers often described in the literature, the typical subsurface layers that are susceptible to liquefaction are loose to medium dense saturated sandy-soil matrices.

During an earthquake, the soil is exposed to shearing stresses and the soil grains tend to reorganize and densify, with less space voids, as water in the pore spaces is forced out. Simultaneously, the propagation of shear waves causes the loose sand to contract, if drainage of pore water is impeded, resulting in an increase in pore water pressure. Due to the seismic shaking occurs rapidly, the cohesionless soil is subjected to undrained-like loading. The increase in pore water pressure causes an upward flow of water to the ground surface, where it emerges in the form of mud spouts or sand boils [Ishihara, K. (1985)].

The development of high pore-water pressures due to the ground shaking and the upward flow of water may turn the sand into a liquefied condition, which has been termed liquefaction. For this state of liquefaction, the effective stress is zero and the individual soil particles are released from any confinement, as if the soil particles were floating in water [Ishihara, K. (1985)].

Another definition of liquefaction is the transformation of a granular material from a solid to a liquid because of the increase of pore-water pressure and the reduced effective stress [Marcuson WF (1978)]. The increase of pore-water pressure is induced due to the predisposition of granular materials to compact when they are subjected to cyclic shear deformations. The chance of state occurs most readily in loose to moderately dense granular soils with poor drainage, such as silty sands or sands and gravels capped by or containing seams of impermeable sediment, [NCEER/NSF, Youd et al. 2001]. Because of that, liquefaction typically occurs in soil with a high groundwater table, which also leads profiles with lower initial effective confinement. The effects of liquefaction are most commonly observed in low-lying areas or adjacent rivers, lakes, bays, and oceans [Robert W. Day (2002)].

The basic mechanism that produce liquefaction behavior can be divided into two main categories: flow liquefaction and cyclic mobility.

1.1.1 Flow liquefaction

Flow liquefaction can occur when the static shear stress in a liquefiable soil deposits is grater that the steady-state strength of the soil. It can produce devastating flow slide failures during or after earthquake shaking. Flow can occur only in loose soils.

It produces the most dramatic effects "although that occurs much less frequently". It is characterized by the sudden nature of their origin, the speed with they develop and the large distance over which the liquefied materials after moving [Kramer, S. L. (1996)].

1.1.2 Cyclic mobility

In contrast of flow liquefaction, cyclic mobility can occur when the static shear stress is less than the steady-state strength and the cyclic shear stress is large enough that the steady-state strength is exceeded momentarily. Deformations produced by cyclic mobility develop incrementally but can become substantial by the end of a strong and/or long-duration earthquake. Cyclic mobility can occur in both loose and dense soils, but the level of deformation decreases remarkably with increased density [Kramer, S. L. (1996)].

One example of a special case of cyclic mobility is level-ground liquefaction, producing movement known as ground oscillation during earthquake shaking, but produces little permanent lateral soil movement. Level ground liquefaction failures are caused by the upward flow of water that occurs when seismically induced excess pore pressure dissipate [Kramer, S. L. (1996)].

1.1.3 Susceptibility

Due to the liquefaction has been seen observed to occur at the same location when site conditions are unchanged [Youd, T. L. (1984)], evidence of the historical occurrence of liquefaction, either observed or in the form of paleo-liquefaction, can be a signal of liquefaction susceptibility. By the same way, geological conditions give indications susceptibility to liquefaction; soils deposited in fluvial deposits, and colluvial and aeolian deposits when saturated, are likely to be susceptible to liquefaction [Bozorgnia, Y. and Bertero, V. V. (2004)].

Liquefaction is also observed in alluvial-fan, alluvial-plain, beach, terrace, playa and estuarine deposits, but not as consistently as in those listed formerly. Younger soils are generally more susceptible to liquefaction than order deposits. The physical composition of a soil deposit will play a strong role in determining its liquefaction susceptibility [Kramer, S. L. (1996)]. Uniformly graded clean sands composed of rounded particles are inherently more susceptible to liquefaction. Well-graded soils and soils with angular particles are less susceptible. Further, the presence the fines, particularly plastic fines (PI>7), tends to decrease liquefaction susceptibility. [Idriss, I. M. (1999).].

The liquefaction susceptibility of a given soil is also influenced by its state, i.e. its in-situ effective stress and relative density conditions. The tendency of a soil to contract, or density, under cyclic loading conditions has long been known to be influenced by both density and effective stress. Loose soils are much more susceptible to liquefaction than dense soils and, for a given density, soils under high effective confining pressures are more susceptible to liquefaction than soils at a low effective confining pressure. High values of the state parameter [Been, K. and Jefferies, M. G. (1985)] defined as the difference between the void ratio and the steady void ratio, indicate increasing contractiveness and, hence, increasing susceptibility to liquefaction; the state parameter can be estimated from CPT resistance [Been, K. et al. (1986, 1987a)].

1.1.4 Initiation

If a soil deposit has been determined to be susceptible to liquefaction, the second step in a liquefaction hazard evaluation is consideration of the potential for initiation of liquefaction. This generally involves characterization of the intensity of seismic loading that the soil will be subjected to and characterization of the liquefaction resistance of the soil. By characterization both loading and resistance in common terms, the two can be compared to determine the liquefaction potential of soil.

➢ Approaches

Several approaches to the characterization of loading and resistance have been proposed for the liquefaction problem. Historically, the cyclic stress method has been commonly used for evaluation of liquefaction potential.

In the cyclic stress approach, both the loading imposed on the soil by the earthquake and the resistance of the soil to liquefaction are characterized in terms of cyclic shear stress. By characterizing both loading and resistance in common terms, they can be directly compared to quantify the potential for liquefaction. The cyclic stress approach benefits from the fact that cyclic stress amplitudes can be computed relatively easily and accurately, and from the fact that it has been verified as a conservative predictor of liquefaction by field observations. The cyclic stress method represents the classic approach to evaluation of liquefaction potential. It has been thoroughly tested and validated as a useful practical approach for evaluation of liquefaction potential, Bozorgnia, Y. and Bertero, V. V. (2004).

➢ Characterization of liquefaction loading

The level of loading imposed on a potentially liquefiable soil is a function of the ground motion the soil is subjected to. It is important to recognize that the entire ground motion effects the soil; therefore, the amplitude, frequency content and duration of the motion are all potentially important, Bozorgnia, Y. and Bertero, V. V. (2004).

Cyclic Stress Approach -For the purpose of liquefaction evaluation using the cyclic stress approach, loading is typically characterized in terms of the cyclic stress ratio, CSR, which is defined as the ratio of the equivalent cyclic shear stress τ_{cyc} to the initial vertical effective stress, σ'_{vo}

$$CSR = \frac{\tau_{cyc}}{\sigma'_{vo}}$$

➢ Characterization of liquefaction resistance

Liquefaction resistance is also typically expressed by means of the same parameters used to characterize earthquake loading. For the cyclic approach, liquefaction resistance is expressed in terms of cyclic stress ratio commonly referred to as the cyclic resistance ratio, CRR. The cyclic resistance ratio is defined as the cyclic stress ratio that just causes initial liquefaction. In practice, liquefaction resistance is typically determined by correlation to in-situ penetration resistance and more recently by the spectral analysis of surface waves (SASW). Shear wave velocity (Vs) tests, tend to be used in special situations and thus are used less often than the SPT and CPT in liquefaction evaluations.

1.1.5 Consequences of liquefaction

Triggering liquefaction can have several consequences for soil properties and site as well as physical damage, economic loss and potential loss of life [National Academies of Sciences, Engineering, and Medicine, (2016)]. Among the consequences due to the liquefaction of the soil can be mentioned;

➢ Alteration of Ground Motion

Ground motion frequency change often occurs suddenly when liquefaction is triggered because of the rapid reduction in shear stiffness at high pore pressure ratios. This process affects the response of buildings, bridges, pipelines, and other elements of infrastructure underlain by liquefiable soils.

➢ Lateral Spreading and Flow Sliding

Initial cutting tensions under sloping ground conditions can cause permanent lateral deformations of the soil after liquefaction. These lateral deformations are known in practice as lateral spreading and flow sliding.

➢ Liquefaction Induced Settlement

Volume loss due to a dissipation of excess pore pressure in the liquefied soil during and after an earthquake generally results in settlements of the soil surface. Settlement can cause damage to the structures if the settlement is not uniform under the structure. The settlement may also leave a gap underneath the structures supported by piles, causing damages to services buried in the ground and alter the drain on the site.

➢ Damage to foundations

Damage to structures supported on shallow foundations is typically produced by differential vertical and horizontal displacements. This is particularly true for structures supported by spread footings or lightly reinforced mats, as is often the case with residential and light commercial structures.

- **Damage to Retaining Structures**

Bulging or tilting of retaining walls, sliding of the wall, and damage to the structures in or behind the wall may occur if the induced liquefaction increases in the pressure of the earth and the decreases in the lateral resistance are not included in the design.

All these consequences of liquefaction are very important in the design and analysis of engineering structures; however, they are outside the context of this thesis.

1.1.6 Advanced numerical methods in simultaneous determination of liquefaction and its consequences

Advanced numerical methods that use the principles of mechanics and incorporate appropriate constitutive relationships offer a more detailed and flexible approach to predicting liquefaction and its consequences than empirical and semi-empirical methods [National Academies of Sciences, Engineering, and Medicine, (2016)].

In a nutshell, it could be stated that through numerical methods the generation and dissipation of excess pore-water pressures are modelled within an effective stress framework. There are two distinct class of constitutive relations as defined below:

1. Loosely-coupled approach: An external relation is implemented to classical elasto-plastic constitutive models (i.e. mostly Mohr-Coulomb) to link the volumetric deformations to earthquake induced shear deformations (e.g. Martin et al., (1975), Byrne, P. M. (1991));
2. Fully-coupled approach: Fully consistent plasticity model is defined to define not only the generation and dissipation of excess pore water pressures, but also stress-strain responses. Examples could be given as Cubrinovski and Ishihara, (2002), Boulanger, R.W. (2010). and Dafalias, Y.F., and M.T. Manzari. (2004). In general, fully coupled models provide the most realistic modelling of the soil response during seismic excitations, however calibration of their numerous parameters needs an extensive set of information regarding the soil under consideration.

It should be noted that implementation and use of advanced numerical models is out of context of this thesis, yet the results of two loosely coupled models, National Academies of Sciences,

Engineering, and Medicine, (2016), are going to be presented in Chapter 4 as the numerical benchmark to compare the predictions of simplified in-situ based triggering approaches.

CHAPTER 2 SIMPLIFIED ASSESSMENT OF LIQUEFACTION TRIGGERING

Computation or estimation of two main variables is required for analysis and evaluation of liquefaction resistance of soils by the simplified approach. The first is determine the demand on a soil layer, expressed in terms of cyclic stress ratio (CSR) that will be induced by the earthquake. Then, the cyclic resistance ratio (CRR) is the variable needed to estimate the capacity of the soil to resist liquefaction.

2.1 Evaluation of Cyclic Stress Ratio (CSR)

As was explained before, for the liquefaction evaluation is using the cyclic stress approach, loading is typically characterized in terms of the cyclic stress ratio, CSR. As a first step, rigid body maximum shear stress is calculated and then a portion (usually 65%) is taken to represent the cyclic nature of the loading, representing a value arrived at by comparing rates of porewater pressure generation caused by transient earthquake shear stress histories with rates caused by uniform harmonic shear stress histories [Seed H. B. et al. (1975) and Liu A.H. et al. (2001)].

In order to represent the deformable nature of the geological layers, maximum cyclic shear stress acting on the rigid body is further reduced by a depth reduction factor called r_d, which represents the average rate at which peak shear stress attenuates with depth. In mathematical form, therefore, the cyclic stress ratio can be defined as:

$$CSR = 0.65 \frac{a_{max}}{g} \frac{\sigma_{vo}}{\sigma'_{vo}} r_d$$

Where a_{max} is the maximum horizontal acceleration at ground surface that would be expected to occur in the absence of liquefaction, i.e. the value of a_{max} predicted by an attenuation relationship or a total stress ground response analysis in which excess pore pressure generation is not considered NCEER/NSF, Youd et al. (2001) σ_{vo} and σ'_{vo} are the initial total and effective vertical stresses, and r_d is a depth reduction factor that accounts for the effect of soil compliance on shear

stress amplitude. It should be noted that this value of a_{max} may differ from the actual value of a_{max} that would occur at the surface of a liquefiable soil profile.

To account for the fact that peak acceleration alone is an insufficient measure of earthquake loading, frequency content and duration effects are accounted for using earthquake magnitude as a proxy in the form of a magnitude scaling factor, *MSF*, NCEER/NSF, Youd et al. (2001) recommend estimation of the *MSF* using.

$$MSF = \left(\frac{7.5}{M_w}\right)^n$$

Where n is within the range of 2.56 to 3.3 $M_w \leq 7.5$, and is equal to 2.56 for $M_w > 7.5$. Magnitude scaling factor is used to correct the resistance which is calibrated for Mw=7.5. In other words, either the demand (CSR) should be divided to MSF or the capacity (CRR) should be multiplied by MSF.

2.1.1 Shear stress reduction coefficient (rd)

This coefficient accounts for flexibility (deformability) of the soil profile since it does not behave as a rigid body during the earthquake. According to Seed H.B. and Idriss I.M. (1971), r_d describes the ratio of cyclic stresses for a flexible soil column to the cyclic stresses for a rigid soil column. $r_d = 1.00$ corresponds to either a rigid soil column response or the value at the ground surface. However, this ratio reduces rapidly as depth increases, knowing that fact, they proposed a range of r_d values how is shown in the Figure 2-1.

Later, Liao, S. S. C. and Whitman, R. V. (1986), formulated a routine for estimate average values of r_d having z, in meters, as the depth from the ground surface.

$$r_d = 1.00 - 0.00765 * z \quad for\ z \leq 9.15m$$

$$r_d = 1.174 - 0.0267 * z \quad for\ 9.15m < z \leq 23m$$

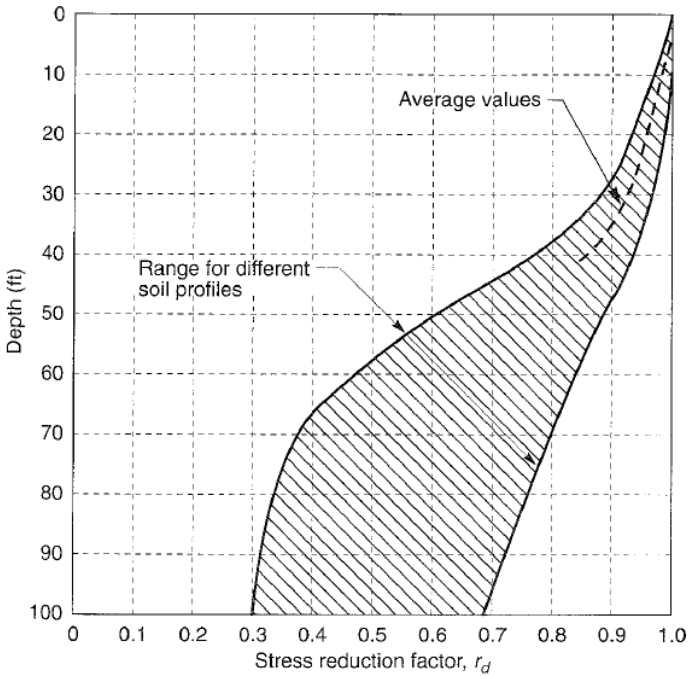

Figure 2-1 r_d profiles as proposed by Seed and Idriss, 1971

An additional formulation is given by NCEER/NSF, Youd et al. (2001) as an approximation of a mean curve of the range proposed by Seed and Idriss (1971), Figure 2-1.

$$r_d = \frac{(1.000 - 0.4113 * z^{0.5} + 0.04052 * z + 0.001753 * z^{1.5})}{(1.000 - 0.4177 * z^{0.5} + 0.05729 * z - 0.006205 * z^{1.5} + 0.001210 * z^2)}$$

Then, Idriss, I. M. (1999), in extending the work of Golesorkhi, R. (1989), where his analyses had shown that r_d is particularly dependent on the earthquake ground motion characteristics, Figure 2-2. Consequently, r_d could be adequately expressed as a function of depth and earthquake magnitude (M) following the equations:

For $z \leq 34m$:

$$r_d = exp(\alpha(z) + \beta(z)M)$$

$$\alpha(z) = -1.012 - 1.126\, sin\left(\frac{z}{11.73} + 5.133\right)$$

$$\beta(z) = 0.106 + 0.118\, sin\left(\frac{z}{11.28} + 5.142\right)$$

For $z > 34m$:

$$r_d = 0.12exp(0.22M)$$

Where, z is the depth in meters and M is the moment magnitude of the earthquake.

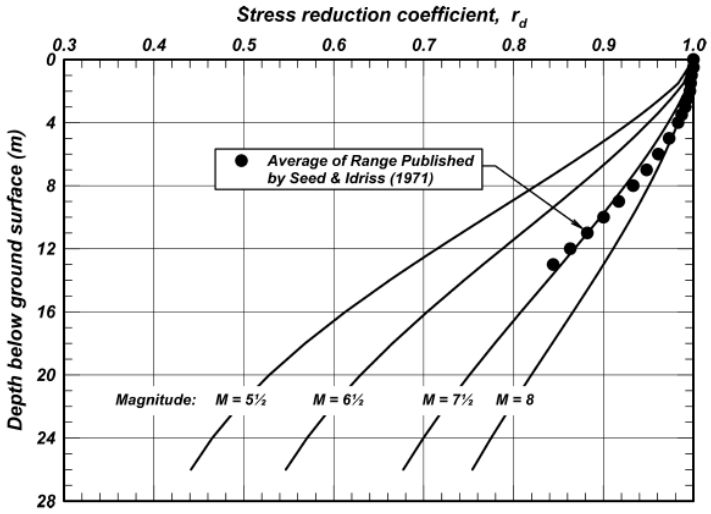

Figure 2-2 Stress reduction coefficient r_d variation with depth and earthquake magnitude (Idriss 1999)

Cetin, K. O. (2000), using ground response analyses that were run using 50 sites and 42 ground motions, reassessed the $r_d$factor, regressed to evaluate the median r_d for a given depth, peak ground acceleration, and moment magnitude. The variance was estimated from the dispersion of the simulations. The median $r_d$results can be calculated using the following equations.

For $d < 20m$:

$$r_d = \left[\frac{1 + \frac{-9.147 - 4.173 \cdot a_{max} + 0.652 \cdot M_W}{10.567 + 0.089 \cdot e^{0.089 \cdot (-d \cdot 3.28 + 7.760 \cdot a_{max} + 78.576)}}}{1 + \frac{-9.147 - 4.173 \cdot a_{max} + 0.652 \cdot M_W}{10.567 + 0.089 \cdot e^{0.089 \cdot (-7.760 \cdot a_{max} + 78.576)}}}\right]$$

For $d \geq 20m$:

$$r_d = \left[\frac{1 + \frac{-9.147 - 4.173 \cdot a_{max} + 0.652 \cdot M_W}{10.567 + 0.089 \cdot e^{0.089 \cdot (-d \cdot 3.28 + 7.760 \cdot a_{max} + 78.576)}}}{1 + \frac{-9.147 - 4.173 \cdot a_{max} + 0.652 \cdot M_W}{10.567 + 0.089 \cdot e^{0.089 \cdot (-7.760 \cdot a_{max} + 78.576)}}}\right] - 0.0014(d \cdot 3.28 - 65) \pm \sigma_{\varepsilon_{r_d}}$$

Where, the standard deviation for r_d is given as:

For $d < 12.2m$:

$$\sigma_{\varepsilon_{r_d}} = (d \cdot 3.28)^{0.864} * 0.00814$$

For $d \geq 12.2m$:

$$\sigma_{\varepsilon_{r_d}} = 40^{0.864} * 0.00814$$

d = depth in meters

a_{max} = is in gravitational acceleration

M_W = earthquake moment magnitude

Afterwards, Cetin, K. O. et al. (2004) base on previous studies suggested for the nonlinear shear mass participation factor r_d the following equations;

For $d < 20m$:

$$r_d = \left[\frac{1 + \frac{-23.013 - 2.949 a_{max} + 0.999 M_W + 0.0525 V^*_{s,12m}}{16.258 + 0.201 * e^{0.341(-d + 0.0785 V^*_{s,12m} + 7.586)}}}{1 + \frac{-23.013 - 2.949 a_{max} + 0.999 M_W + 0.0525 V^*_{s,12m}}{16.258 + 0.201 * e^{0.341(0.0785 V^*_{s,12m} + 7.586)}}}\right]$$

For $d \geq 20m$:

$$r_d = \left[\frac{1 + \frac{-23.013 - 2.949 a_{max} + 0.999 M_W + 0.0525 V^*_{s,12m}}{16.258 + 0.201 * e^{0.341(-d + 0.0785 V^*_{s,12m} + 7.586)}}}{1 + \frac{-23.013 - 2.949 a_{max} + 0.999 M_W + 0.0525 V^*_{s,12m}}{16.258 + 0.201 * e^{0.341(0.0785 V^*_{s,12m} + 7.586)}}}\right] - 0.0046(d - 20) \pm \sigma_{\varepsilon_{r_d}}$$

Where, the standard deviation for r_d is given as:

For $d < 12m$:

$$\sigma_{\varepsilon_{r_d}} = d^{0.850} * 0.0198$$

For $d \geq 12m$:

$$\sigma_{\varepsilon_{r_d}} = 12^{0.850} * 0.0198$$

d = depth in meters

a_{max} = is in gravitational acceleration

M_W = earthquake moment magnitude

$V_{s,12m}^*$ = equivalent shear wave velocity defined as:

$$V_s^* = \frac{H}{\sum \frac{h_i}{V_{s,i}^*}}$$

Where, H is the total soil profile thickness (m), h_i is the thickness of the i^{th} sub-layer (m) and $V_{s,i}^*$ is the shear wave velocity within the i^{th} sub-layer (m/s). If estimation of $V_{s,12}^*$ is considered difficult for a given case, then $V_{s,12}^*$ can simply be taken as approximately 150–200 m/s (500–650 ft/s) for most potentially liquefiable sites with adequate accuracy for many engineering applications, Cetin, K. O. et al. (2004).

2.1.2 Magnitude scaling factor (MSF)

Magnitude scaling factor (MSF) relationships are used in liquefaction triggering correlations to approximately account for how the characteristics of the irregular cyclic loading produced by different magnitude earthquakes affect the potential for triggering of liquefaction. MSF relationships depend on the characteristics of both the imposed loading and the soil's loading response, as expected for any type of fatigue problem. MSF relationships developed for sands (e.g., Seed et al. 1975, Idriss 1999, Liu et al. 2001, Green and Terri 2005). In this research, the MSF value will be estimated according to the suggested or each methodology.

2.2 Evaluation of Cyclic Resistance Ratio (CRR)

From the cyclic approach, liquefaction resistance is expressed in terms of cyclic resistance ratio, CRR. Numerous field tests have been implemented for the evaluation of liquefaction resistance, including the standard penetration test (SPT), the cone penetration test (CPT), shear-wave velocity measurements (Vs), NCEER/NSF, Youd et al. (2001) and correlated with the observed cases of liquefaction.

In present day, due to the difficulties associated with sampling and laboratory testing and advanced skills needed in the numerical models, still in-situ tests constitute the state of practice for routine liquefactions investigations. To be more specific, the methodologies based on SPT and CPT are mostly preferred for liquefaction resistance assessment, because of there are more extensive databases and experience, however, Vs have been becoming more familiar in the recent years. In the follows will explained the mainly approaches for the correlation between the resistance of soil to initiation or "triggering" of liquefaction under earthquake shaking and soil resistance based on in-situ tests.

2.2.1 Standard Penetration Test (SPT)

Along with the CPT, the standard penetration test SPT is one of the most commonly used tests for characterization of liquefaction resistance. SPT consists of driving a standard split-tube sampler 18-inches into the soil, counting the number of blows required to drive the device three consecutive 6-inch intervals (18 inches total). The actual number of blows required to drive the sampler the final 12 inches is the standard penetration resistance, or N value. ASTM D1586, (1999). Several factors influence SPT results as describes the equation:

$$(N_1)_{60} = N_m \cdot C_N C_E C_B C_R C_S$$

Where, N_m is the measured standard penetration resistance. C_N =factor to normalize N_m to a common reference effective overburden stress; C_E = correction for hammer energy ratio (ER); C_B = correction factor for borehole diameter; C_R = correction factor for rod length; and C_S = correction for samplers with or without liners.

Due to the SPT N-values will increase with increasing effective overburden stress, an overburden stress correction factor should be considering Seed, H. B., and Idriss, I. M. (1982). This factor is commonly calculated from equation suggested by Liao, S. S. C. and Whitman, R. V. (1986),

$$C_N = \left(\frac{P_a}{\sigma'_{vo}}\right)^m$$

where C_N normalizes N_m to an effective overburden pressure σ'_{vo} of approximately 100 kPa (1 atm) P_a. The exponent m is equal to 0.5. C_N should not exceed a value of 1.7 according to NCEER/NSF, Youd et al. (2001). There are other researches that have been recommended limits of 1.6 to 2.0 for C_N, as Cetin, K. O. et al. (2004), who suggest 1.6 as maximum value.

Then, Idriss, I. M. and Boulanger, R. W. (2004, 2008), recommended that the value of the exponent m as follows;

$$m = 0.784 - 0.0768\sqrt{(N_1)_{60cs}}$$

However, that expression requires iteration for computing m based on $(N_1)_{60cs}$.

Additional, Kayen, R. E. et al. (1992) suggested the following equation for effective overburden pressure correction factor.

$$C_N = \frac{2.2}{\left(1.2 + \frac{\sigma'_{vo}}{P_a}\right)}$$

Another factor that influenced the SPT liquefaction analyses results is C_E due to the hammer energy ratio, ER. Therefore, it is extremely important to understand the actual SPT hammer energy when measuring N_m values in the field. Values suggested by Seed, H. B. et al. (1984), Skempton, A. W. (1986) and NCEER/NSF, Youd et al. (2001) as listed in Table 2-1, following the next expression

$$C_E = \frac{ER}{60\%}$$

Table 2-1 Correction for hammer energy efficiency

Equipment	Approximate ER**	C_E **
Safety Hammer	0.4 to 0.75	0.7 to 1.2
Donut Hammer	0.3 to 0.6	0.5 to 1.0
Donut Hammer*	0.7 to 0.85	1.1 to 1.4
Automatic-Trip Hammer (Donut or Safety Type)	0.5 to 0.8	0.8 to 1.4

**With special Japanese "throw" release*

***The ranges shown can vary if equipment and/or monitoring and procedures are not good*

The correction factor for nonstandard borehole diameters C_B whose values as given in the Table 2-2, in correspondence to NCEER/NSF, Youd et al. (2001).

Table 2-2 Correction for borehole diameters

Borehole diameter	C_B **
65 to 115mm	1.00
150mm	1.05
200mm	1.15

Short rod correction factor, C_R accounts for the effect of rod length on the energy transferred to the sampling rods during the primary hammer impact. The rod length is the sum of the rod stick-up length (length above the ground surface) and the sampling depth. The values of C_R recommended in NCEER/NSF, Youd et al. (2001) given before by Seed, H. B. et al. (1984) and Skempton, A. W. (1986) are listed in the Table 2-3.

Table 2-3 Rod Correction recommended values

Borehole diameter	C_R
Rod length < 3 m	0.75
Rod length 3-4 m	0.80
Rod length 4-6 m	0.85
Rod length 6-10 m	0.95
Rod length 10-30 m	1.00

The factor C_S is the correction for no standardized sampler configuration. For standard sampler are set equal to unity. However, for samplers with an indented space for interior liners, but with

liners omitted during sampling Seed, H. B. et al. (1984, 1985) recommend used the following expression,

$$C_S = 1 + \frac{(N_1)_{60}}{100} \qquad for\ ;\ 10 \leq (N_1)_{60} \leq 30$$

With limits as $1.10 \leq C_S \leq 1.30$.

Based on the feature that increase in relative density of soil increases both the penetration resistance and liquefaction resistance potential; Seed, H. B. et al. (1983) suggested an empirical correlation where $N_{1,60}$ and CSR were chosen as the capacity and demand parameters, respectively. Then, in Seed, H. B. et al. (1984), a methodology is proposed for assess liquefaction resistance, through triggering curves as is illustrated in the Figure 2-3.

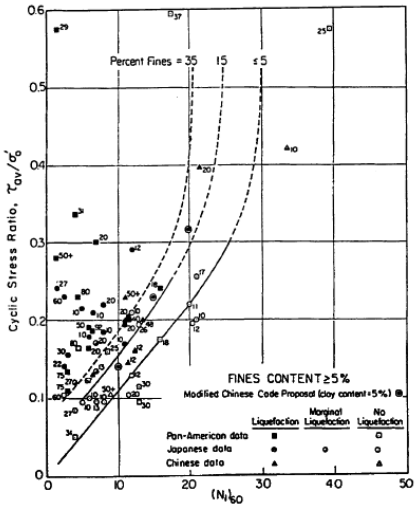

Figure 2-3 Relationship between Stress Ratios Causing liquefactions and $N_{1,60}$ recommended by Seed et al. (1984), for Magnitude 7.5.

CRR curves on the Figure 2-3, also known as; SPT clean sand curve, were conservatively positioned to separate regions with data indicative of liquefaction from regions with indicative of no liquefaction and were established for granular soils with fines contents of 5% or less, 15%, and 35%.

After Seed, H. B. et al. (1984), several changes to the SPT criteria have been formulated. One of the first adjustments consists in a projection of the curve for low values of $N_{1,60}$. This modification was done mainly to achieve greater consistence with CRR curves developed for CPT and Vs shear wave velocity procedures. That approximation for clean sand curve, recommended by the workshop NCEER/NSF, Youd et al. (2001), follows the equation:

$$CRR_{7.5} = \frac{1}{34 - (N_1)_{60}} + \frac{(N_1)_{60}}{135} + \frac{50}{[10 * (N_1)_{60} + 45]^2} - \frac{1}{200}$$

This equation is valid for $(N_1)_{60} < 30$. For $(N_1)_{60} \geq 30$, clean granular soils are too dense to liquefy and are classed as no liquefiable. Several other researchers proposed other forms of $CRR_{7.5}$ curves, among them Cetin et al. (2004) and Idriss and Boulanger (2014) constitute the most popular ones.

➢ Cetin et al. (2004)

Cetin, K. O. et al. (2004) presents adjusted correlations for assessment of the likelihood of initiation (or "triggering") of soil liquefaction. The intention of their correlations eliminates several sources of bias intrinsic to previous, similar correlations.

$$P_L = \Phi\left(-\frac{\left(N_{1,60} \cdot (1 + 0.004 \cdot FC) - 29.53 \cdot ln(CSR_{eq}) - 29.53 \cdot ln(M_w) - 3.70 \cdot ln\left(\frac{\sigma_v'}{P_a}\right) + 0.05 \cdot FC + 16.85\right)}{2.70}\right)$$

Where; P_L = probability of liquefaction in decimals (i.e., P_L=30% is represented as 0.30), CSR_{eq} = is not "adjusted" for magnitude or duration effects (correction for duration effects occurs within the equation itself), FC = percent fines content (by dry weight) expressed as an integer (e.g., 12% fines is expressed as FC=12), P_a = atmospheric pressure (=1 atm) in the same units as the in-situ vertical effective stress σ_v' and Φ= standard cumulative normal distribution.

Also, the cyclic resistance ratio for a given probability of liquefaction can be expressed as

$$CRR = exp\left[\frac{\left(N_{1,60} \cdot (1 + 0.004 \cdot FC) - 29.53 \cdot ln(M_w) - 3.70 \cdot ln\left(\frac{\sigma_v'}{P_a}\right) + 0.05 \cdot FC + 16.85 + 2.70 \cdot \Phi^{-1}(P_L)\right)}{13.32}\right]$$

Where, $\Phi^{-1}(P_L)$ = inverse of the standard cumulative normal distribution (i.e., mean=0, and standard deviation=1).

Figure 2-4, shows the correlations suggested by Cetin, K. O et al. (2004), representing the resistance of soils to liquefaction referred by cyclic resistance ratio (CRR).

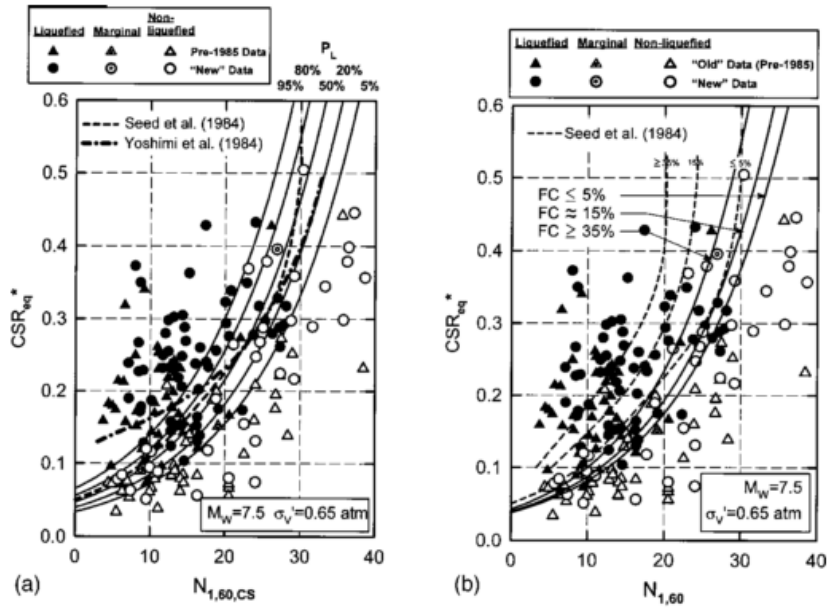

Figure 2-4 (a) Probabilistic standard penetration test-based liquefaction triggering correlation for Mw=7.5 and σ_v' =1.0 atm and (b) "deterministic" standard penetration test-based liquefaction triggering correlation for Mw=7.5 and σ_v' = 0.65 atm, Cetin, K. O et al. (2004)

➢ Idriss, I. M. and Boulanger, R. W. (2014)

Idriss, I. M. and Boulanger, R. W. (2004, 2008, 2014), proposed a correlation between the cyclic resistance ratio (CRR) adjusted to M = 7.5 and σ_v' = 1 atm and the equivalent clean sand $(N_1)_{60cs}$ value for cohesionless soils, as developed by, is expressed as:

$$CRR_{M=7.5,\sigma_v'=1atm} = exp\left(\frac{(N_1)_{60cs}}{14.1} + \left(\frac{(N_1)_{60cs}}{126}\right)^2 - \left(\frac{(N_1)_{60cs}}{23.6}\right)^3 + \left(\frac{(N_1)_{60cs}}{25.4}\right)^4 - 2.8\right)$$

This relationship $CRR_{M=7.5,\sigma'_v=1atm}$ and $(N_1)_{60cs}$ can be understood in the Figure 2-5.

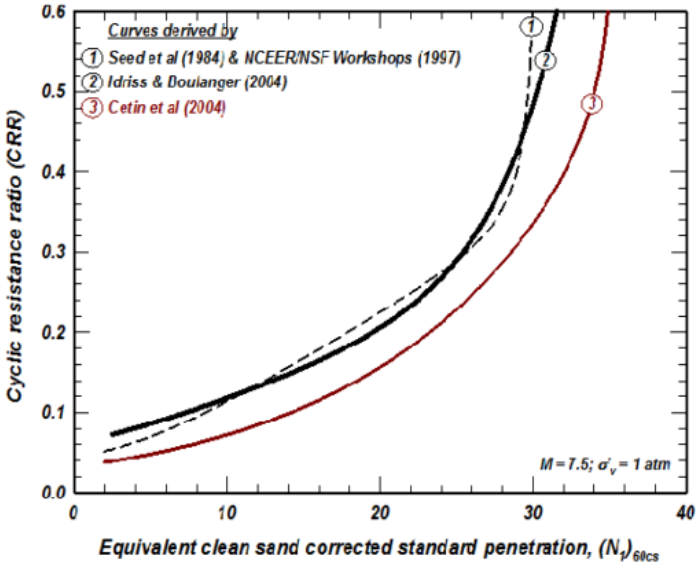

Figure 2-5 SPT-based liquefaction triggering curves components

➢ Influence of fines content

First recognized by Seed, H. B. et al. (1984), there is an increase of CRR with fines content, FC, as illustrated in the Figure 2-3, where they reproduced curves of CRR for various fines contents. Then, a revised correction for fines contents was develop by NCEER/NSF, Youd et al. (2001), where they judged that despite the influence of plasticity, among other characteristics of soil, in the liquefaction resistance could be based solely on fines content with engineering caution and judgment. Therefore, for correction of $(N_1)_{60}$ to equivalent clean sand $(N_1)_{60cs}$ they suggested the following equations:

$$(N_1)_{60cs} = \alpha + \beta\,(N_1)_{60}$$

Where α and β are coefficients determined by the next relationships:

$$\alpha = 0 \quad for \;\; FC \leq 5\%$$
$$\alpha = exp[1.76 - (190/FC^2] \quad for \;\; 5\% < FC < 35\%$$
$$\alpha = 5.0 \quad for \;\; FC \geq 35\%$$

$$\beta = 1.0 \quad for \quad FC \leq 5\%$$
$$\beta = [0.99 - (FC^{1.5}/1000] \quad for \quad 5\% < FC < 35\%$$
$$\beta = 1.2 \quad \text{for} \quad \text{FC} \geq 35\%$$

In the same way, Cetin, K. O et al. (2004), based on the overall (regressed) correlation among additional considerations the values of $N_{1_{60}}$ are further corrected for fines content as:

$$N_{1_{60CS}} = N_{1_{60}} \cdot C_{FINES}$$

The fines correction is equal to approximately 1.0 for fines contents of $FC \leq 5\%$, in other words, for those values there is not adjustment, and reaches a maximum value for FC $\geq$ 35%. As is shown in the Figure 2-4 (b), the maximum fines correction is somewhat smaller than the former maximum correction of +10 blows/ ft proposed by Seed, H. B. et al. (1984). The C_{FINES} relationship is given as close approximation as:

$$C_{FINES} = (1 + 0.004 \cdot FC) + 0.05\left(\frac{FC}{N_{1_{60}}}\right)$$
$$lim: 5\% < FC < 35\%$$

Where FC is fines content expressed as an integer (e.g., 27% fines as $FC = 27.0$). Additionally, for fines contents less than 5% is given a $FC = 0$ while for fines contents greater than 35% is used $FC = 35$.

Another proposed correlation for fines contents is suggested by Idriss, I. M. and Boulanger, R. W. (2004, 2008) and it is expressed in terms of equivalent clean sand $(N_1)_{60cs}$, which is obtained using the following equation:

$$(N_1)_{60cs} = (N_1)_{60} + \Delta(N_1)_{60}$$

Where the adjustment $\Delta(N_1)_{60}$ is function of FC, which is empirically derived from the liquefaction case history data, and accounts for the effects that fines content has on both the CRR and the SPT blow count. As was exposed before by Seed, H. B. et al. (1984), the liquefaction case histories suggest that the liquefaction triggering correlation shifts to the left as the fines content (FC)

increases. Having this in consideration Idriss, I. M. and Boulanger, R. W. (2004, 2008) developed their equivalent clean sand adjustment expressed as:

$$\Delta(N_1)_{60} = exp\left(1.63 + \frac{9.7}{FC + 0.01} - \left(\frac{15.7}{FC + 0.01}\right)^2\right)$$

where FC is in percent. The resulting relationships is illustrated in Figure 2-6 along with: (a) the equivalent clean sand adjustments recommended by NCEER/NSF, Youd et al. (2001), based on the curves originally published by Seed, H. B. et al. (1984), and (b) the equivalent clean sand adjustments recommended in Cetin, K. O et al. (2004).

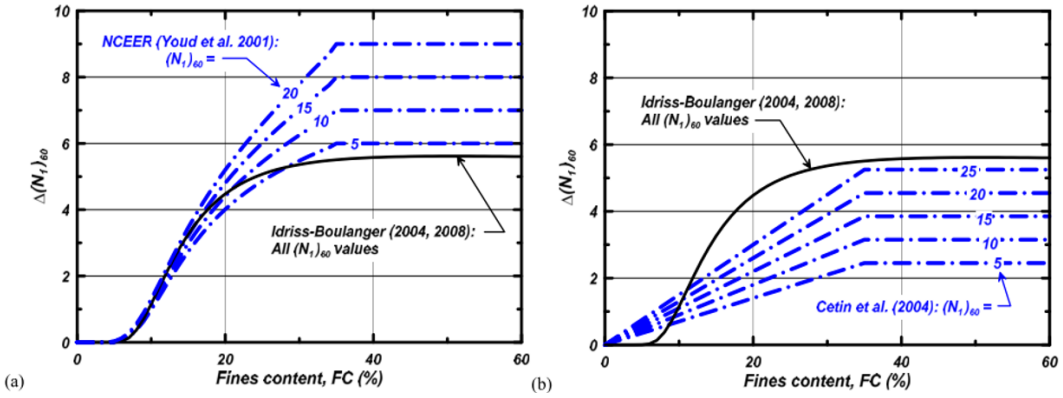

Figure 2-6 Variation of $\Delta(N_1)_{60}$ with fines content

2.2.2 Cone Penetration Test (CPT)

During the last two decades, cone penetration test (CPT) has been quickly becoming one the most popular type of in-situ test because it is fast, economical, and provides continuous profiling of geo-stratigraphy and soil properties evaluation. It proposes repeatable and reliable data (not operator-dependent).

Test consists of pushing a cylindrical steel cone shaped probe into the ground at a constant velocity with rate of 20 mm/s and measuring the resistance to penetration of the cone and of a surface sleeve. The cone resistance q_c is the force acting on the cone Q_c divided on the projected area of the cone A_c. The sleeve fraction resistance f_s is the frictional force that turns on the friction sleeve, F_s, divided by its surface area, A_s. As well, the CPTu or piezocone allows to measure the pore

pressure. The pore pressure generated during cone penetration is measured by a pore pressure sensor as; u_1 when measured on the cone face and u_2 when measured just behind the cone, Robertson, P. K. and Wride, C. E. (1998).

The tip resistance from the cone penetration test can also be used as a measure of liquefaction resistance. One of the CPT advantages is that a nearly continuous profile of penetration resistance is developed for stratigraphic interpretation. This capability makes the CPT particularly advantageous for developing liquefaction-resistance profiles. Similar to what has been represented in SPT, interpretations based on the CPT must be verified with a few well-placed boreholes to confirm soil types and further verify liquefaction- resistance interpretations, NCEER/NSF, Youd et al. (2001).

It should be noted that the current day of practice three different updated methodologies are often being used to assess the potential of liquefaction trigger: Robertson (2009), Moss et al. (2006), and Boulanger and Idriss (2015).

- **Robertson's woks**

Recommended CPT correlation for sand-like soils can be assessed by means of the following the equations given by Robertson, P. K. and Wride, C. E. (1998).

$$CRR_{7.5} = 93\left[\frac{(Q_{tn,cs})}{1000}\right]^3 + 0.08$$

If $50 \leq Q_{tn,cs} \leq 160$

$$CRR_{7.5} = 0.833\left[\frac{(Q_{tn,cs})}{1000}\right] + 0.05$$

If $Q_{tn,cs} < 50$

Where the $Q_{tn,cs}$ is the equivalent clean sand penetration resistance that comes from the normalized CPT penetration resistance Q_{tn} defined as follows;

$$Q_{tn,cs} = K_c Q_{tn}$$

Having K_c as a correction factor that is a function of behavior characteristics (e.g. combined influence of fines content and plasticity) of the soil.

Another concept is the behavior type index I_c which allows to differentiate soil types characterized as clays from soil types characterized as sands and silts and is defined by Robertson, P. K. (1990) and it is computed as follow;

$$I_c = [(3.47 - logQ_{tn})^2 + (log\ F + 1.22)^2]^{0.5}$$

Where

$$Q_{tn} = \left(\frac{q_t}{P_{a2}}\right)\left(\frac{P_a}{\sigma'_{vo}}\right)^n$$

And

$$F = \left[\frac{f_s}{(q_c - \sigma_{vo})}\right] * 100\%$$

Having; n = stress exponent, F is the normalized friction ratio (in percent); f_s is the CPT sleeve friction stress; σ_{vo} and σ'_{vo} are the total effective overburden stresses respectively P_a is a reference pressure in the same units as σ'_{vo} and P_{a2}

The stress exponent n should be computed through iteration stating form values of $n = 1.0$ and satisfying the equating; where at the end of the iteration should be $n \leq 1.0$

$$n = 0.381(I_c) + 0.05\left(\frac{\sigma'_{vo}}{P_a}\right) - 0.15$$

Another relationship is between I_c and the correction factor K_c and Robertson (1990) proposes by the following;

$$K_c = 1.0 \qquad if \quad I_c \leq 1.64$$

$$K_c = 5.581 \cdot I_c^3 - 0.403 \cdot I_c^4 - 21.63 \cdot I_c^2 + 33.75 \cdot I_c - 17.88 \qquad if \quad I_c > 1.64$$

Robertson, P. K. (2009a, 2009b) recommended the following CPT-based approach that can be applied to all soils (i.e. no I_c cut-off):

Taking everything into consideration there are a few more conditions for computing $CRR_{7.5}$ base on I_c values;

- When $I_c \leq 2.50$, assume soils are sand-like
  Using the previous conditions for K_c and I_c, and following Robertson, P. K. and Wride, C. E. (1998) recommendations;

$$Q_{tn,cs} = K_c Q_{tn}$$

- When $I_c > 2.70$, assume soils are clay-like, where;

$$CRR_{7.5} = 0.053 Q_{tn} K_{\propto}$$

- when $2.50 < I_c < 2.70$, transition region, according to Robertson, P. K. and Wride, C. E. (1998), equivalent clean sand penetration resistance is;

$$Q_{tn,cs} = K_c Q_{tn}$$

  Where:

$$K_c = 6 * 10^{-7} (I_c)^{16.76}$$

The correction factor $K_{\propto}$ permits to account to static shear stress. For well-designed structures where the factor of safety for static loading is large, $K_{\propto}$ is generally close to 0.9. For heavily loaded soils under static conditions, $K_{\propto}$ can be significantly less than 1.0.

➢ Moss et al. (2006)

About soil liquefaction assessment concerns, Moss, R. E. S., et al. (2006) presented a methodology for both probabilistic and deterministic assessment of seismic soil liquefaction

triggering potential based on the cone penetration test CPT. Consequently, the following equation can be used to calculate the probability of liquefaction:

$$P_L = \Phi\left(-\frac{\left[q_{c,1}^{1.045} + q_{c,1}(0.110R_f) + (0.001R_f) + c(1 + 0.850R_f) - 7.177ln(CSR) - 0.848ln(M_w) - 0.002ln(\sigma_v') + 20.923\right]}{1.632}\right)$$

Where; $q_{c,1}$ normalized tip resistance (MPa); R_f friction ratio (percent); c = normalization exponent; CSR equivalent uniform cyclic stress ratio; σ_v' effective overburden stress (kilopascal); and $\Phi(P_L)$ cumulative normal distribution. Also, the cyclic resistance ratio for a given probability of liquefaction can be computing as;

$$CRR = exp\left[\frac{q_{c,1}^{1.045} + q_{c,1}(0.110R_f) + (0.001R_f) + c(1 + 0.850R_f) - 0.848ln(M_w) - 0.002ln(\sigma_v') + 20.923 + 1.632\Phi^{-1}(P_L)}{13.32}\right]$$

Where, $\Phi^{-1}(P_L)$ = inverse of the standard cumulative normal distribution (i.e., mean=0, and standard deviation=1).

The normalized tip resistance $q_{c,1}$, according to Moss, R. E. S., et al. (2006), depends on the exponent that allows to normalize the tip resistance for a given level of overburden stress, by means of the following equation;

$$q_{c,1} = C_q \cdot q_c$$

Where

$$C_q = \left(\frac{P_a}{\sigma_v'}\right)^c \leq 1.7$$

C_q tip normalization factor; $q_c$raw tip resistance (MPa); P_a reference stress (1 atm, in compatible units); σ_v' effective overburden stress (same units as P_a) and c normalization exponent that can be calculated using the iterative equation

$$c = f_1 \cdot \left(\frac{R_f}{f_3}\right)^{f_2}$$

Where

$$f_1 = x_1 \cdot {q_c}^{x_2} \quad \text{where;} \quad x_1 = 0.78 \ \text{ and } \ x_2 = -0.33$$

$$f_2 = -(y_1 \cdot {q_c}^{y_2} + y_3) \quad \text{where;} \quad y_1 = -0.32\,, \quad y_2 = -0.35 \quad \text{and} \quad y_3 = 0.49$$

$$f_3 = abs[log(10 + q_c)]^{z1} \quad \text{where;} \quad z_1 = 1.21$$

R_f friction ratio (the ratio of sleeve to tip resistance, f_s/q_c in percent)

To normalize the tip resistance appropriately, an iterative procedure is necessary; first at all estimate an initial of the normalization exponent c, for instance, it can be taken as 0.5, Liao, S. S. C. and Whitman, R. V. (1986), secondly normalized the tip resistance $q_{c,1}$, then revised estimate of the normalization exponent c using the normalized tip resistance $q_{c,1}$ which is compared to the initial normalization exponent estimate, finally repeated until an acceptable convergence tolerance is achieved.

➢ Boulanger and Idriss (2015)

Boulanger, R. W. and Idriss, I. M. (2015) based on updated case history database and through the methodology for developing the probabilistic relationships for liquefaction triggering that they already had presented in Boulanger, R. W. and Idriss, I. M. (2014) and in previous works, revised relationships for the magnitude scaling factor (MSF) and for estimating fines contents from CPT data when laboratory test data are not available.

First at all, it is important explain their methodology. Idriss, I. M. and Boulanger, R. W. (2004, 2008) proposed cyclic resistance ratio (CRR) adjusted to M = 7.5 and σ'_v = 1 atm and expressed in terms of equivalent clean-sand q_{c1Ncs} that can be was assessed using the following relationship,

$$CRR_{M=7.5,\sigma'_v=1atm} = exp\left(\frac{q_{c1Ncs}}{113} + \left(\frac{q_{c1Ncs}}{1000}\right)^2 - \left(\frac{q_{c1Ncs}}{140}\right)^3 + \left(\frac{q_{c1Ncs}}{137}\right)^4 - C_0\right)$$

where C_0 = is unknown as fitting parameter that permits scaling the relationship while maintaining its shape. This relationship is not strongly constrained by the case history data for low or high values of q_{c1Ncs}, and thus its shape was also guided by checking its consistency with the SPT-based correlation by Boulanger and Idriss (2012) in terms of implied q_c/N_{60} ratios and relative state parameter indices for common values of $CRR_{M=7.5,\sigma'_v=1atm}$ and P_L. As a result of that, among

another contemplations, Boulanger, R. W. and Idriss, I. M. (2015) considered as appropriate value for $C_0 = 2.8$ for deterministic approach.

For determining the equivalent clean-sand q_{c1Ncs} values, is used the following expression:

$$q_{c1Ncs} = q_{c1N} + \Delta q_{c1N}$$

The overburden correction factor, C_N could be expressed in terms of q_{c1Ncs}. The use of following equation requires iteration that could be stating for instance using the lower value of the stress exponent $m = 0.254$.

$$C_N = \left(\frac{P_a}{\sigma_v'}\right)^m \leq 1.7$$

Where;

$$m = 1.338 - 0.249(q_{c1Ncs})^{0.264} \qquad with \quad 0.254 \leq m \leq 0.782$$

with q_{c1Ncs} has limit values in the interval from 21 to 254.

The equivalent clean-sand adjustment Δq_{c1N} that can be seen in the Figure 2-7, is given by the following equation;

$$\Delta q_{c1N} = \left(11.9 + \frac{q_{c1N}}{14.6}\right) exp\left(1.63 - \frac{9.7}{FC + 2} - \left(\frac{15.7}{FC + 2}\right)^2\right)$$

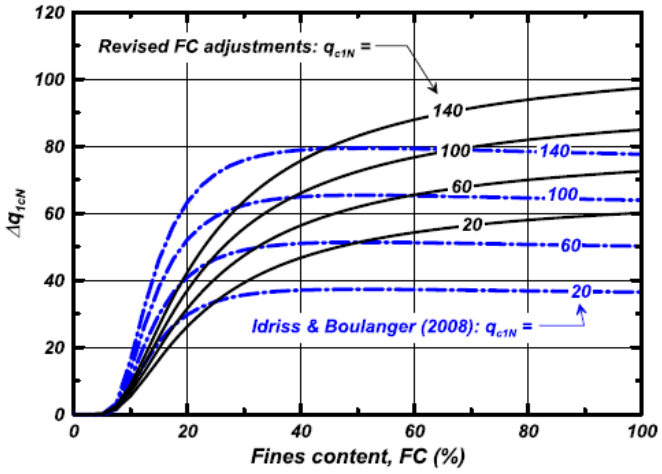

Figure 2-7 Equivalent clean sand adjustments for CPT-based liquefaction triggering procedures

The revised CPT-based liquefaction triggering procedure suggested Boulanger, R. W. and Idriss, I. M. (2014), included a recommended relationship and approach for estimating FC, fines content percent, and soil classifications from the I_c index as follows;

$$FC = 80(I_c + C_{FC}) - 137 \qquad with \;\; 0\% \leq FC \leq 100\%$$

where C_{FC} is a fitting factor (it is by default is 0.0) This expression with C_{FC} = -0.29, 0.0, and 0.29 (i.e., ± an amount equal to the standard deviation in the general correlation) as is shown in the Figure 2-8. A site-specific value for C_{FC} should come from individual geologic strata (for instance; common source material and deposition).

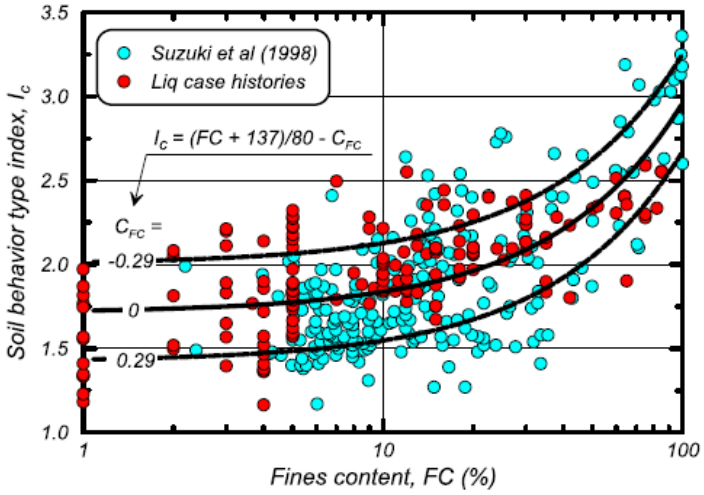

Figure 2-8 Recommended correlation between I_c and FC with plus or minus one standard deviation against the data set by Suzuki et al. (1998) and the liquefaction database

The soil behavior type index I_c is computed as F;

$$I_c = [(3.47 - logQ_{tn})^2 + (log\, F + 1.22)^2]^{0.5}$$

where Q and F are normalized tip and sleeve friction ratios computed as,

$$Q = \left(\frac{q_c - \sigma_{vo}}{P_{a2}}\right)\left(\frac{P_a}{\sigma'_{vo}}\right)^n \qquad with \;\; 0.5 \leq n \leq 1.0$$

$$F = \left[\frac{f_s}{(q_c - \sigma_{vo})}\right] * 100\%$$

Where, he exponent n varies from 0.5 in sands to 1.0 in clays Robertson, P. K. and Wride, C. E. (1998).

➢ Cyclic Resistance Ratio CRR from State Parameter ψ

The cyclic resistance ratio CRR can be estimated directly through the state parameter ψ, which indicates the potential dilation or contraction behavior of the soil during shearing. This can be accomplished by the suggested methodology of Jefferies, M.G. & Been, K. (2015). Similarly, developed empirical correlations allow estimating the state parameter.ψ from CPT results alone. Those correlations were developed through a review of data available at the time that featured both CPT results and laboratory measures of λ_{10} in the same soil.

As results of their previous investigations, Jefferies, M.G. & Been, K. (2015) suggest the following equation to calculate CRR knowing the state parameter ψ:

$$CRR = 0.06 * e^{-9\psi}$$

Methods to obtain ψ from the CPT were first proposed by Been et al. (1986), who synthesized a body of calibration chamber data to develop the following expression:

$$\psi = \frac{-ln\left(\frac{Q}{k}\right)}{m}$$

Where Q is normalized dimensionless cone tip friction ratio and, k and m are soil specific coefficients that depended on soil compressibility λ_{10}.

$$k = \frac{0.55}{\lambda_{10} - 0.01} + 8$$

$$m = 8.1 - 2.3log\lambda_{10}$$

Plewes et al. (1992) suggested the following expression for estimating the soil compressibility.

$$\lambda_{10} = \frac{F}{10}$$

Where, F is normalized cone sleeve friction ratio.

2.2.3 Shear Wave Velocity (Vs)

Over the past 30 years, in-situ measurements of small-strain shear-wave velocity V_s has been an alternative to the penetration-based approaches for compute liquefaction resistance due to it provides consistent information about soil resistance.

Although there has been an ongoing dispute on assessing the large-strain response of liquefaction resistance based on a small strain in-situ test, the use of V_s as an index of liquefaction resistance is soundly used by opposing researchers because both V_s and liquefaction resistance are similarly influenced by many of the same factors (e.g., void ratio, state of stress, stress history, and geologic age) [e.g. Andrus, R. D., and Stokoe, K. H., II. (2000)].

According to Andrus, R. D., and Stokoe, K. H., II. (2000), using V_s brings some advantages; of which can be mentioned the possibility of performed on small laboratory specimens, allowing direct comparisons between laboratory and field behavior, also, the measurements can be perform in soils that are hard to sample, such as gravelly soils where penetration tests may be unreliable. Moreover, V_s is a basic mechanical property of soil materials, directly related to small-strain shear modulus G_{max} by;

$$G_{max} = \rho V_s^2$$

where ρ = mass density of soil.

Making the contrast with V_s, SPT and CPT penetration methods have the advantage of correlating more directly with relative density, which has a strong effect on the cyclic behavior of saturated soil according to Idriss, I.M. and Boulanger, R.W. (2008). On the other hand, V_s is considerably less sensitive to problems of soil compression and reduced penetration resistance when soil fines

are present, compared with SPT and CPT penetration methods. Therefore, V_s requires only minor corrections for fines content (FC) [Kayen, R., et al. (2013)].

➢ NCEER Workshop

In practice there are three facts concerning the use of V_s for liquefaction-resistance evaluations. First; seismic wave velocity measurements are made in the range of small strains, but on the other hand pore-water pressure buildup and the onset of liquefaction are medium- to high-strain phenomena. Secondly, in seismic testing there is not possibility to obtain samples for classification of soils and identification of no liquefiable soft clay-rich soils. And the third fact is that thin, low V_s strata may not be detected if the measurement interval is too large. Thus, in practice is recommended to drill adequate number boreholes in order to detect and delineate thin liquefiable strata, no liquefiable clay-rich soils, and silty soils above the ground-water table that might become liquefiable should the water table rise. NCEER/NSF, Youd et al. (2001).

For evaluating liquefaction resistance, NCEER/NSF, Youd et al. (2001) recommend follow the traditional procedures that make the correction of penetration resistance taking into account the overburden stress, as a consequence, V_s is also corrected to a reference overburden stress using the following equation, where V_s is measured with both the directions of particle motion and wave propagation polarized along principal stress directions and that one of those directions is vertical Stokoe, K. H et al. (1985).

$$V_{s1} = V_s \left(\frac{P_a}{\sigma'_{vo}}\right)^{0.25}$$

Where V_{s1}= overburden-stress corrected shear wave velocity; P_a= atmospheric pressure approximated by 100kPa and σ'_{vo} initial effective vertical stress in the same units as P_a.The Figure 2-9 shows the compassion between many authors who made the relationship $CRR - V_{s1}$

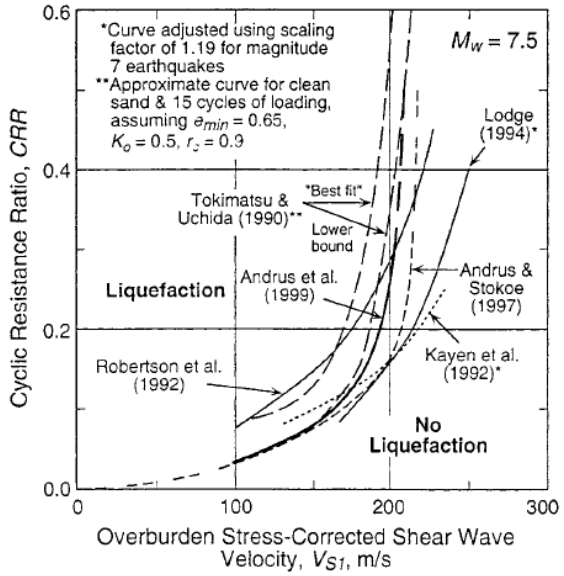

Figure 2-9 Comparison relationships between Liquefaction Resistance and Overburden Stress-Corrected Shear Wave Velocity for Granular Soils

Andrus, R. D., and Stokoe, K. H., II. (1997) proposed the following relationship between CRR and V_{s1} that was developed for uncemented, Holocene-age soils with 5% or less fines using field performance data from 20 earthquakes and over 50 measurement sites.

$$CRR = a\left(\frac{V_{s1}}{100}\right)^2 + b\left(\frac{1}{V_{s1}^* - V_{s1}} - \frac{1}{V_{s1}}\right)$$

where V_{s1}^* = limiting upper value of V_{s1} for liquefaction occurrence; and a and b are curve fitting parameters.

CRR versus V_{s1} curves recommended for engineering practice by Andrus, R. D., and Stokoe, K. H., II. (2000) for magnitude 7.5 earthquakes and uncemented Holocene-age soils with various fines contents are shown in Figure 2-10.

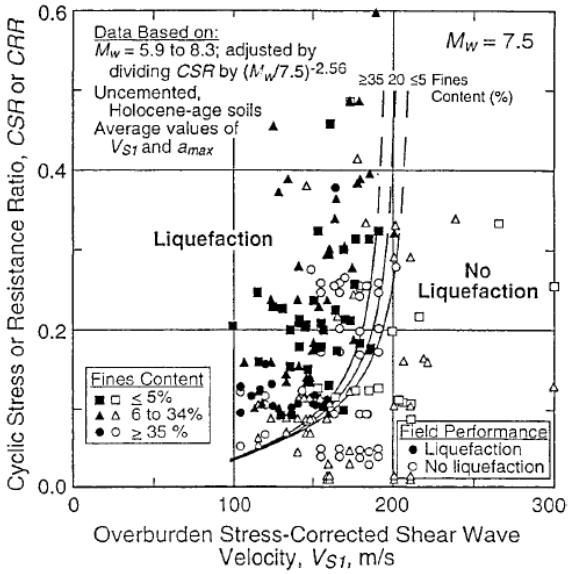

Figure 2-10 Liquefaction Relationship Recommended for Clean, Uncemented Soils with Liquefaction Data from Compiled Case Histories (Reproduced from Andrus, R. D., and Stokoe, K. H., II. (2000))

The three curves shown were determined by an iterative process of varying the values of a and b. The final values of a and b used to draw the curves were 0.022 and 2.8, respectively. Values of were assumed V_{s1}^* to vary linearly from 200 m/s for soils with fines content of 35% to 215 m/s for soils with fines content of 5% or less.

➢ Kayen et al., 2013

The methodology suggested by Kayen, R., et al. (2013) is the product of an 11-year international project to gather new Vs site data. Toward that objective, shear-wave velocity test sites were identified, and measurements made for 301 new liquefaction field case histories in China, Japan, Taiwan, Greece, and the United States over a decade. These new data are combined with previously published case histories to build a global catalog of 422 case histories of V_s liquefaction performance. As a result of the research, the authors propose probabilistic correlations for seismic soil liquefaction occurrence.

In the Kayen, R., et al. (2013) wok, the case histories were evaluated for seismic demand CSR and soil capacity V_{s1}, and using a Bayesian regression and structural reliability methods a probabilistic treatment was done for V_s. In addition, uncertainties of the variables comprising both the seismic

demand and the soil capacity were estimated and included in the analysis. A dual procedure is used to compute the final form of the governing equation.

The model coefficients were determined for V_{s1}, CSR, M_w, and σ'_{v0} from the entire data set. In the second follow-up analysis, these coefficients were fixed, and the model coefficient for FC was determined, which produced the lowest model error for the portion of the data set with FC data. Therefore, a cumulative normal distribution Φ is used as following, to develop the probability models for liquefaction based on the V_{s1}.

$$P_L = \Phi\left(-\frac{((0.0073 \cdot V_{s1})^{2.8011} - 1.946 \cdot ln(CSR) - 2.6168 \cdot ln(M_w) - 0.0099 \cdot ln(\sigma'_{v0}) + 0.0028 \cdot FC)}{0.4809}\right)$$

Where; P_L = probability of liquefaction in decimals (i.e., P_L=30% is represented as 0.30), CSR = is not "adjusted" for magnitude or duration effects (correction for duration effects occurs within the equation itself), FC = percent fines content (by dry weight) expressed as an integer (e.g., 12% fines are expressed as FC=12) and Φ= standard cumulative normal distribution.

For the deterministic assessment of liquefaction susceptibility, the writers recommend the P_L=15% contour for use as the single deterministic boundary for V_{s1}-based liquefaction evaluation. The P_L=15% contour adheres to the original intent of Seed H.B. and Idriss I.M. (1971) to have inherent conservatism in the boundary.

Also, the cyclic resistance ratio for a given probability of liquefaction can be expressed as

$$CRR = exp\left[\frac{\left((0.0073 \cdot V_{s1})^{2.8011} - 2.6168 \cdot ln(M_w) - 0.0099 \cdot ln(\sigma'_{v0}) + 0.0028 \cdot FC - 0.0028 \cdot \Phi^{-1}(P_L)\right)}{1.946}\right]$$

The deterministic factor of safety against triggering of seismic soil liquefaction is computed as the ratio of the soil capacity to resist liquefaction at P_L(15%), $CRR_{P_L(15\%)}$ and the corresponding seismic demand (CSR).

$$FS_{liq} = \frac{CRR_{P_L(15\%)}}{CSR}$$

The factor of safety can be determined either for the given earthquake magnitude and effective overburden stress or from values of CRR and CSR converted to the reference condition of M_w = 7.5, σ'_{v0}= 1 atm.

2.3 Liquefaction-Induced lateral displacements and Liquefaction-Induced ground settlements

Liquefaction-induced ground deformations have caused significant damage to engineered structures and lifelines during past earthquakes. Both ground settlements and lateral spreads are the pervasive types of liquefaction-induced ground deformations for level to gently sloping sites, (Zhang; P. et al 2002)

2.3.1 Mechanism of Liquefaction-Induced lateral spreads

Test of One-g shake table performed by (Sasaki et al. 1991; Yasuda et al. 1992) and centrifuge model tests done by (Abdoun 1997; Taboada-Urtuzuastegui and Dobry 1998), and their research, supports the hypothesis that lateral spread results from distributed residual shear strains throughout the liquefied layers. The residual shear strains in liquefied layers are primarily a function of maximum cyclic shear strains , and biased in situ static shear stresses, Zhang; P. et al (2002).

The estimation of Maximum Shear Strains γ_{max} from CPT data, depends of the liquefaction factor of safety and relative density D_r. Relative densities can be estimated from correlations of CPT results. The correlation between D_r and cone tip resistance (q_c) suggested by (Tatsuoka et al. 1990) and recommended by Zhang; P. et al (2002) is;

$$D_r = -85 + 76log(q_{c1N}) \quad [q_{c1N} \leq 200]$$

Where, q_{c1N} is normalized CPT tip resistance.

➢ Lateral Displacement Index LDI

Integrating the calculated Maximum Shear Strains γ_{max} values with depth will produce a value that is defined as the lateral displacement index LDI, Zhang; P. et al (2002).

$$LDI = \int_0^{Z_{max}} \gamma_{max} dz$$

Where, Z_{max} is maximum depth below all the potential liquefiable layers.

On the other hand, the γ_{max} values are estimated base on factor of safety FS according to the following expressions, and which mathematically describe the curves seen in the Figure 2-11.

$$if\ D_r = 90\%, \quad \gamma_{max} = 3.26(FS)^{-1.80} \quad for\ 0.7 \leq FS \leq 2.0$$
$$if\ D_r = 90\%, \quad \gamma_{max} = 6.2 \quad for\ FS \leq 0.7$$
$$if\ D_r = 80\%, \quad \gamma_{max} = 3.22(FS)^{-2.08} \quad for\ 0.56 \leq FS \leq 2.0$$
$$if\ D_r = 80\%, \quad \gamma_{max} = 10 \quad for\ FS \leq 0.56$$
$$if\ D_r = 70\%, \quad \gamma_{max} = 3.20(FS)^{-2.89} \quad for\ 0.59 \leq FS \leq 2.0$$
$$if\ D_r = 70\%, \quad \gamma_{max} = 14.5 \quad for\ FS \leq 0.59$$
$$if\ D_r = 60\%, \quad \gamma_{max} = 3.58(FS)^{-4.42} \quad for\ 0.66 \leq FS \leq 2.0$$
$$if\ D_r = 60\%, \quad \gamma_{max} = 22.7 \quad for\ FS \leq 0.66$$
$$if\ D_r = 50\%, \quad \gamma_{max} = 4.22(FS)^{-6.39} \quad for\ 0.72 \leq FS \leq 2.0$$
$$if\ D_r = 50\%, \quad \gamma_{max} = 34.1 \quad for\ FS \leq 0.72$$
$$if\ D_r = 40\%, \quad \gamma_{max} = 3.31(FS)^{-7.97} \quad for\ 1.0 \leq FS \leq 2.0$$
$$if\ D_r = 40\%, \quad \gamma_{max} = 250(1.0 + FS) + 3.5 \quad for\ 0.81 \leq FS \leq 1.0$$
$$if\ D_r = 40\%, \quad \gamma_{max} = 51.2 \quad for\ FS \leq 0.81$$

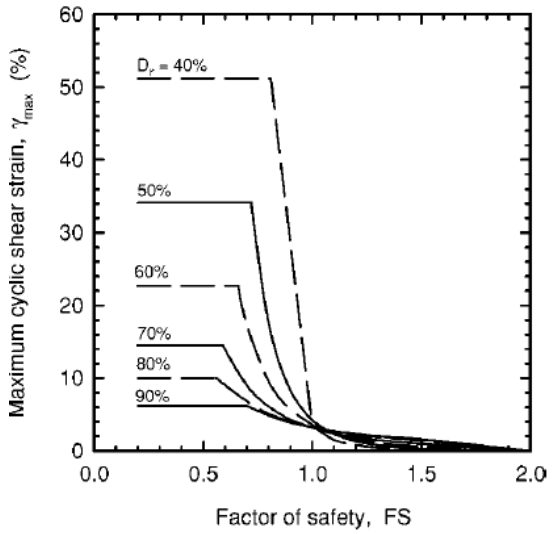

Figure 2-11 Relationship between Maximum Cyclic Shear Strain γ_{max} and Factor of Safety for different Relative Densities D_r for clean sands, Zhang; P. et al (2002).

2.3.2 Calculating ground settlement

For sites with level ground, far from any free face such as river banks and seawalls, it is reasonable to assume that little or no lateral displacement occurs after the earthquake, such that the volumetric strain will be equal or close to the vertical strain. Therefore, If the vertical strain in each soil layer is integrated with depth using the following equation, the result should be an appropriate index of potential liquefaction-induced ground settlement at the CPT location, Zhang, G. et al (2014)

$$S = \sum_{i=1}^{j} \varepsilon_{vi} \Delta z_i$$

Where, S is the calculated liquefaction-induced ground settlement at the CPT location; ε_{vi} is the postliquefaction volumetric strain for the soil sublayer i; Δz_i is the thickness of the sublayer i; and j is the number of soil sublayers.

The correlations between $(q_{c1N})_{cs}$ and postliquefaction volumetric strain (ε_v) for different FS were developed on the basis of the curves shown in Figure 2-12. The equations for these relationships are given as;

$$if \quad FS \leq 0.5, \quad \varepsilon_v = 102(q_{c1N})_{cs}^{-0.82} \quad for\ 33 \leq (q_{c1N})_{cs} \leq 200$$

$$if \quad FS = 0.6, \quad \varepsilon_v = 102(q_{c1N})_{cs}^{-0.82} \quad for\ 33 \leq (q_{c1N})_{cs} \leq 147$$

$$if \quad FS = 0.6, \quad \varepsilon_v = 2411(q_{c1N})_{cs}^{-1.45} \quad for\ 147 \leq (q_{c1N})_{cs} \leq 200$$

$$if \quad FS = 0.7, \quad \varepsilon_v = 102(q_{c1N})_{cs}^{-0.82} \quad for\ 33 \leq (q_{c1N})_{cs} \leq 110$$

$$if \quad FS = 0.7, \quad \varepsilon_v = 1701(q_{c1N})_{cs}^{-1.42} \quad for\ 110 \leq (q_{c1N})_{cs} \leq 200$$

$$if \quad FS = 0.8, \quad \varepsilon_v = 102(q_{c1N})_{cs}^{-0.82} \quad for\ 33 \leq (q_{c1N})_{cs} \leq 80$$

$$if \quad FS = 0.8, \quad \varepsilon_v = 1690(q_{c1N})_{cs}^{-1.46} \quad for\ 80 \leq (q_{c1N})_{cs} \leq 200$$

$$if \quad FS = 0.9, \quad \varepsilon_v = 102(q_{c1N})_{cs}^{-0.82} \quad for\ 33 \leq (q_{c1N})_{cs} \leq 60$$

$$if \quad FS = 0.9, \quad \varepsilon_v = 1430(q_{c1N})_{cs}^{-1.48} \quad for\ 60 \leq (q_{c1N})_{cs} \leq 200$$

$$if \quad FS = 1.0, \quad \varepsilon_v = 64(q_{c1N})_{cs}^{-0.93} \quad for\ 33 \leq (q_{c1N})_{cs} \leq 200$$

$$if \quad FS = 1.1, \quad \varepsilon_v = 11(q_{c1N})_{cs}^{-0.65} \quad for\ 33 \leq (q_{c1N})_{cs} \leq 200$$

$$if \quad FS = 1.2, \quad \varepsilon_v = 9.7(q_{c1N})_{cs}^{-0.69} \quad for\ 33 \leq (q_{c1N})_{cs} \leq 200$$

$$if \quad FS = 1.3, \quad \varepsilon_v = 7.6(q_{c1N})_{cs}^{-0.71} \quad for\ 33 \leq (q_{c1N})_{cs} \leq 200$$

$$if \quad FS = 2.0, \quad \varepsilon_v = 0.0 \quad for\ 33 \leq (q_{c1N})_{cs} \leq 200$$

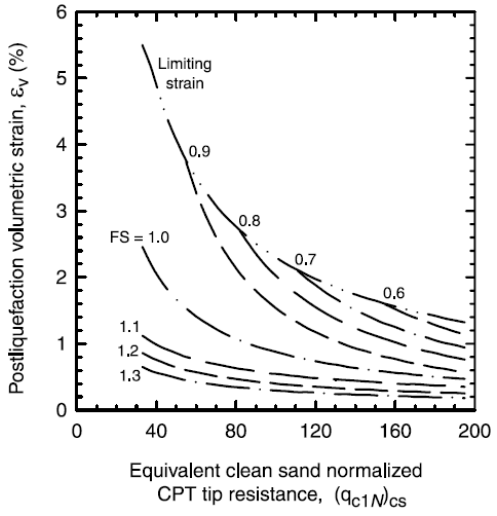

Figure 2-12 Relationship between postliquefaction volumetric strain and equivalent clean sand normalized CPT tip resistance for different factors of safety FS, Zhang, G. et al (2014)

Zhang, P. et al (2002) after reviewing several case studies, suggest a relationship between calculated values of LDI and LD measured. A general trend of increasing LD/LDI with increasing ground slope that can be expressed as;

$$\frac{LD}{LDI} = S + 0.2 \quad (for\ 0.2\% < S < 3.5\%$$

Where, S is the ground slope as percentage.

CHAPTER 3 APPLICATION OF THE SIMPLIFIED ASSESSMENT OF LIQUEFACTION TRIGGERING METHODS

The simplified procedures to measure liquefaction in soils, which are presented in the previous chapter, were programmed in MATLAB and Statistics Toolbox Release (2015a), to facilitate the calculation of potential liquefaction. Additionally, a graphics interface was created that allows the user to import the data from the field test, interact with the methods, and graph and visualize the results in tables. Therefore, by way of the programmed MATLAB package that helps to perform a liquefaction evaluation using the established methods based on the CPT, SPT and Vs tests a case study was analyzed which is shown in the following.

3.1 CASE STUDY

Regarding the assessment of liquefaction using the simplified methods based on the CPT, SPT and Vs tests, explained above, a case study was used with field information that is part of the research that Chiaradonna et al. (2018) under the effect of 2012 event with $Mw = 6.1$. A brief introduction is presented in the next paragraph.

In zone of northern Italy, specifically on the Po river riviera, an earthquake of magnitude of $Mw = 6.1$ took place on May 20, 2012. Among all the effects caused by this seismic event, the appearance of liquefaction stands out, which called the attention of the scientific community. As a consequence of this, the group European research project titled LIQUEFACT, was interested in deepening the study of the area with the purpose of verifying the effectiveness of mitigation measures to reduce the effects of liquefaction.

LIQUEFACT carried out subsoil research and collected existing information from literature and previous studies in order to characterize and define the geotechnical geological model of the area. The specific site selected for the investigation of the subsoil was Pieve di Cento (Bologna).

Moreover, according to Chiaradonna et al. (2018) the shallow layering and the shear wave velocity profile are identified from a borehole and 5 CPTs carried out at the site. As a result, it can be said that the soil column is composed by a sandy silt layer overlaying a silty sand layer that is supposed to be the liquefiable layer. There is a relatively thin clayey layer which is identified in the silty sand deposits from 4.2m and 4.8 m depth, as can be seen in the Figure 3-1, where, also is shown the soil behavior index I_C which is compute from the Robertson (2010) approach.

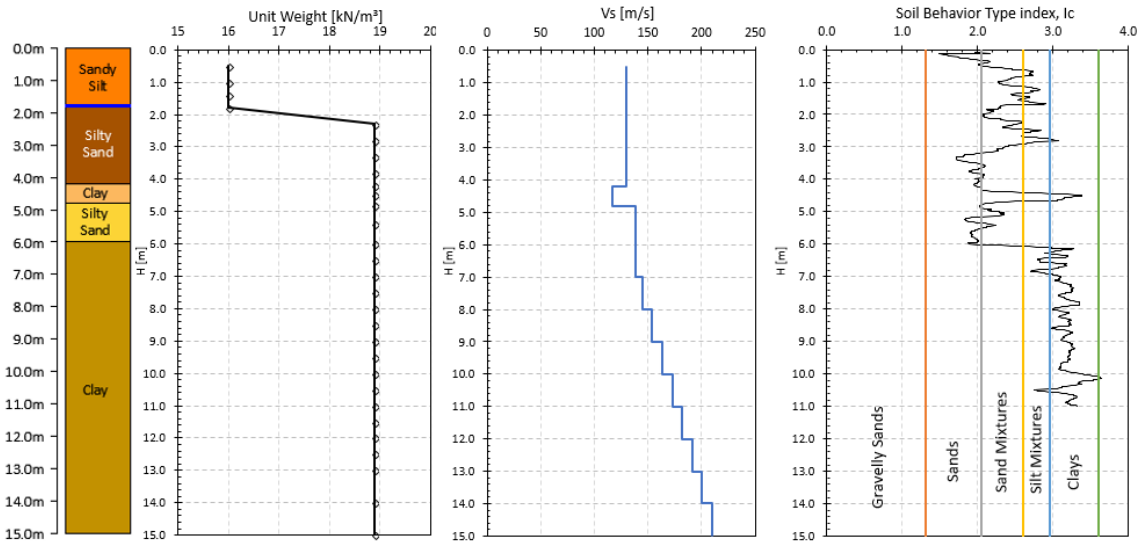

Figure 3-1 Soil column profile, (assumed) unit weight profile, shear wave velocity profile in smaller depth range (0-15 m) and soil behavior index I_C

Additionally, it was established as a limit value for $I_C > 2.6$ Figure 3-2 from which, according to Robertson (2010), the soil is classified as clayey and it is considered to be too much clay-rich to liquefy. Similarly, the soil behavior index I_C was filtered in units of soil above the water table "WT", as also is observed in the liquefaction potential analyzes presented in this document.

As can be seen in the figure, according to the results of the field tests of CPT and the soil behavior index I_C, a thin layer of clay was found around the 2.8m depth, as well as the layer of clay between

4.2m and 4.8m depth corresponding to the soil column profile defined by Chiaradonna et al. (2018).

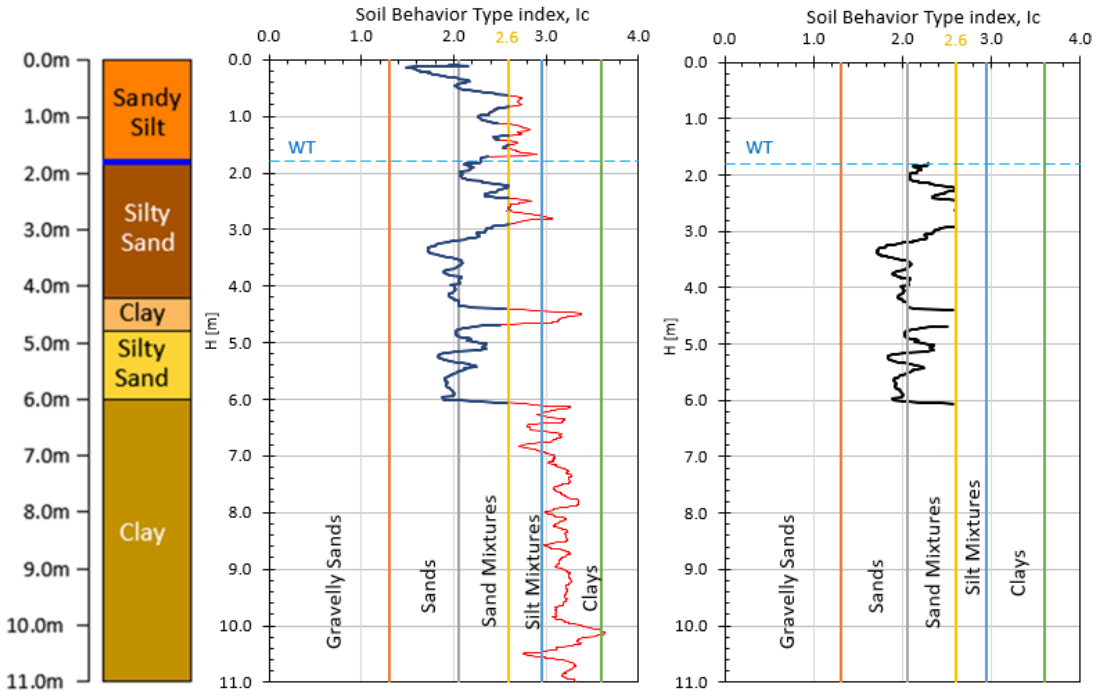

Figure 3-2 Soil column profile, and soil behavior index I_C

Additional to the case study Pieve di Cento (BO), focus of this chapter, another case study was carried out "Cavezzo (MO)", which is summarized and presented in the appendix. For the accomplishment of that case study all the subsoil investigation results and the laboratory tests, among another supplementary information were provided by the LIQUEFACT group.

3.1.1 CPT based methods

In relation to the methods based on CPT to evaluate liquefaction, the proposals of Moss, R. E. S., et al. (2006), that of Boulanger, R. W. and Idriss, I. M. (2015), and Robertson (2010) were used, based on data from field test performed and recollected by Chiaradonna et al., (2018). in the Figure 3-3 shows that information which contains the cone tip resistance, cone sleeve resistance and pore pressure and then the Figure 3-4 illustrates the normalized cone tip resistance and the normalized cone sleeve resistance.

It is important to reference, for this study case, that the magnitude of the earthquake *Mw* 6.1, the ground water table level 1.8m, PGA as computed from local site response analysis as 0.34g, which is defined in Chapter 4.

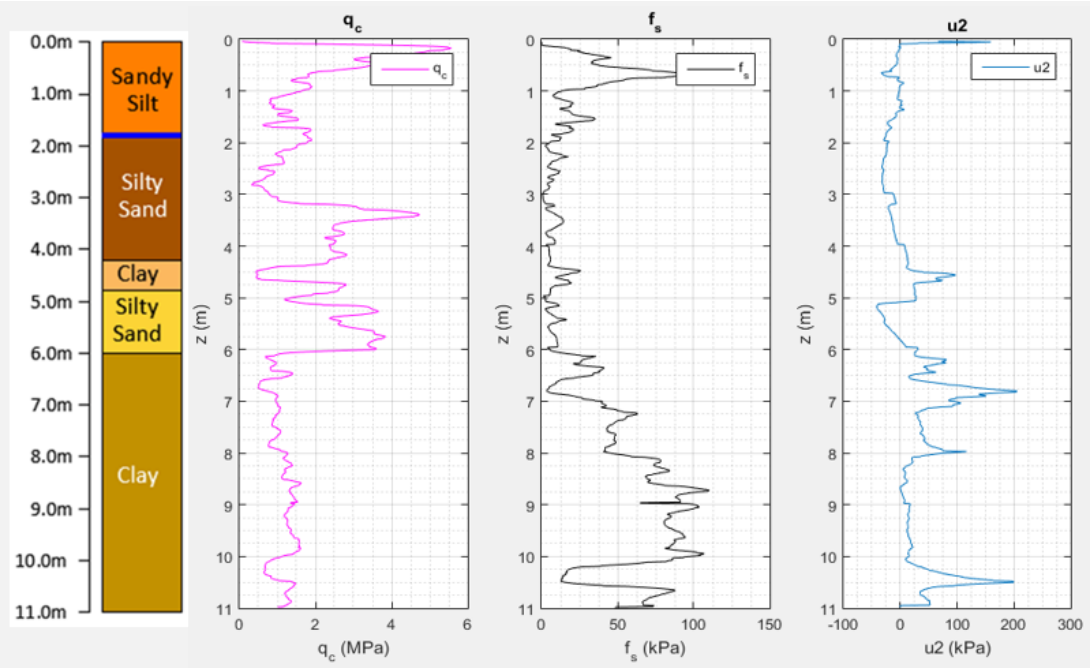

Figure 3-3 Cone tip resistance, cone sleeve resistance and pore pressure, data from Chiaradonna et al. (2018)

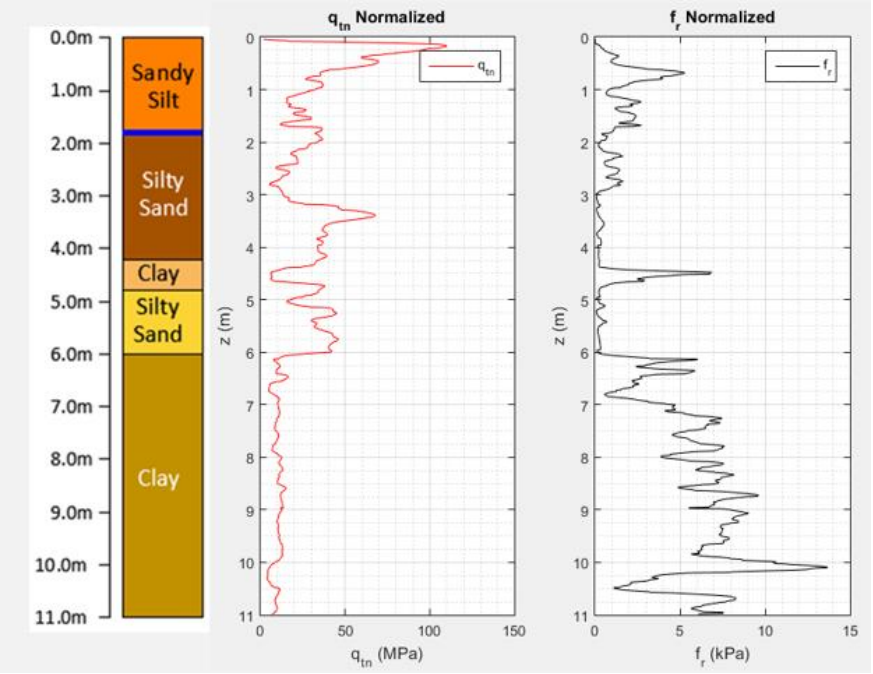

Figure 3-4 Normalized cone tip resistance and normalized cone sleeve resistance obtained by processing data from Chiaradonna et al. (2018)

First, from the data that comes from Chiaradonna et al. (2018) research, the value of clean sand is estimated according to the methodologies proposed by Moss, R. E. S., et al. (2006), Robertson (2010) and Boulanger, R. W. and Idriss, I. M. (2015), as it is shown in the Figure 3-5, Figure 3-6 and Figure 3-7 respectively.

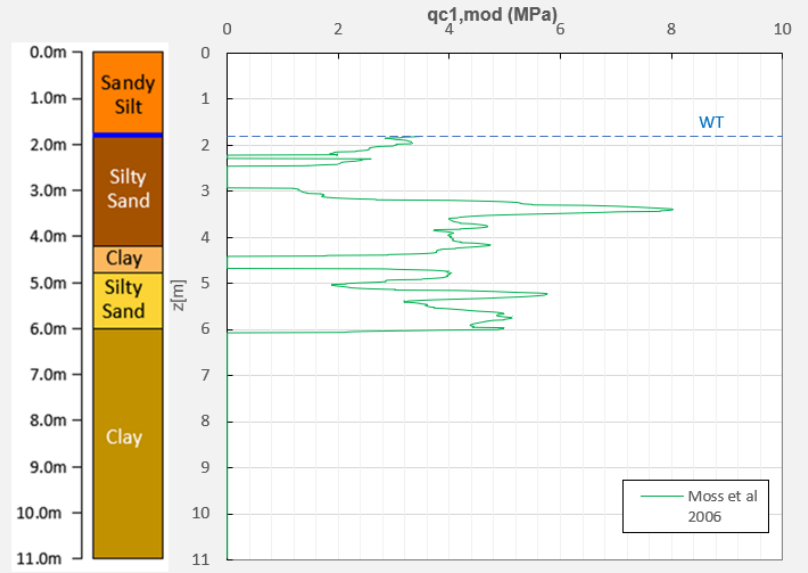

Figure 3-5 Modified normalized CPT tip resistance "clean" sand, Moss, R. E. S., et al. (2006)

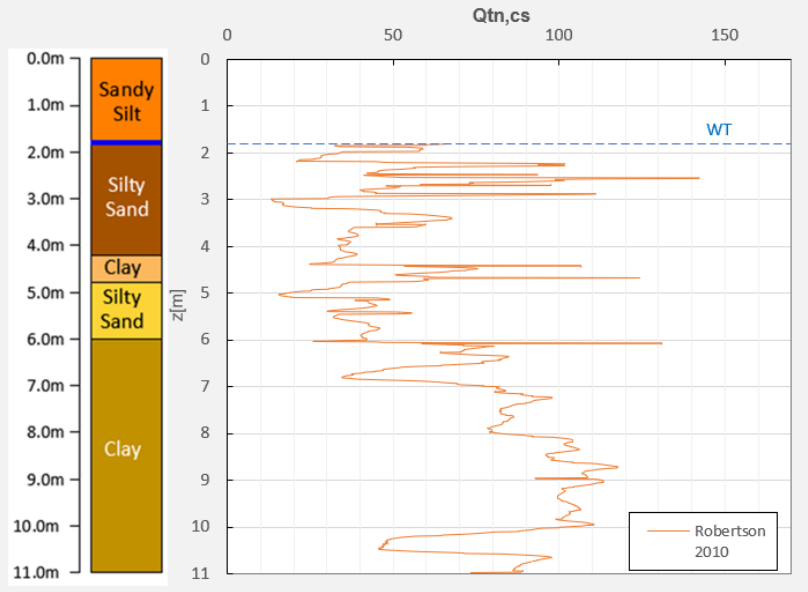

Figure 3-6 Equivalent clean sand penetration resistance, Robertson (2010)

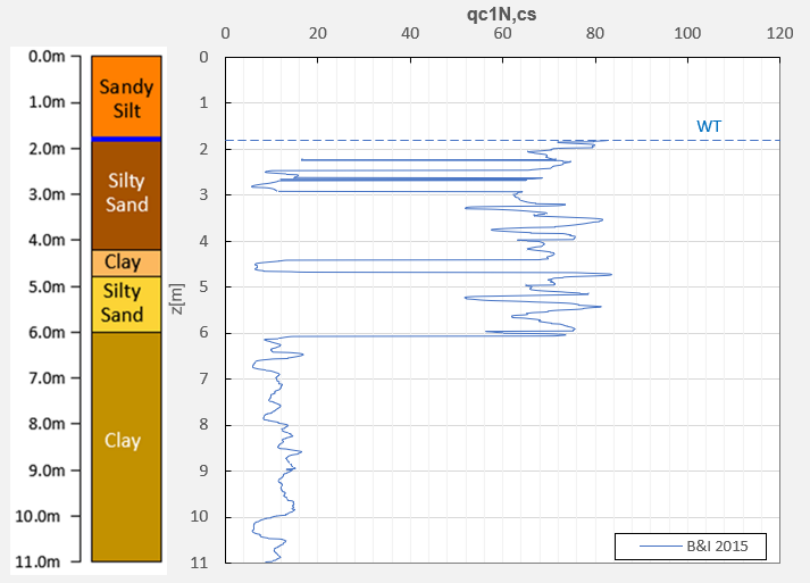

Figure 3-7 Equivalent clean sand penetration resistance, Boulanger, R. W. and Idriss, I. M. (2015)

For the estimation of the stress reduction coefficient r_d it should be clarified that each method used applies a different approach for its calculation. For instance, Robertson 2010 uses the Liao, S. S. C. and Whitman, R. V. (1986) methodology and Boulanger, R. W. and Idriss, I. M. (2015) the r_d extending form work of Golesorkhi, R. (1989), both of those methodologies are based on the variation of stresses due to the depth, however, R. W. and Idriss, I. M. (2015) includes the effect of the *Mw* earthquake moment magnitude . On the other hand, Moss, R. E. S., et al. (2006) applies the Cetin, K. O. (2000) proposal, who incorporates in his method not only the effects of the depth but also the contribution of the a_{max} peak ground surface acceleration and the *Mw* earthquake moment magnitude. In the Figure 3-8 is possible to distinguish the values of r_d based on the already mentioned methodologies.

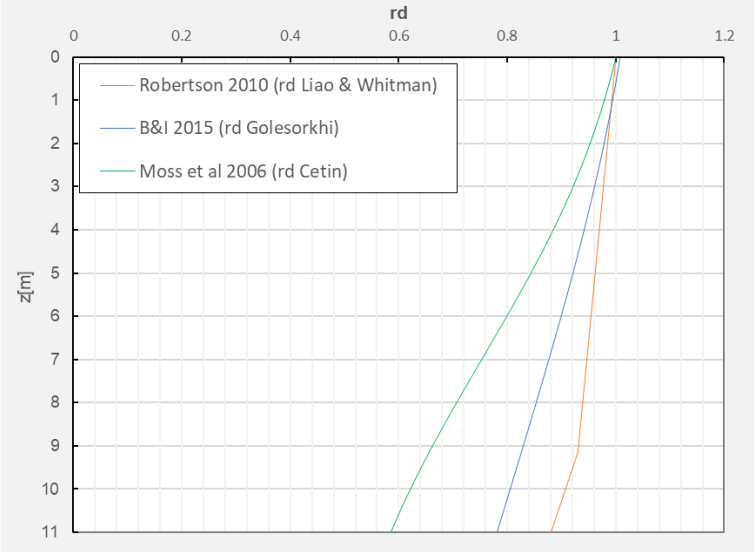

Figure 3-8 Stress Reduction Coefficient r_d

The CPT analysis, which is shown from the Figure 3-9 to Figure 3-12, that was used to estimate CSR cyclic stress ratio, CRR cyclic resistance ratio, Factor of Safety FS and the probability of liquefaction.

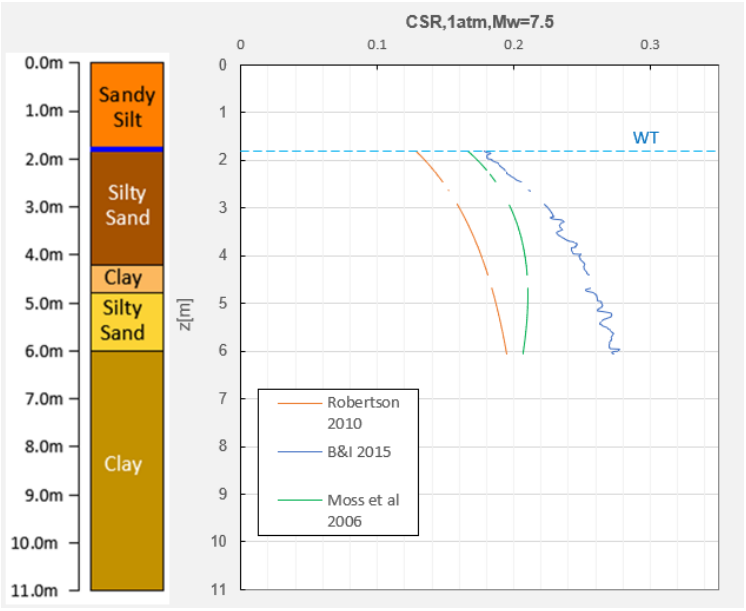

Figure 3-9 CSR Cyclic Stress Ratio assessment results, 1=1tm and Mw=7.5

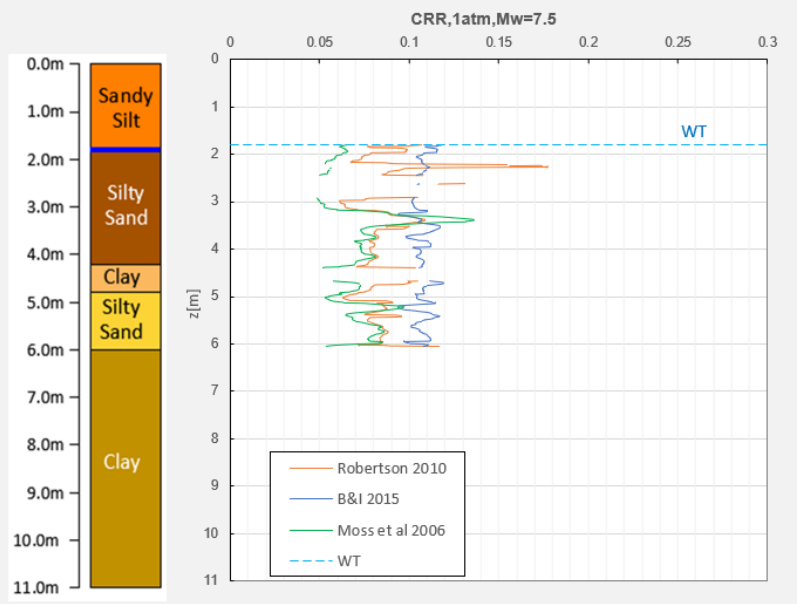

Figure 3-10 CRR Cyclic Resistance Ratio assessment results normalized to 1=1tm and Mw=7.5

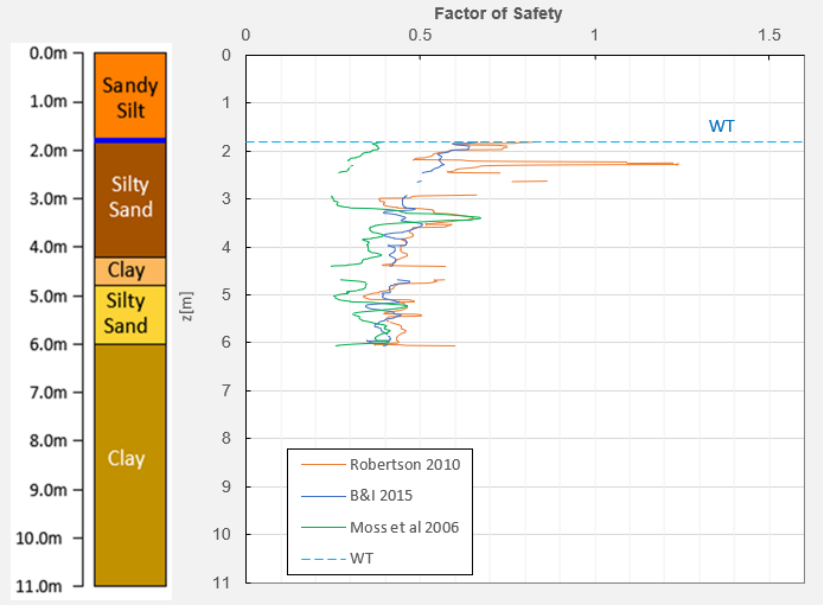

Figure 3-11 Computed factor of Safety for CPT based used methods for assessing liquefaction

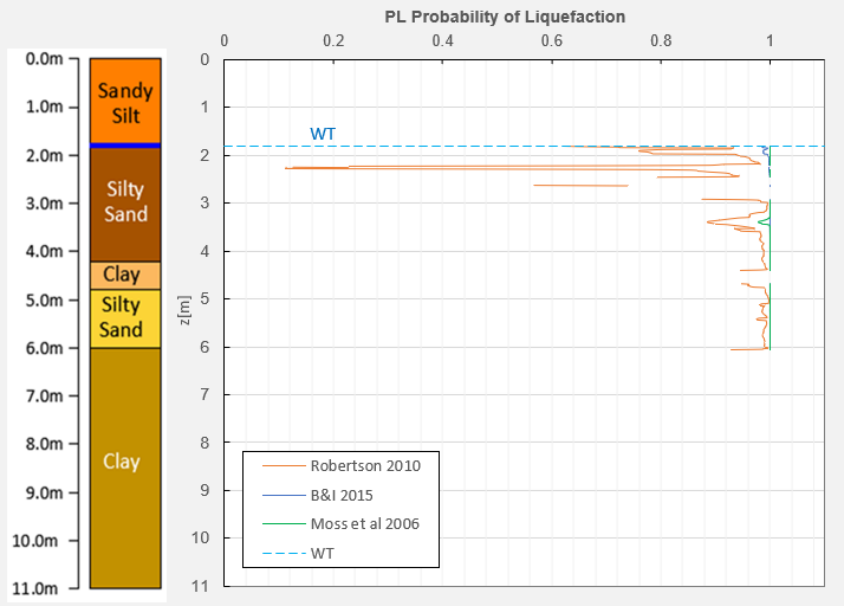

Figure 3-12 Probability of liquefaction CPT based used methods for assessing liquefaction

According to the estimated values of CSR, Figure 3-9, it is evidence that the proposal of Boulanger, R. W. and Idriss, I. M. (2015) provides the largest. On the other hand, Robertson (2010) gives the lowest values up to 7.5m depth where Moss, R. E. S., et al. (2006) becomes the lowest.

As far as CRR values are concerned, Robertson (2010) provides the largest values followed by Boulanger, R. W. and Idriss, I.M. (2015) and then Moss, R. E. S., et al. (2006) that projects the lowest values. Additionally, the three methodological proposals maintain the same tendency regarding the distribution of results as is illustrated in the Figure 3-10.

By observing the results of calculations, from this single application, it is noted that the CPT method of Moss, R. E. S., et al. (2006) for evaluating the liquefaction potential is the most conservative, providing the lowest factors of safety, Figure 3-11. As a consequence of this, Moss, R. E. S., et al. (2006) gives the largest liquefaction probability values unlike Robertson (2010) which provides the highest factors of safety and therefore the lowest liquefaction probabilities, Figure 3-12. The difference can be attributed to the equivalent clean-sand correction factor, Kc, and the magnitude scaling factor, MSF among another factors.

➢ CRR determined from the State Parameter approach

An additional analysis is performed, where the CRR values obtained through the simplified methods are compared with the CRR that are determined from the State Parameter ψ computed according to Jefferies, M.G. & Been, K. (2015). In the Figure 3-13 the comparison of CRR is observed, while in Figure 3-14 the factors of safety are illustrated. From these analyzes and comparing the results obtained, CRR values that are calculated from the state parameter are lower than those that result from the simplified methods as well as factors of safety.

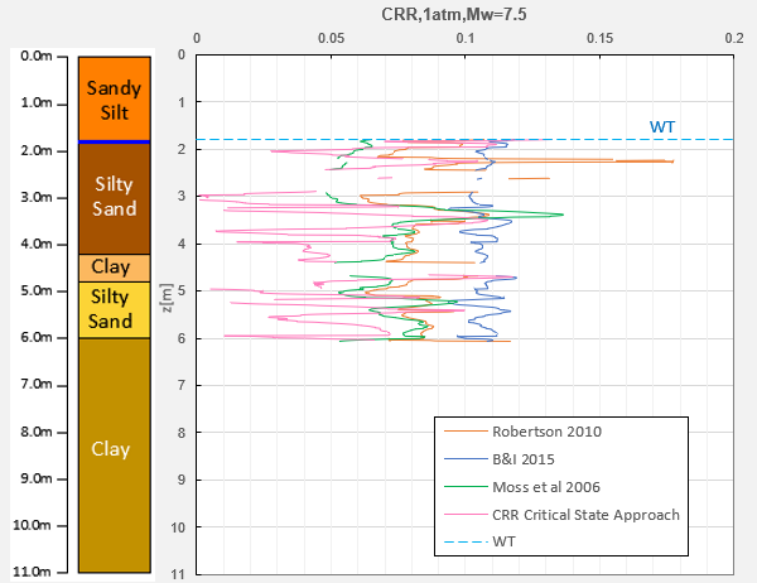

Figure 3-13 CRR Cyclic Resistance Ratio based used methods and CRR from State Parameter suggested by Jefferies, M.G. & Been, K. (2015)

Figure 3-14 Computed FS from CPT based methods used compared to FS for CRR from State Parameter suggested by Jefferies, M.G. & Been, K. (2015)

3.1.2 SPT based methods

Regarding the evaluation of liquefaction using SPT based methods, the methodologies suggested by NCEER / NSF, Youd et al. (2001) and Cetin, K. O. et al. (2004). Because there is no present SPT test data for the study area (until now), it is proceeded to estimate the number blows for 60% energy N_{60}, using the correlation proposed by Robertson (2012), showing in the following, that values provide a reasonable estimate of SPT N_{60} values from CPT data.

$$\frac{(q_t/P_a)}{N_{60}} = 10^{(1.1268-0.2817*FC)}$$

The results obtained from the previous mathematical expression are recorded in the Figure 3-15, together with the content of fine FC, which were estimated following the proposal of Robertson (2010) from the CPT test as well, for which is taken into account Soil Behavior Type Index, I_C.

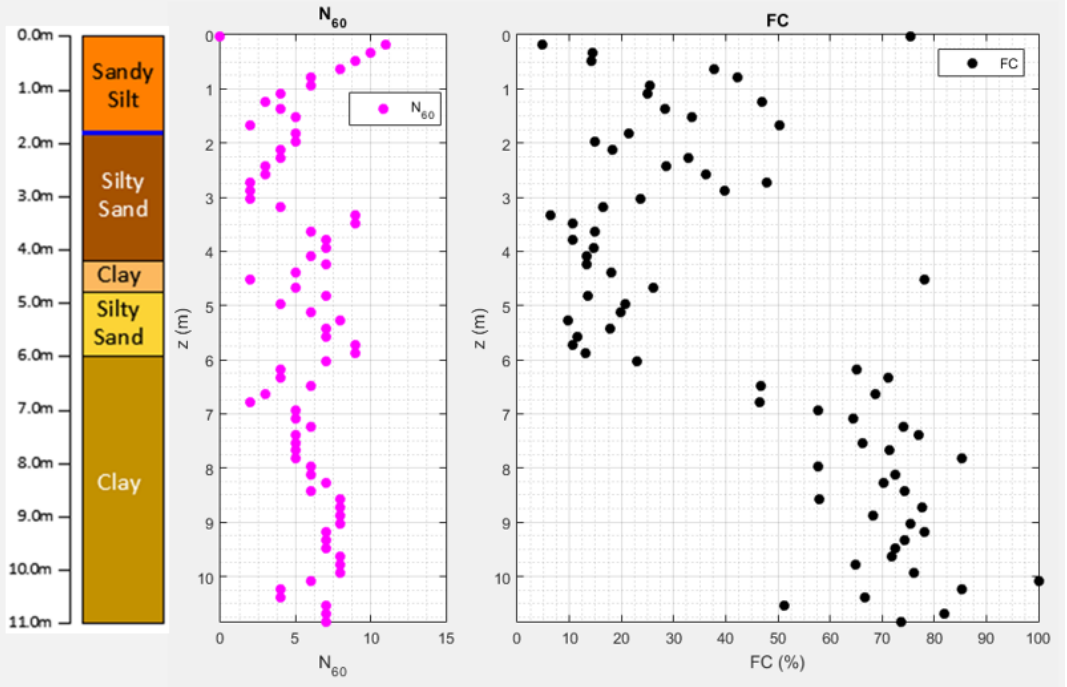

Figure 3-15 SPT estimates values N_{60} and fines content FC

Subsequently, the demand and liquefaction resistance and the factor of safety were calculated from the SPT data, as described below.

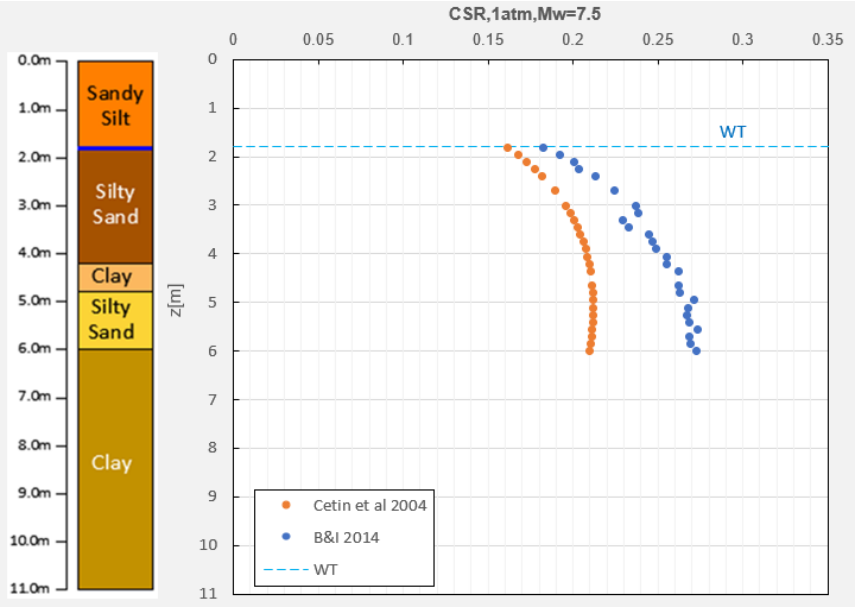

Figure 3-16 SPT based methods, Cyclic Stress Ratio assessment results, 1=1tm and Mw=7.5

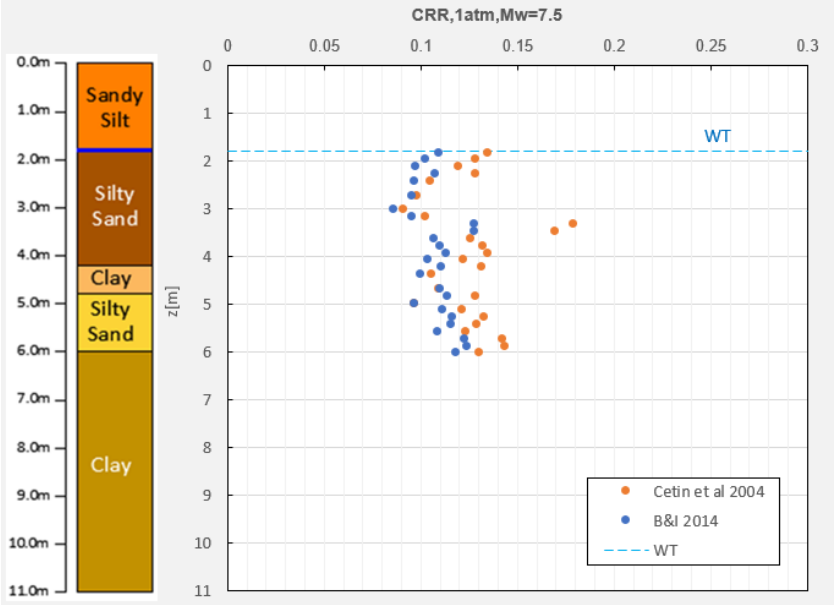

Figure 3-17 SPT based methods, Cyclic Resistance Ratio assessment results normalized to 1=1tm and Mw=7.5

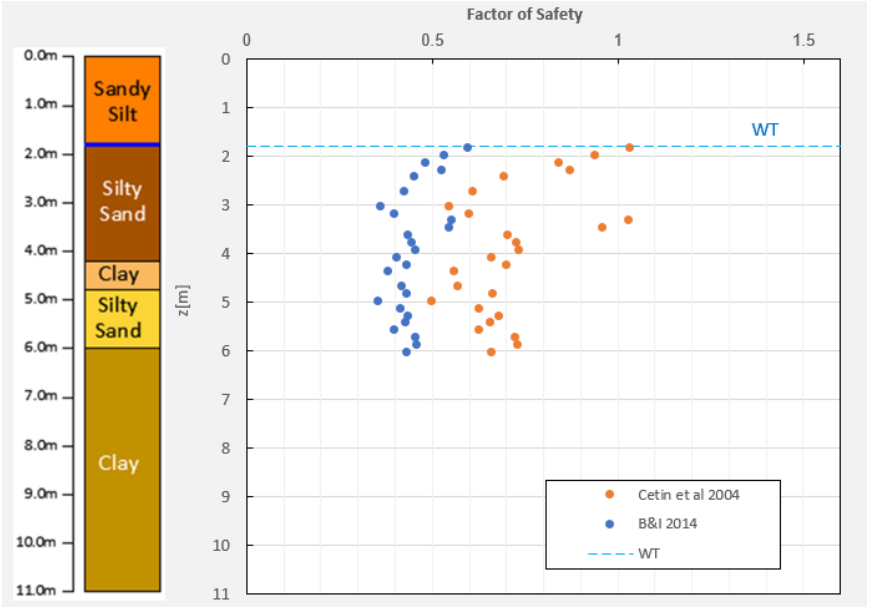

Figure 3-18 SPT based methods, Computed factor of Safety for SPT based used methods for assessing liquefaction

The previous results show that Cetin, K. O. et al. (2004) provides the lower values of CSR Idriss, I. M. and Boulanger, R. W. (2014), Figure 3-16, On the other hand, the two methodologies yield very similar values of CRR, Figure 3-17. Therefore, the estimated factors of safety are higher according to Cetin, K. O. et al. (2004) approach compared with those calculated with Idriss, I. M. and Boulanger, R. W. (2014), Figure 3-18.

3.1.3 Vs based methods

On the other hand, to evaluate liquefaction by means of Vs based methods, as inputs were used the results of the field test, given in detail by Chiaradonna et al. (2018). In that research, the shear wave velocity profile and the soil layering, in larger depth range (from 0m to 230m, the depth where was assumed bedrock), were defined from the interpretation all the available information. In addition, for the shallow layering and the shear wave velocity profile they were identified from a borehole and a Cross-Hole test carried out at the site, Figure 3-19.

The geology of the study area, according to the exploration of the subsoil and secondary sources, show that the soil column consists of a sequence of silty-clay and sandy soil deposits.

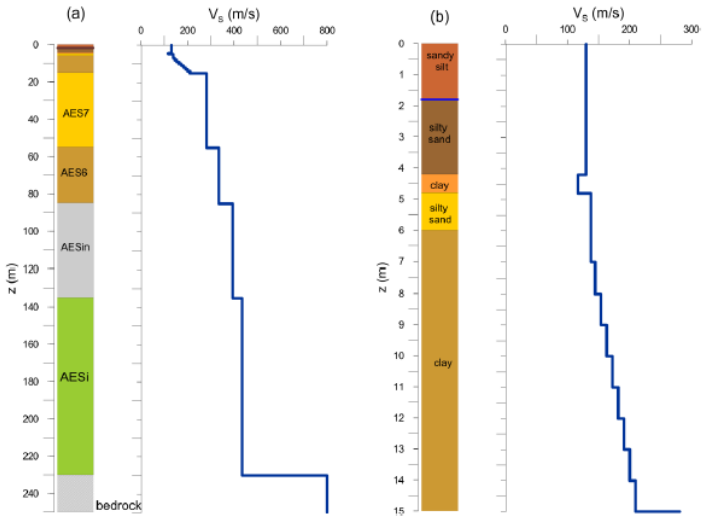

Figure 3-19 Shear wave velocity profile used for Pieve di Cento site. (a): in larger depth range, (b): in smaller depth range, Chiaradonna et al., (2018)

In the same way as in the previous cases, CSR cyclic stress ratio, CRR cyclic resistance ratio and Factor of Safety FS were estimated following the simplified methodologies of NCEER / NSF, Youd

et al. (2001) and Kayen, R., et al. (2013), these results are shown from the Figure 3-20 to the Figure 3-22.

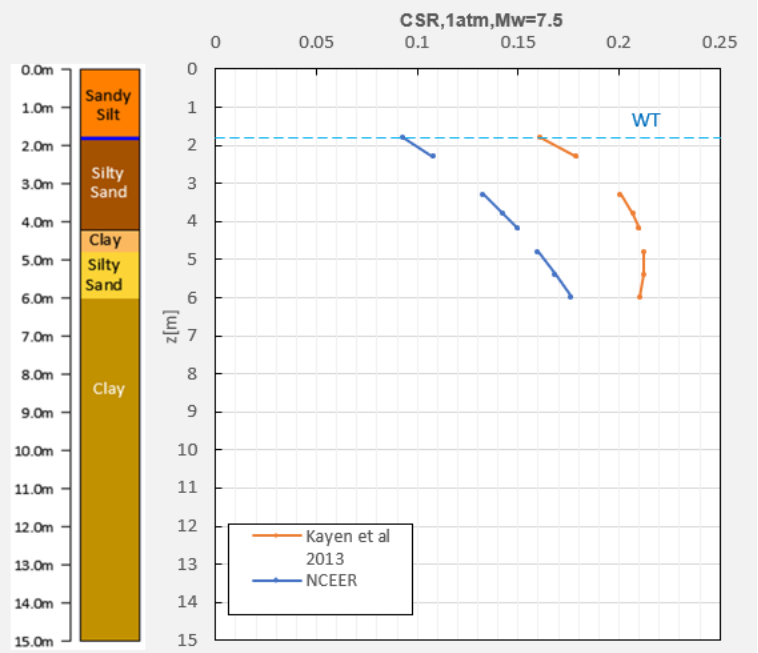

Figure 3-20 Vs based methods, Cyclic Stress Ratio assessment results, 1=1tm and Mw=7.5

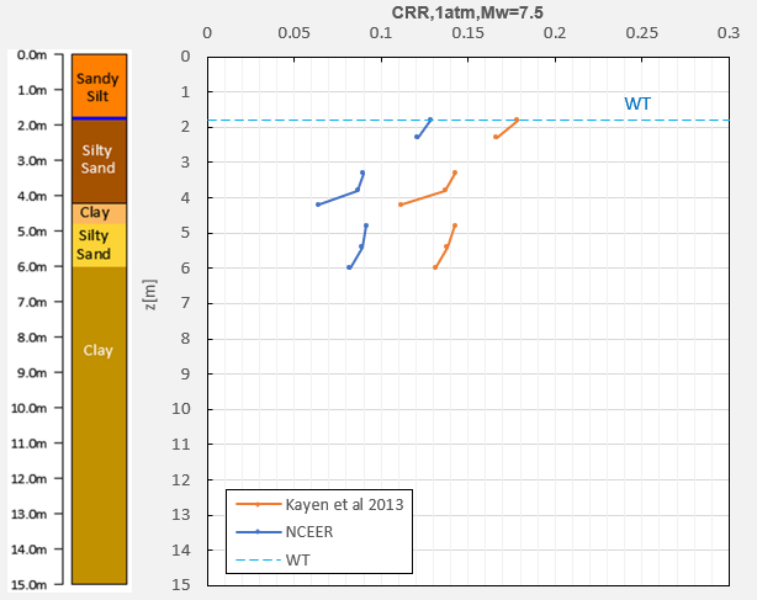

Figure 3-21 Vs based methods, Cyclic Resistance Ratio assessment results normalized to 1 atm and Mw=7.5

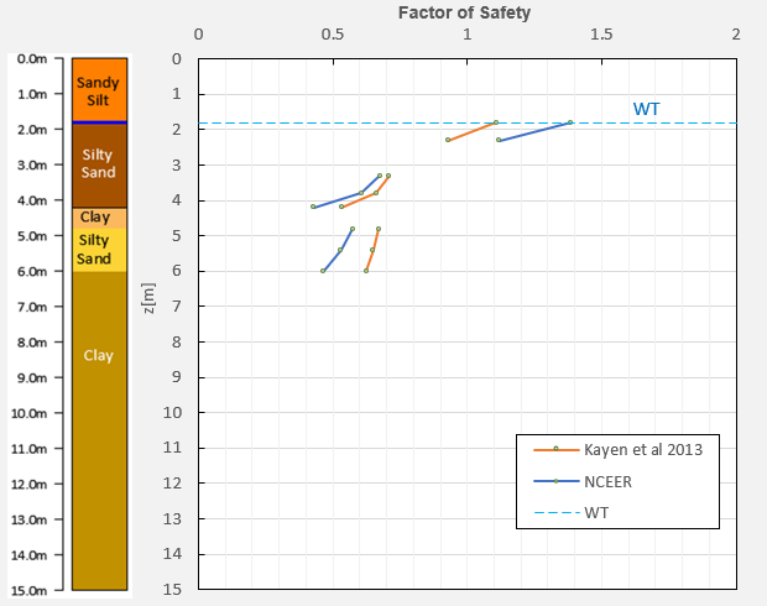

Figure 3-22 Vs based methods, Computed factor of Safety for Vs based used methods for assessing liquefaction

Regarding the results of the Cyclic Stress Ratio CSR, Figure 3-20, it is evident that Kayen, R., et al. (2013) provides higher values up to approximately 6m, after that depth NCEER / NSF, Youd et al. (2001) becomes the one that shows the largest values, following a growing trend. Concerning about CRR values, the two methodologies show the same trend, however, Kayen, R., et al. (2013) gives values around twice as compared to NCEER / NSF, Youd et al. (2001), Figure 3-21.

The factors of safety estimated using the two methodologies differ quite as depth increases, Figure 3-22. The Kayen, R., et al. (2013) approach provides the greatest factors of safety, moreover, it can be notice that these values increase dramatically after approximately 7m depth.

CHAPTER 4 INFLUENCE OF CSR OBTAINED FROM LOCAL RESPONSE ANALYSIS

This chapter shows the application of the simplified methods to calculate liquefaction that have been previously explained, comparing between the potential of liquefaction results that derive from CSR values computed for each method and the potential of liquefaction results that descend from CSR values subtracted after local response analysis.

Therefore, with the aim of establishing relationships and differences between methods based on CSR, it proceeded as follows; first, a local response analysis was performed using the STRATA (Software, version 0.5.9), in order to establish the Peak Ground Acceleration PGA, a_{max}, of the investigated area and mainly to define the Stress Reduction Coefficient rd, to then estimate the reference CSR value to compare the results obtained using the different methods based on SPT, CPT and Vs.

4.1 Local response analysis for computing Stress Reduction Coefficient rd and PGA

The local response analysis was performed using information taken from laboratory test done by Tonni et al., (2015). In Figure 4-1 and Figure 4-2, is observing the dynamic behavior in 1D of the two main soil units defined Sand and Clay. Figure 4-1 presents the shear modulus reduction and damping curves for the unit of soil defined as Sand, as well the Figure 4 2 shows the shear modulus reduction and damping curves of the Clay.

The local response analysis was executed following the EQL Equivalent Linear methodology through the software STRATA that allows defining the dynamic behavior in 1D of the two main soil units defined as Sand and Clay.

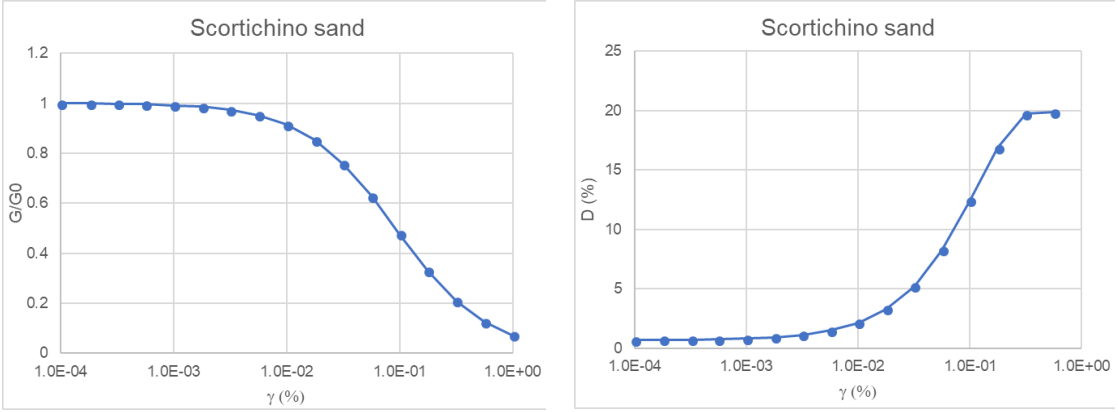

(a) **(b)**

Figure 4-1 (a) shear modulus reduction and (b) damping curves Sand Scortichino, source; Tonni et al., (2015).

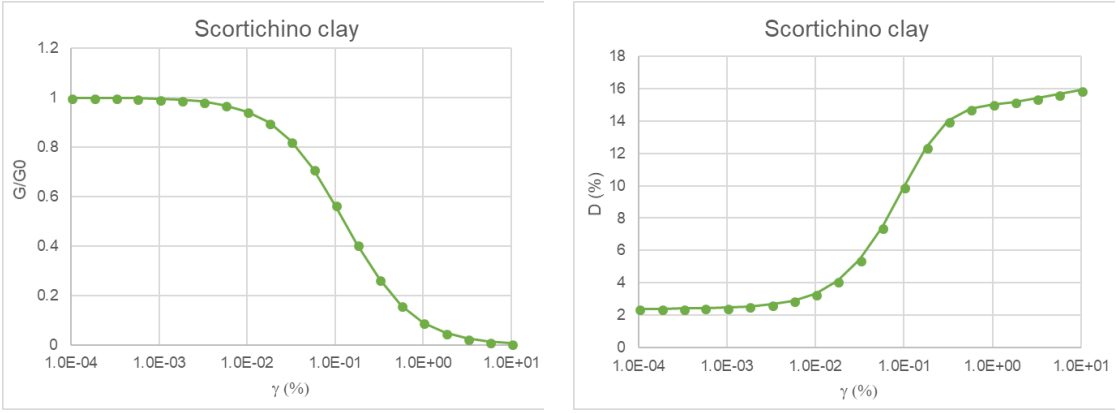

(a) **(b)**

Figure 4-2 (a) shear modulus reduction and (b) damping curves Clay Scortichino, source; Tonni et al., (2015).

Due to the considerable distance of the closest stations with respect to the epicenter in the 2012 earthquake, Chiaradonna et al. (2018). had to deconvolve the EW component of the acceleration record at MRN station to the bedrock; Subsequently, the deconvolved outcrop motion was scaled down to account for the epicentral distance of the test site. Finally, the deconvoluted movement spread from the bedrock (230 m depth) up to 15m depth. As a result of that, were obtained the obtained ground motion at 15 m in terms of acceleration time history, Figure 4-5, and the correspondent acceleration response spectrum, Figure 4-4.

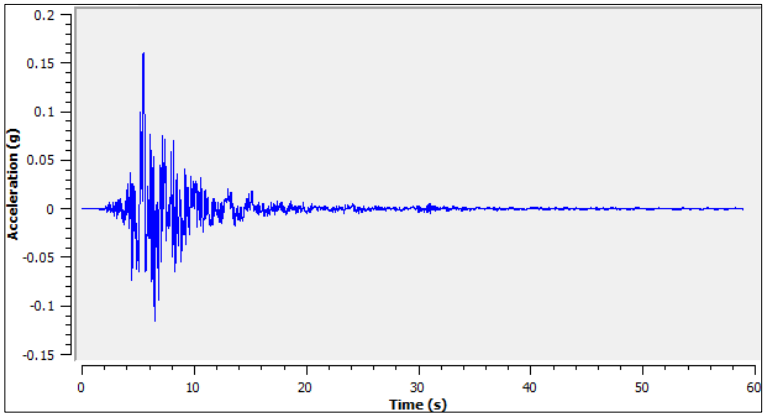

Figure 4-3 Deconvolved input motion at 15 m

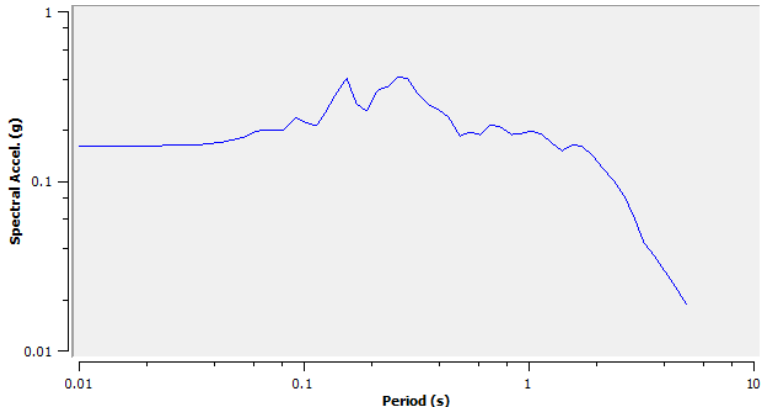

Figure 4-4 Acceleration response spectrum

Accordingly, from the local site response analysis were obtained the PGA in Figure 4-5 and the Stress Reduction Coefficient rd in Figure 4-6. Those inputs allow calculating CSR that is used as a reference to compare the estimated results from the simplified methods for liquefaction potential assessment. Consequently, in the Figure 4-5 is obtained a_{max}=0.34g at surface, as well as from the Figure 4-6 Stress Reduction Coefficient r_d data is extracted.

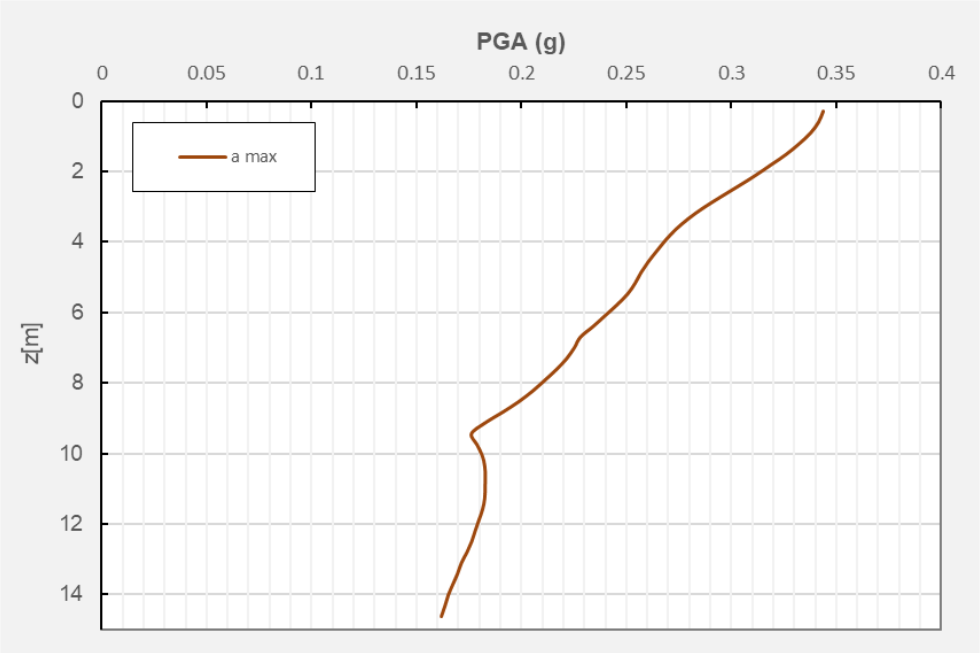

Figure 4-5 Peak Ground Acceleration profile from local response analysis, a_{max}=0.34g at surface

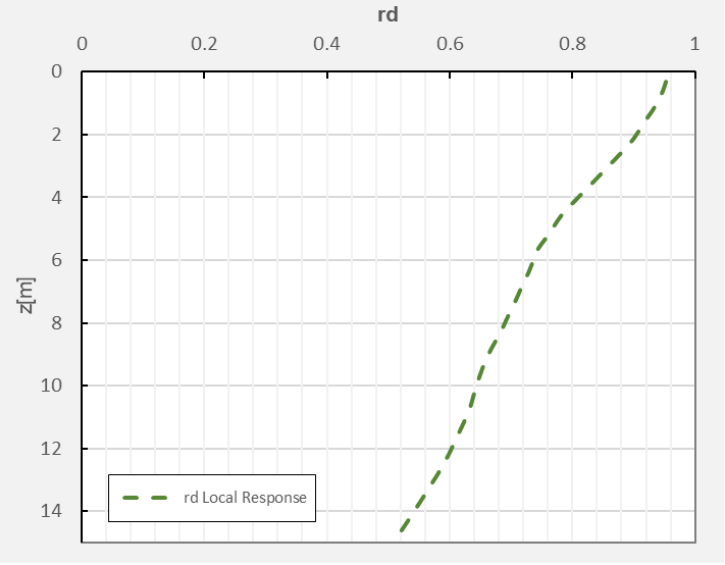

Figure 4-6 Stress Reduction Coefficient r_d, from local response analysis

4.2 Comparison; CPT based methods

First, a comparison is made between the Stress Reduction Coefficient r_d values obtained by means of the simplified methods with respect to the results of the local response analysis, as can be seen in the Figure 4-7. According to the trend described by the curves, Moss, R. E. S., et al. (2006) presents a better correlation with the local response analysis because its results are somehow of the same order.

Moreover, the results obtained by the method of Robertson (2010) who applies the formula suggested by Liao, S. S. C. and Whitman, R. V. (1986), defers with respect to the results coming from the analysis of local response. This is mainly due to the fact that this formula is one of the first empirical approaches and only considers the effect of depth. On the other hand, the formula used by Boulanger, R. W. and Idriss, I. M. (2015) considers the effect of depth and additionally the contribution of the earthquake moment magnitude, in some way differs with respect to the analysis of local response results.

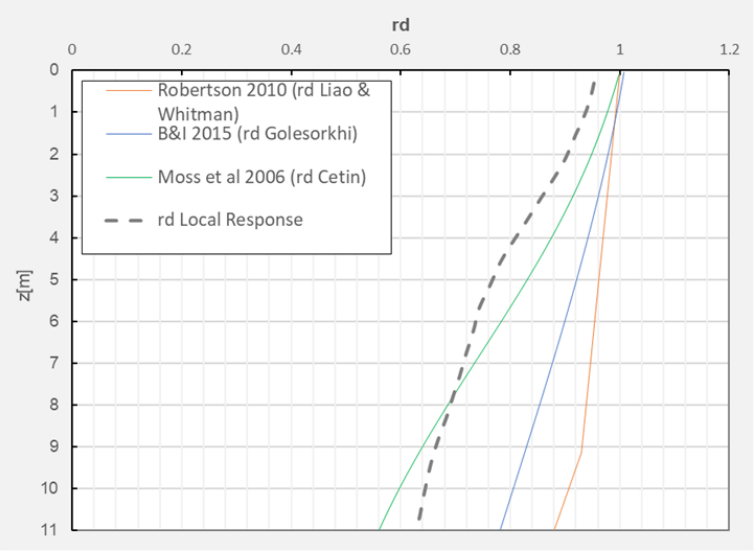

Figure 4-7 Stress Reduction Coefficient r_d comparison

The Figure 4-8 shows the comparison of CSR (projected to M=7.5) between the already explained CPT based methods. Note that the 'shape' 'of the curve of the results computed from local response coincides quite well with the methods simplified specifically with the curve of the results obtained from the method suggested by Boulanger, R. W. and Idriss, I. M. (2015) and Moss et al. (2006).

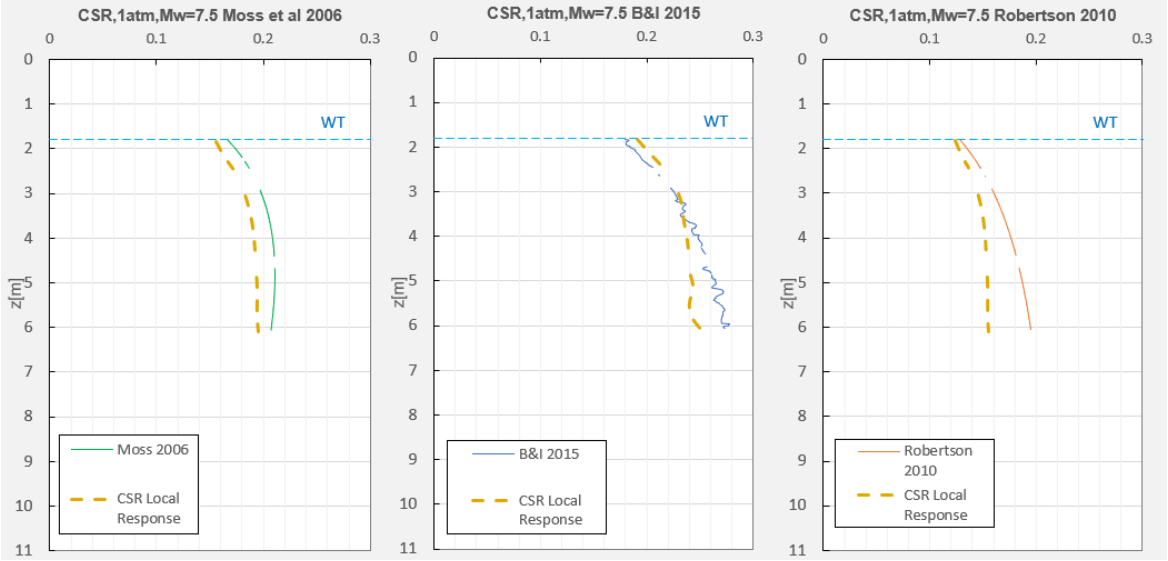

Figure 4-8 CSR from CPT based methods and Local Response

The values for CRR where calculated for the methods of Moss, R. E. S., et al. (2006), Robertson (2010) and R. Boulanger, R. W. and Idriss, I. M. (2015). Based on the results it is notice that Boulanger, R. W. and Idriss, I. M. (2015) shows the greater values of CRR Cyclic Resistance Ratio, while Moss, R. E. S., et al. (2006) gives the lower values. However, and despite of the small differences in the results, the three methods follow the same pattern, Figure 4-9, with a remarkable pick of CRR in the Robertson (2010) results, in about 2.2m depth.

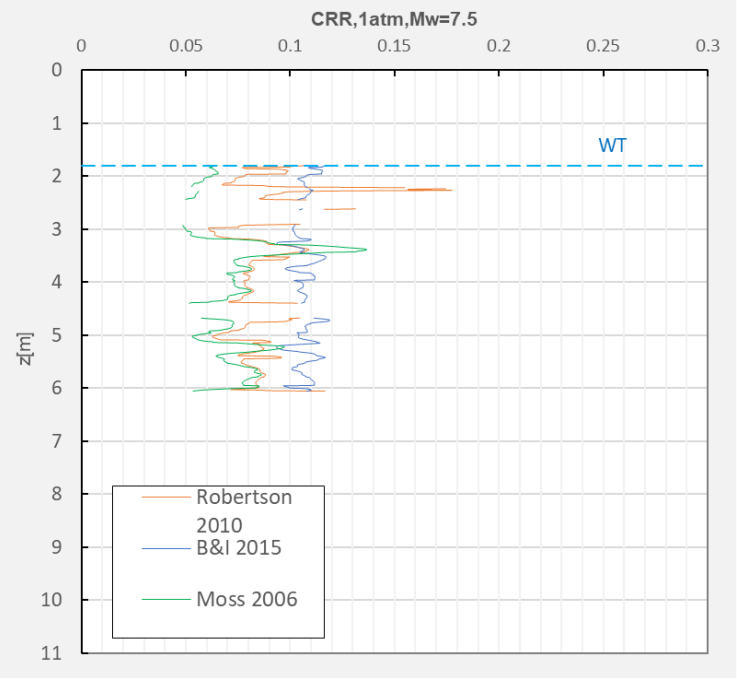

Figure 4-9 CRR from CPT based methods

The factor of safety calculated using the simplified methods, obtaining the CRR data according to each author, the estimated values are shown in the Figure 4-9 , and the CSR according to the local response analysis are recorded in the Figure 4-10. No significant differences are noted between the results of the factor of safety, however, it can be seen that Boulanger, R. W. and Idriss, I. M. (2015) offers slightly higher factors of safety values.

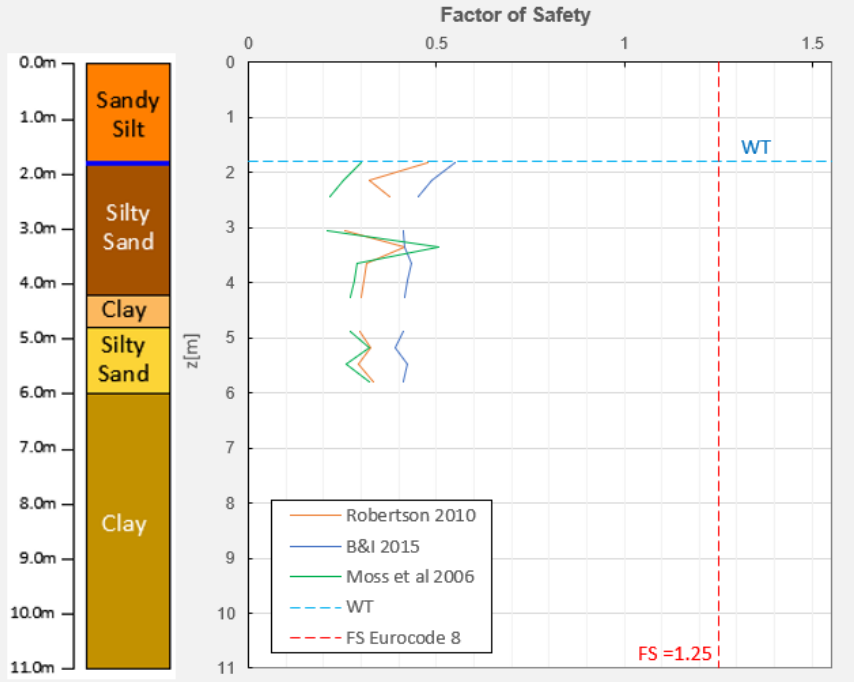

Figure 4-10 CPT based methods Local Response, Computed factor of Safety with CSR from local response

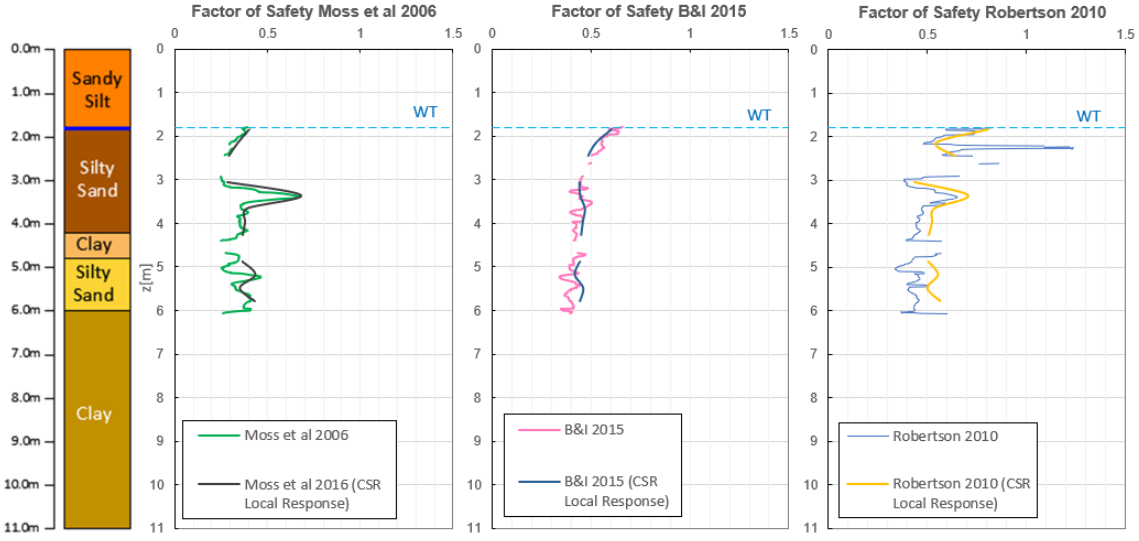

Figure 4-11 CPT - Comparison factor of Safety based (CSR from methods and CSR from local response analysis)

In order to compare the factor of safety of the simplified methods, based on CPT from the CSR estimation in a conventional manner, with respect to the factor of safety that result from the calculation of CSR by means of the local response analysis. The results are plotted in both cases as can be seen in the Figure 4-11. The tendency for slightly lower factors of safety in the case of simplified methods compared with those obtained with the estimated CSR of the local response analysis is clear. This trend is a bit more marked in the case of Robertson (2010). It should be noted that any generalization must be avoided given that only one case study is presented.

➢ lateral displacements and ground settlements

Additionally, lateral displacement and ground settlements were estimated for the approach of liquefaction analysis from CPT test suggested by Robertson (2010) comparing the results of the factor of safety FS obtained by CSR through the method and for the factors of safety FS by means of the CSR provided by the site response analysis. Therefore, following the guidelines of Zhang, P. et al (2002) for lateral displacement and the case of the settlement of the settlement the method suggested by Zhang, G. et al (2014) were calculated as illustrated in Figure 4-12 and in Figure 4-13 respectively.

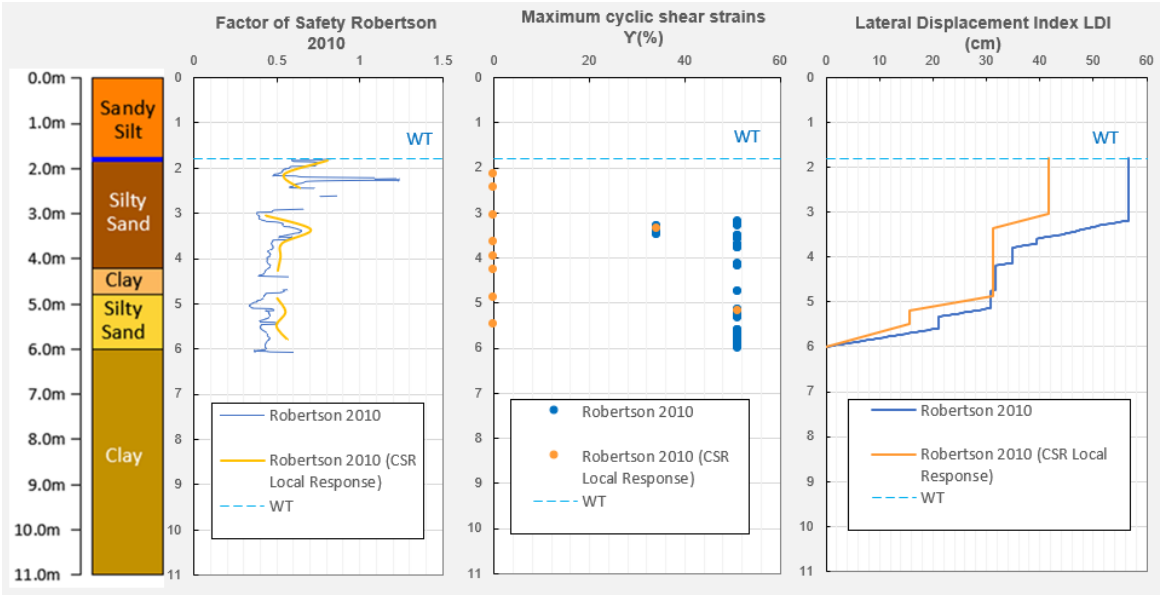

Figure 4-12 Factor of Safety FS, Maximum Cyclic Shear Strain γ_{max} and Lateral Displacement Index LDI, CPT based Robertson (2010) approach

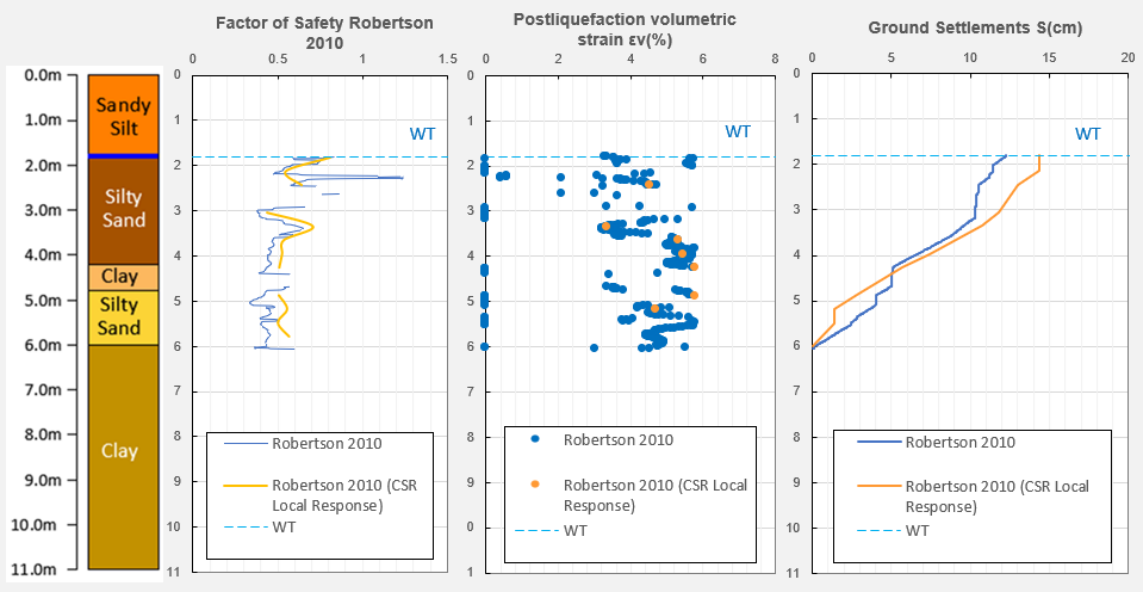

Figure 4-13 Factor of Safety, Postliquefaction Volumetric Strain ε_v and Liquefaction-induced ground settlements $S(cm)$ using CPT based Robertson (2010) approach

From the previous results it is evident that lateral displacements are lower for the factor of safety obtained from CSR site response analysis. On the other hand, the settlements induced by liquefaction are slightly lower in the case of the factor of safety calculated with the CSR obtained from the Robertson (2010) method. Since only one case study was analyzed, this behavior should not be considered general.

4.3 Comparison; SPT based methods

From the results of the local response analysis, CSR was estimated and projected to M=7.5, Figure 4-15,and was compared with the values calculated by the simplified methods of Cetin, K. O. et al. (2004) and Idriss, I. M. and Boulanger, R. W. (2014) in the case of SPT. It is evident that the numbers of CSR from local response have good similarity with those given by Idriss, I. M. and Boulanger, R. W. (2014) and unlike what can be seen from the results of Cetin, K. O. et al. (2004) which are slightly smaller.

Regarding the factors of safety, the CRR data were estimated according to what was proposed by each methodology, that is, the method suggested by Cetin, K. O. et al. (2004) and the one suggested

by Idriss, I. M. and Boulanger, R. W. (2014). The Figure 4-14 illustrates the CRR obtained values from each of methods used.

In addition, the CSR values were estimated from the local response analysis, how is shown in the Figure 4-15, and the factors of safety shown in the Figure 4-16 were obtained. It is clear to that the results of Cetin, K. O. et al. (2004) are slightly greater than Idriss, I. M. and Boulanger, R. W. (2014) results of the factors of safety.

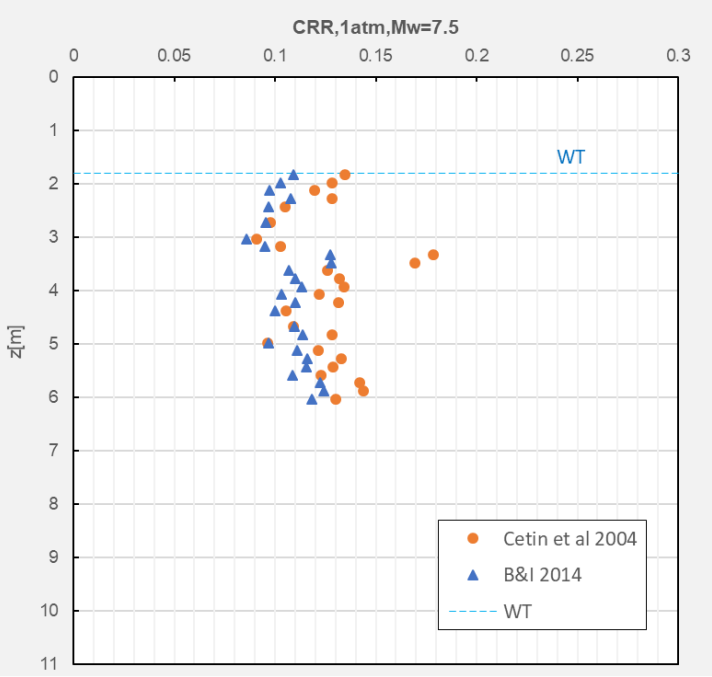

Figure 4-14 CRR from SPT based methods

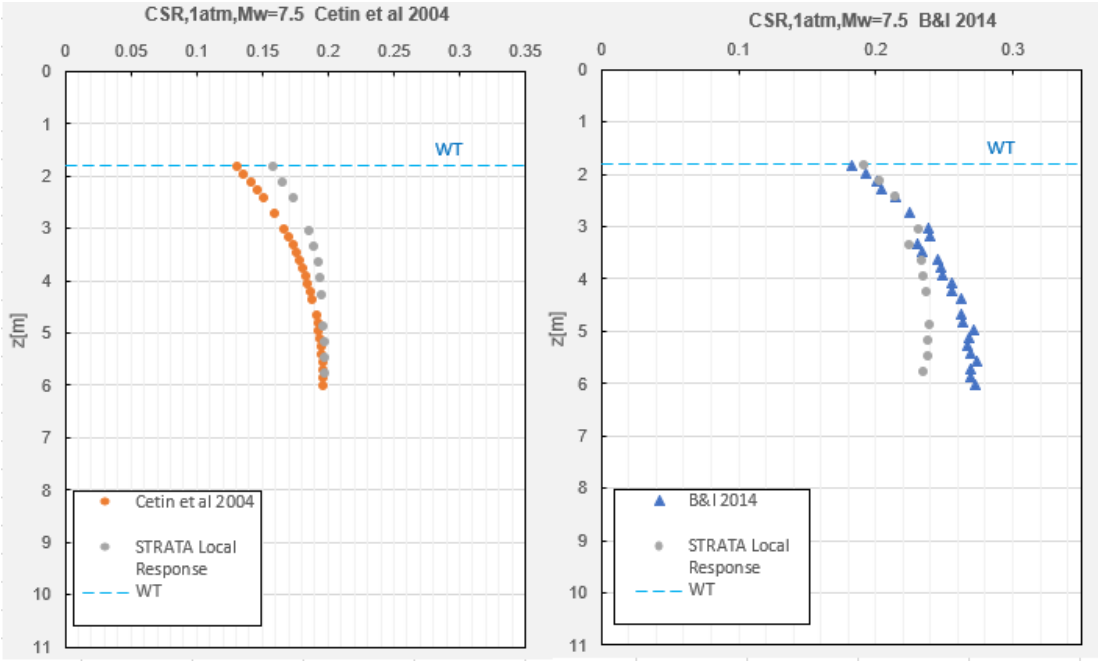

Figure 4-15 CSR from SPT based methods and Local Response

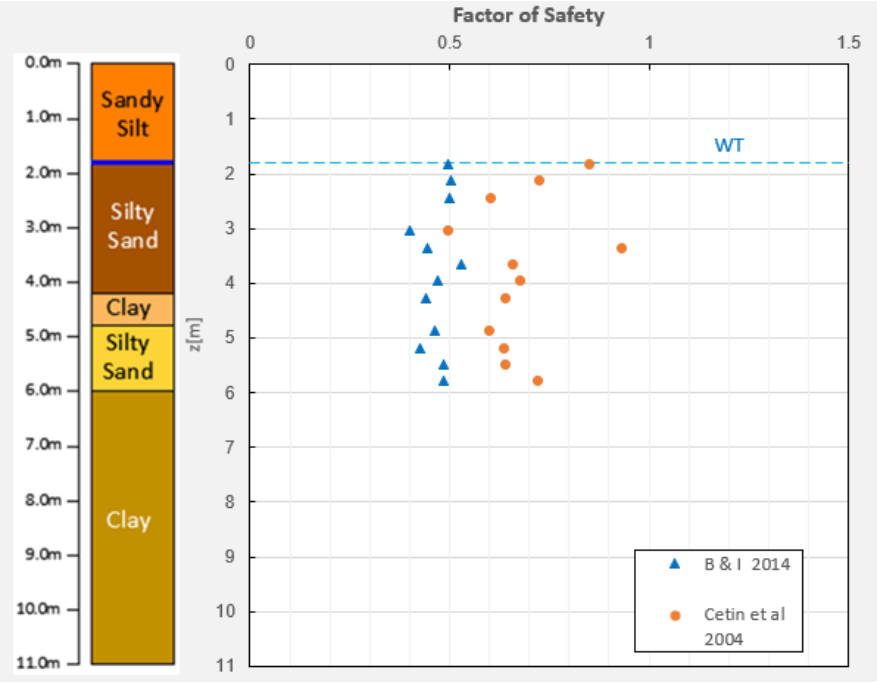

Figure 4-16 SPT based methods Local Response, Computed factor of Safety with CSR from local response

Additionally, a comparison was made between the factor of safety obtained by means of the simplified methods and that obtained through the local response analysis., Figure 4-17. It is noted, of the results obtained that Cetin, K. O. et al. (2004) yields higher factors of safety through calculating CSR in a conventional manner than the results of the factors of safety that are derived from the local response analysis. On the other hand, the factors of safety according to both the methodologies are quite homogeneous and do not show a considerable difference.

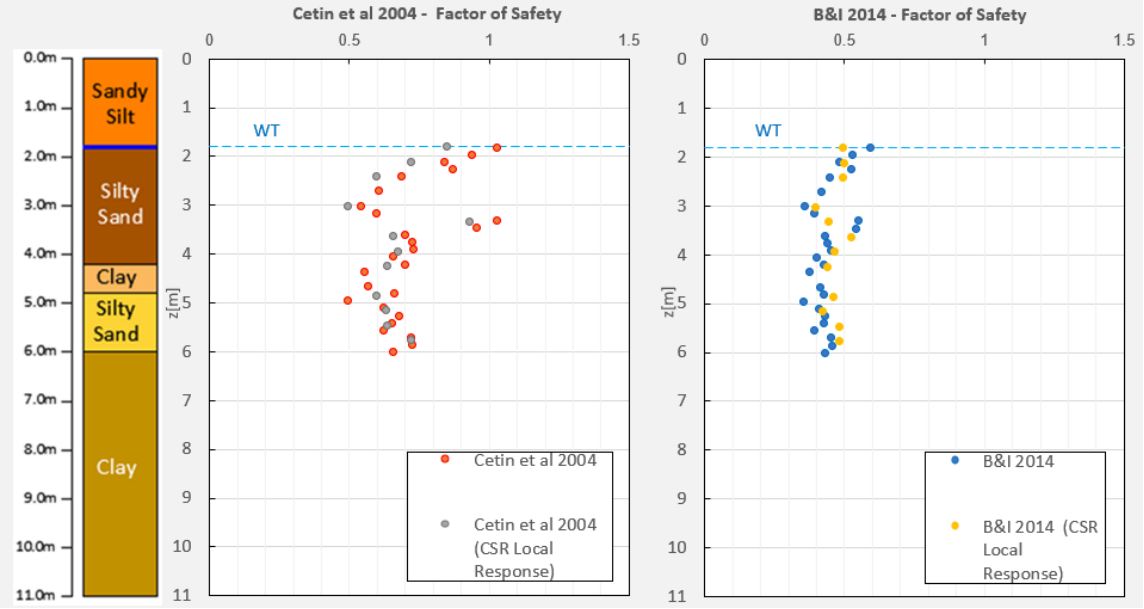

Figure 4-17 SPT - Comparison factor of Safety based (CSR from methods and CSR from local response analysis)

4.4 Comparison; Vs based methods

In this part, CSR computation from Vs results is presented using the simplified methods to evaluate the liquefaction potential and the estimated CSR results from the local response analysis. In the Figure 4-18, a noteworthy difference can be noted between the methodology of Kayen, R., et al. (2013) and the proposal of NCEER / NSF, Youd et al. (2001). NCEER / NSF, Youd et al. (2001) gives larger CSR results comparing to Kayen, R., et al. (2013). Another trend to highlight is that NCEER / NSF, Youd et al. (2001) results follows somehow the same pattern of CSR results that were calculated by local response analysis.

On the other hand, in the Figure 4-19 can be seen the results for the CRR that were estimated from Vs based methods. It can be notice that Kayen, R., et al. (2013) displays higher values for CRR than NCEER / NSF, Youd et al. (2001).

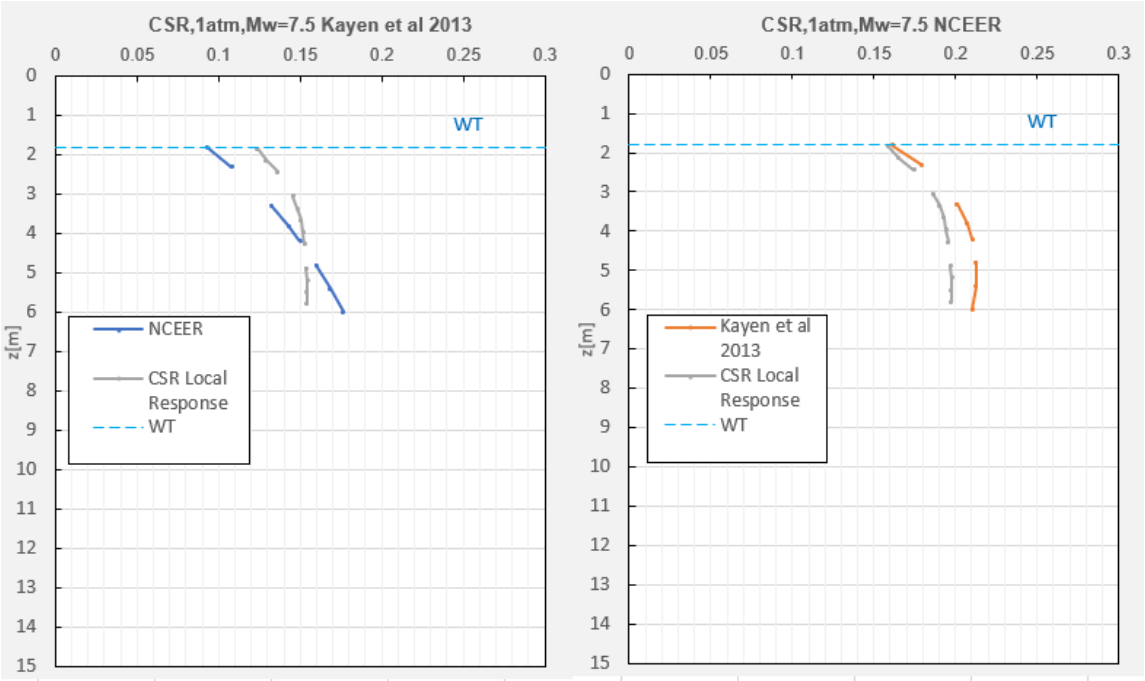

Figure 4-18 CSR from Vs based methods and Local Response

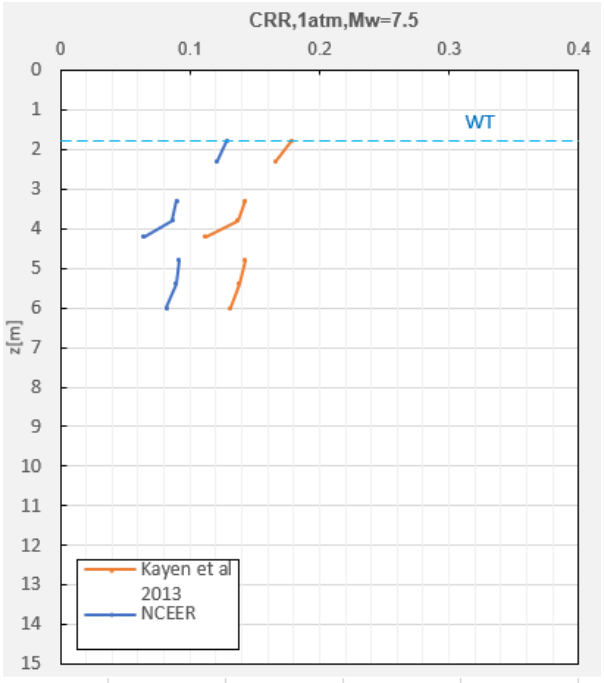

Figure 4-19 CRR from Vs based methods

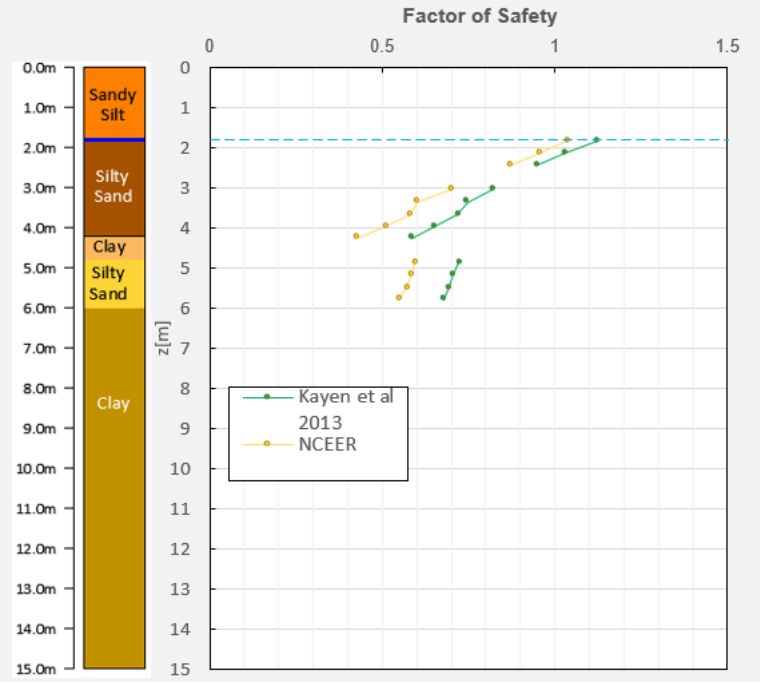

Figure 4-20 Vs based methods Local Response, Computed factor of Safety with CSR from local response

Simultaneously, the factor of safety was calculated for the method of Kayen, R., et al. (2013) as for the proposal of NCEER / NSF, Youd et al. (2001), Figure 4-20. From the results obtained, it is evident that Kayen, R., et al. (2013) offers greater factors of safety compared to NCEER / NSF, Youd et al. (2001) that is more conservative in terms of factors of safety according to the pattern that follows the results.

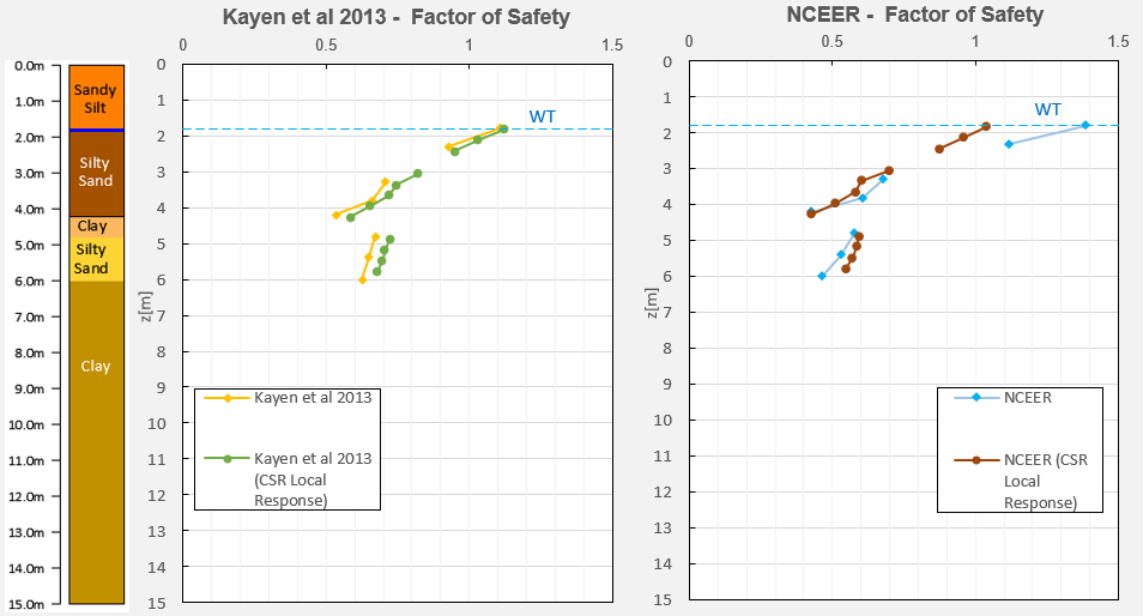

Figure 4-21 Vs - Comparison factor of Safety based (CSR from methods and CSR from local response analysis)

Similarly, factors of safety have been plotted for methods of Kayen, R., et al. (2013) and of NCEER / NSF, Youd et al. (2001), comparing the estimated values through the conventional method and through the local response analysis, Figure 4-21. The proposal of Kayen, R., et al. (2013) results of factors of safety looks quite like the estimated values through local response analysis.

A further comparison is performed between factors of safety estimated using CSR values subtracted after analysis local response, Figure 4-22. Additionally, a contrast with the r_u values from Chiaradonna et al. (2018) research. The excess pore pressure expressed as a pore pressure ratio r_u defined as the ratio of the excess pore pressure to the initial vertical effective stress. The pore-pressure ratio is an index of how close a soil is to liquefaction and can be considered as an indication of liquefaction triggering.

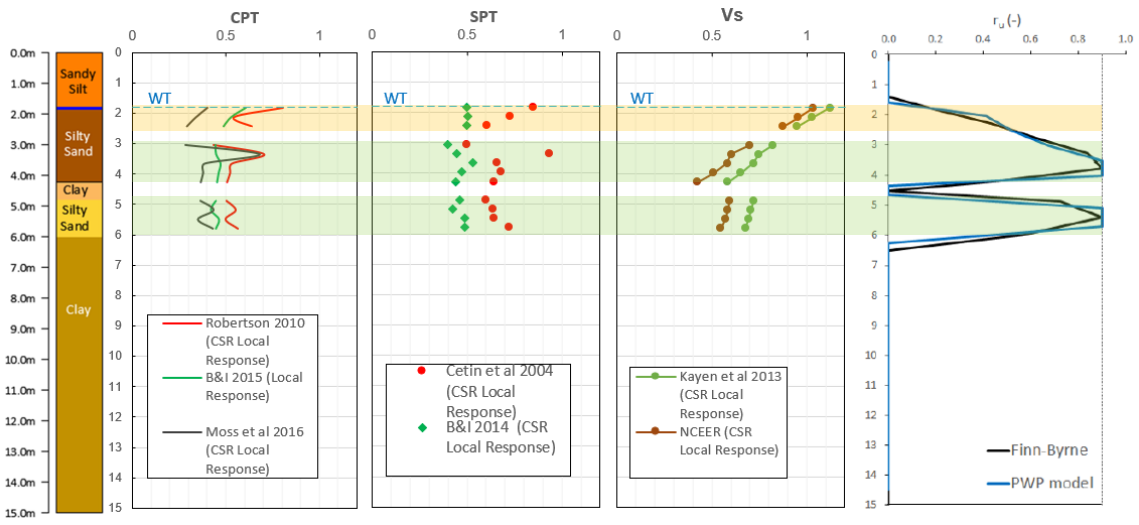

Figure 4-22 CPT, SPT and Vs - Comparison factor of Safety based (CSR from local response analysis) and r_u from Chiaradonna et al. (2018)

In Figure 4-22, factor of safety profiles of seven studies are compared with the excess pore water pressure ratio (r_u=σ'$_{vo}$/Δu) computed through numerical means (Chiaradonna et al., 2018). It could be observed that all of the methods provide reliable evaluations for the depths 3-4 and 5-6 meters (shown by light green rectangles). Yet, there is a common tendency in the simplified to overestimate the severity of the situation where r_u is only around 0.5 (shown with light orange rectangle), most likely because of the unreasonably high seismic demands calculated through coupled means. As the final observation, it seems that for the specific case study approximation, Robertson (2010)-CPT, Cetin, K. O. et al. (2004)-SPT, and Kayen, R., et al. (2013) appear to provide the most suitable comparisons.

CHAPTER 5
CODE - USER MANUAL

5.1 System Overview

The code is designed to be run with MATLAB ©, and allows the civil engineer or user to perform soil liquefaction analysis trough simplified methods based on the fields test for soils investigation; CPT, SPT or Shear Wave velocity, Vs. The organization of the code lets the user enter in data of the fields test from a .txt file and select the base method for accomplish liquefaction analysis. Therefore, users are capable of generating the results of liquefaction analysis, obtain the results in tables and graphically.

5.1.1 Project code and functions

The following is a list of the codes and references given as MATLAB's function that are used during preforming of liquefactions analysis:

- liquefaction.m (main script)
- cpt_boulanger_idriss_2014.m
- cpt_moss_et_al_2006.m
- cpt_robert_2010.m
- spt_boulanger_idriss_2014.m
- spt_cetin_et_al_2004.m
- vs_kayen_et_al_2013.m
- vs_youd_nceer_2001.m

It is important that all files; code functions and field data files be in the same folder "BASE FOLDER".

5.1.2 Organization of the Manual

This manual is divided into 4 major sections, listed and defined below.

General Information: Contains basic information about the code, such as functions performed and a description of the program.
System Summary: This section provides a general overview of the system.
Getting Started: This section provides a general walk-through guide to the system, from beginning to exit.
Reporting: This section describes the various reports that can be generated by the system.

5.1.3 Acronyms and Abbreviations

GUI MATLAB – Graphical User Interface in MATLAB
BASE FOLDER – The main folder that contains all file (MATLAB files and field test files)

5.2 System Configuration

Users are provided with a GUI to interact with the field test data, select the analysis method, and choose liquefaction simplified method, among other actions. That interface allows to complete tasks such as import data, test type selection, inputs modification and resets import data, along with the evaluation of liquefaction.

5.2.1 Data Flows

Users are presented with an interface from which they can select a variety evaluation of liquefaction methods and insert inputs such as earthquake magnitude, peak ground acceleration, and water table level. The GUI then prompts the user to input specific data and import the field test recorded in a .txt or CVS file. The Figure 5-1 gives an overview of the sequence of events that should be done once users starts to perform the liquefaction analysis.

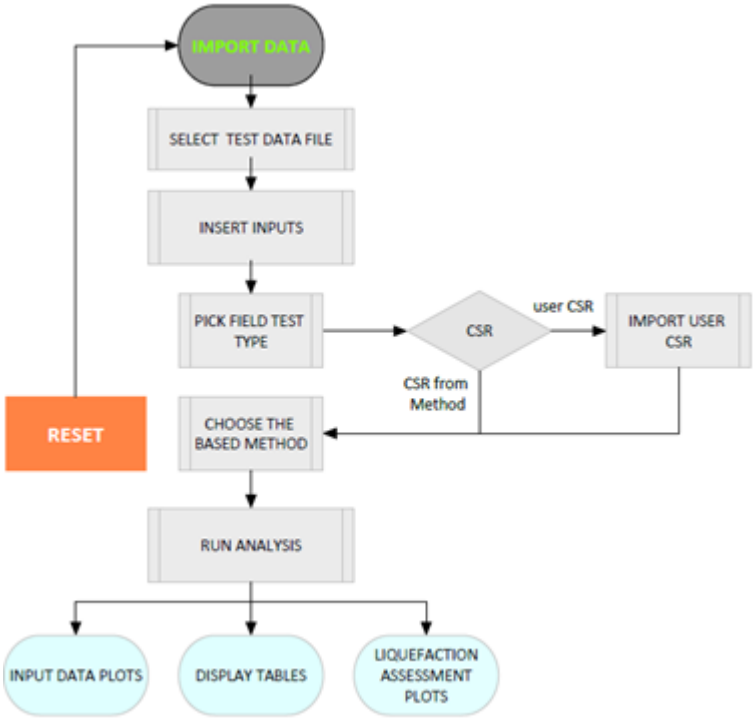

Figure 5-1 Data flows

5.3 System Menu

A set of options are provided for users in order to perform liquefaction analysis based on a list of simplified methods.

5.3.1 Main Interface

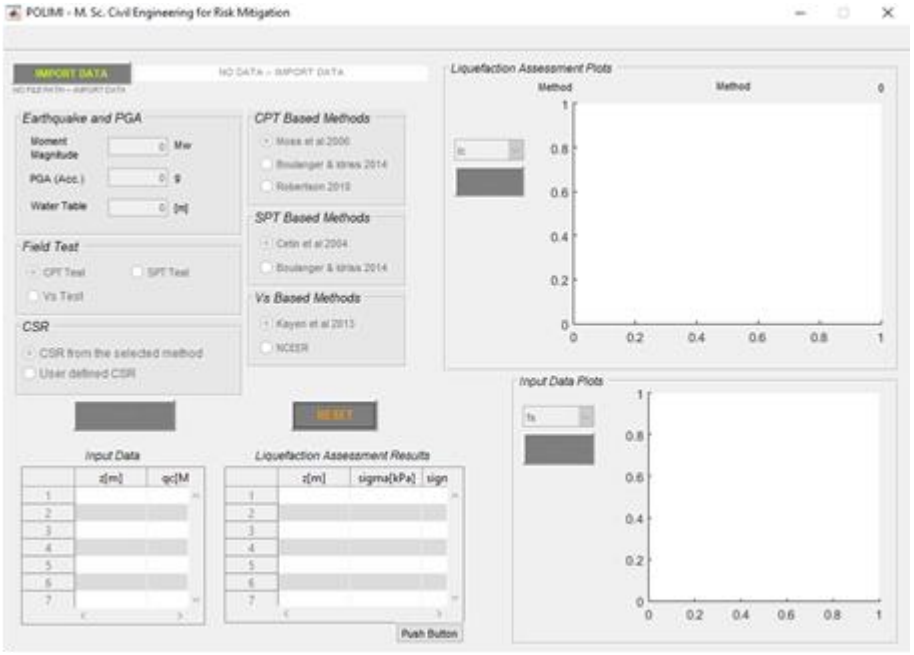

Figure 5-2 Main interface

Upon beginning the code, running the main script call “liquefaction.m”, users are presented with the main interface (pictured above). By clicking the labeled tabs, users can perform the following actions, Figure 5-2:

- Import data
- Input data (Earthquake, water table and PGA)
- Pick Field Test
- Select how compute CSR
- Choose methods (CPT, SPT and Vs)
- RUN
- Input Data Plots
- Liquefaction Assessment Plots
- Input Data (Table)
- Liquefaction Assessment Results (Table)

5.3.2 Import data

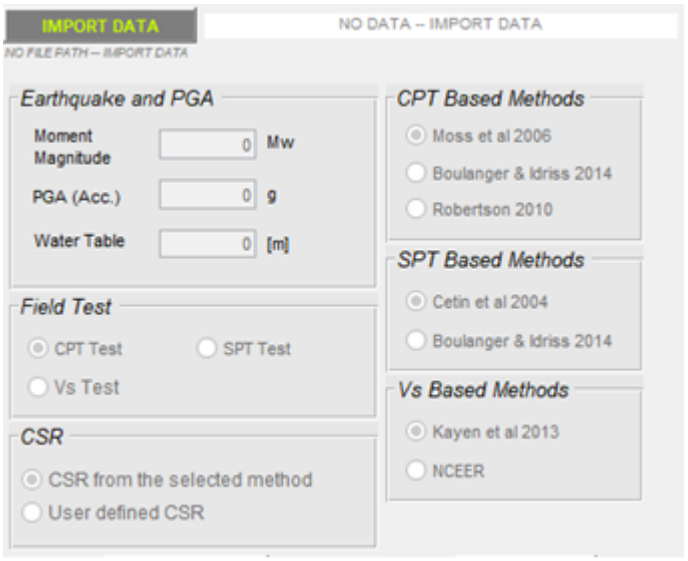

Figure 5-3 Import data interface

The users are able to import the field tests data from a file .txt or CVS by clicking in the button IMPORT DATA, Figure 5-3. The files that contain the tests data must follow the next indications and must be saved in the BASE FOLDER.

➢ CPT field data

In the case for the information obtained from CPT tests, the file that holds the information must contains in 4 columns separated by space and starting with the "depth" in meters, then "cone tip resistance qcin" MPa, then "cone sleeve resistance fs" in MPa and finally the "pore pressure u" in MPa as shows the Figure 5-4.

z (m)	qc (MPa)	fs (MPa)	u (MPa)
3	0 0	0	
3.02	1.502811	0.013038952	0.036991489
3.04	1.413078	0.012179143	0.035953191
3.06	1.325033	0.012896095	0.036991489
3.08	1.379744	0.013036286	0.048940426
3.1	1.624189	0.012893429	0.054655319
3.12	1.801967	0.012893429	0.046344681
3.14	1.846411	0.014036286	0.041148936

Figure 5-4 CPT field data

➢ SPT field data

Concerning the data filed that come from an SPT test, the imported file must contain the "depth" in meters as a first column, then the "raw Nspt" and the third value is the "FC fines content in percentage" i.e. 25% should be written as 25. The Figure 5-5 illustrates how must organize the information for SPT, where the columns are separated by space.

z(m)	(Nm)	FC(%)
2.3	4	69
3	6	33
3	5	20
3.4	3	33
3.4	5	17
3.4	10	25

Figure 5-5 SPT field test

➢ Vs field data

When the user has tests of shear wave velocity as inputs for liquefaction analysis, in order to import then, those values, in a .txt file, must be separated by space stating with the "depth in meters" then the "Vs shear wave velocity given in m/s" the third column is the "FC fines content in percentage" and the four column is the "unit weight of the soil in kN/m³" as is showing in the following Figure 5-6.

H(m)	Vs_(m/s)		FC(%)	gamma(kN/m3)
2.05	41	13	19	
2.1	41	18	19	
2.15	42	28	19	
2.2	42	2	19	
2.25	42	4	19	
2.3	43	14	19	

Figure 5-6 Vs field test

5.3.3 Input data

In this section, the field data have been already imported and users simply by writing in the text boxes can insert the values of Moment magnitude of the earthquake, the peak ground acceleration in a fraction of the gravity and water table level, as is illustrated in Figure 5-7.

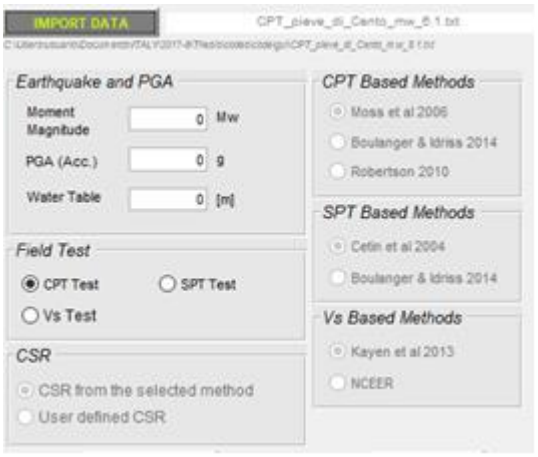

Figure 5-7 Input data

5.3.4 Pick Field Test

Users are able to pick the kind of test in the panel “Field Test”, Figure 5-8, according to the information that comes from field, either CPT test or SPT test or Vs test.

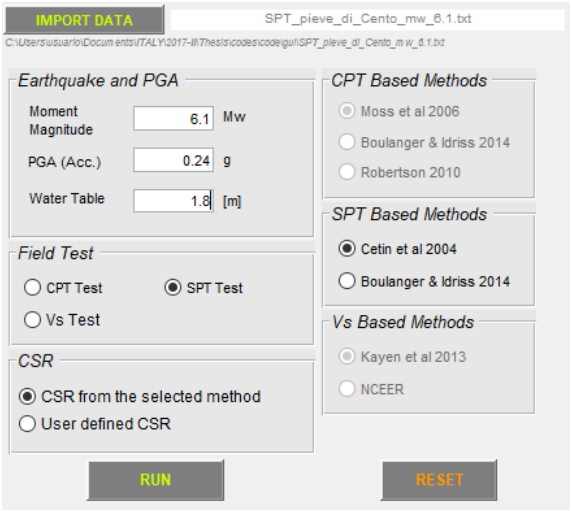

Figure 5-8 Pick data field test

5.3.5 Select how to compute CSR

The code allows the users to choose how to compute the CSR. The first option is based on the selected method, CPT, SPT or Vs and the second option permits the users to import their own values of CSR estimated from local site response analysis, Figure 5-9.

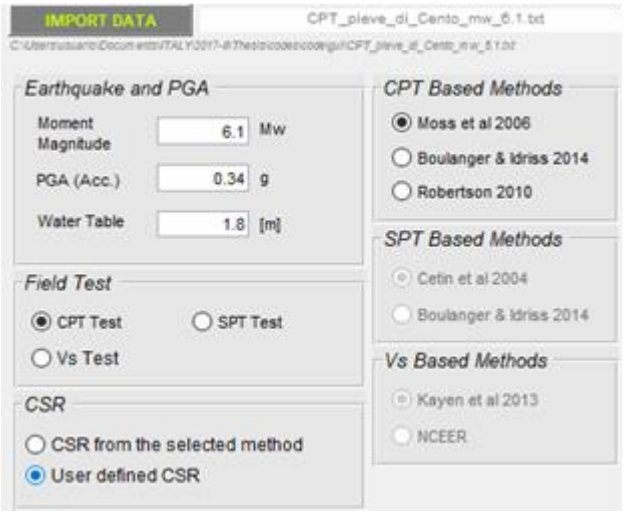

Figure 5-9 Selecting how computing CSR

Whether the users want to use their own CSR, that information must be in the BASE FOLDER and should be listed in a space separated .txt or CVS file, as shows the following Figure 5-10, where the first column is the “depth in meters” and the second the values of “CSR provided by the user”.

z (m)	CSR_user
3	0
3.02	0.117129759
3.04	0.117324239
3.06	0.117515719
3.08	0.117704229
3.1	0.117889803
3.12	0.118072472

Figure 5-10 Imported file

5.3.6 Choose methods (CPT, SPT and Vs)

After choosing the field test method and the technique for computing CSR the users can simply pick on the panel “CPT Based Methods” or “SPT Based Methods” or “Vs Based Methods” the preferred author for developing the liquefaction analysis, Figure 5-11.

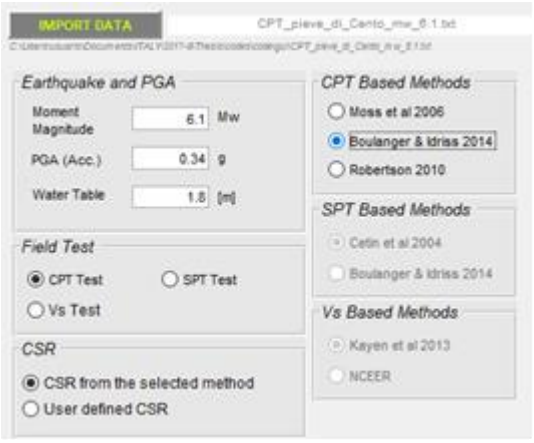

Figure 5-11 Choosing methods for assessing

5.3.7 RUN

After having been selected the kind of based method and having chosen the CSR to compute procedure, the users can perform the analysis just clicking on button RUN. Then the MATLAB GUI will display the Input Data Table and the Liquefaction Assessment Results Table, Figure 5-12.

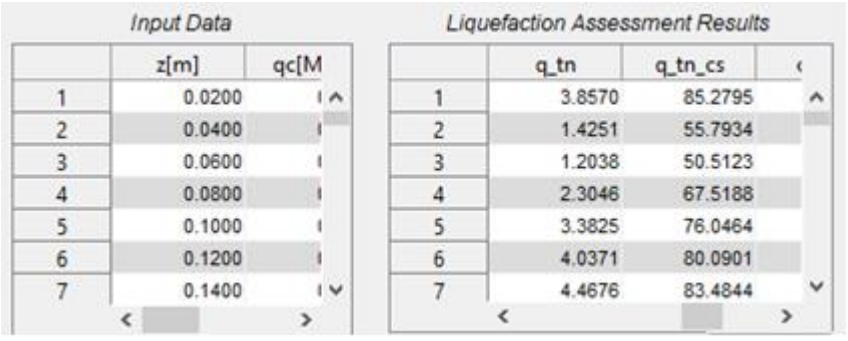

	z[m]	qc[M
1	0.0200	
2	0.0400	
3	0.0600	
4	0.0800	
5	0.1000	
6	0.1200	
7	0.1400	

	q_tn	q_tn_cs
1	3.8570	85.2795
2	1.4251	55.7934
3	1.2038	50.5123
4	2.3046	67.5188
5	3.3825	76.0464
6	4.0371	80.0901
7	4.4676	83.4844

Figure 5-12 Input Data Table and the Liquefaction Assessment Results Table

Moreover, the user by a pop-up menu can select the input data and main results and plot them as is visible in Figure 5-13.

Input Data Plots: Liquefaction Assessment Plots:

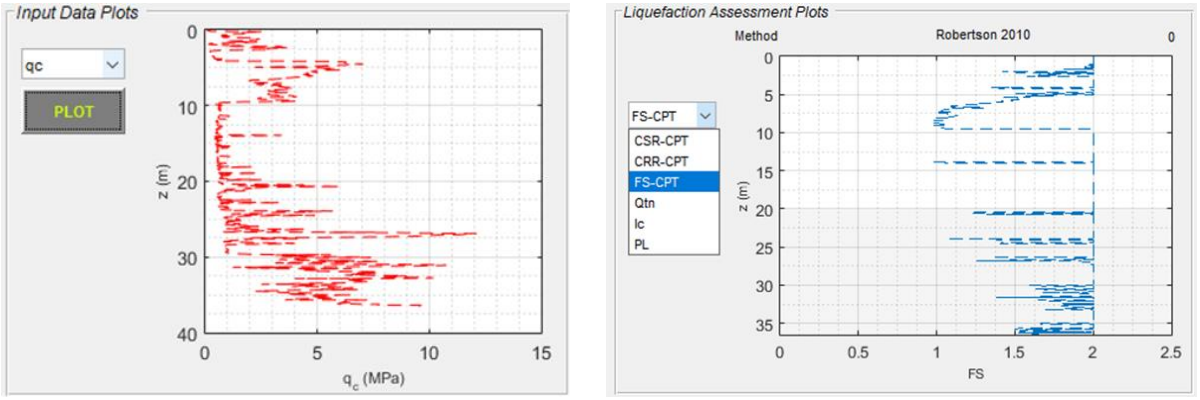

Figure 5-13 Inputs and results plots

5.3.8 Reset

Users are able to permanently renew the analysis from the beginning, by clicking on the option RESET, Figure 5-14. Choosing that option all tables and plots will be empty the inputs must be inserted again and the field data as well.

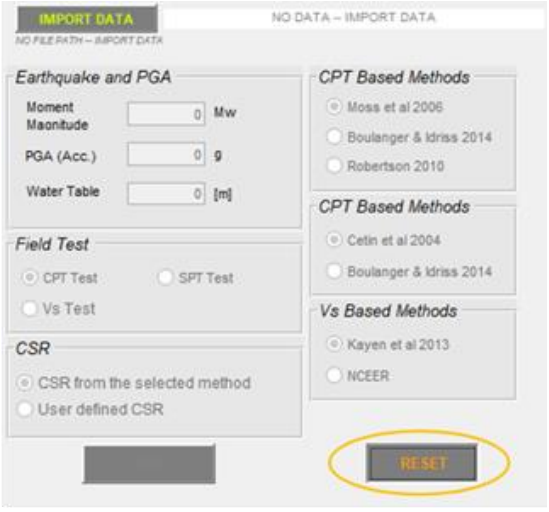

Figure 5-14 Reset interface

5.3.9 Exporting Data txt file

Exporting to a .txt file is done during the execution of the code, and the file of results can be found in the BASE FOLDER.

5.4 Exit System

Users should ensure that all their liquefaction are completed, and their results may be saved automatically in order to close the MATLAB GUI.

CHAPTER 6
CONCLUSIONS

As for the state of the art of liquefaction assessment concerns, it requires rigorous efforts not only by academic researchers and geotechnical engineers but also by facility owners and stakeholders involved in the risk assessment due to liquefaction effects, which is a crucial aspect in topics such urban planning and developing of infrastructure in general.

Addressing the aforementioned need, many methods have been developed to evaluate the soil liquefaction triggering and its consequences through in-situ, laboratory, and numerical methods. Therefore, it is crucial to know strengths and pitfalls of the used methods to construct proper engineering judgement on the selected in-situ test and selected liquefaction-trigger evaluation method.

This thesis contributes by the implementing the frequently used seven CPT, SPT, and Vs-based methods into MATLAB platform, which could be efficiently used in the future. Secondly, an example benchmarking is presented to compare the performance of the implemented methodologies. As the benchmark case illustration, observed liquefaction of Pieve di Cento site during 2012 Emilia event is presented. The results of the simplified methodologies are compared with numerical simulation results that are presented in Chiaradonna et al. (2018) as the ongoing work within the confines of LIQUEFACT project.

It is shown for the specific case study that simplified methods differ in defining the CSR and CRR even if one uses the rd relation computed through local site response analyses. The deviation in CSR is found to be stemming from Magnitude Scaling Factors (MSF), whereas the deviations in CRR are found to be method specific. Yet, the output Factor of Safety (FS) profiles show significant similarities, this underlines the significance of using the same MSF and CRR evaluations defined exclusively as in the selected in-situ method under consideration.

When one compares the tendency for the prediction of the layers expected to liquefy with the advanced numerical simulations, it is verified that the methodologies stay on the conservative side. More specifically, in CPT-based evaluations, the level of conservatism increases as Robertson

(2010), Idriss and Boulanger (2014), and Moss et al. (2006); in SPT-based evaluations Idriss and Boulanger (2014) is found to be more conservative than Cetin et al. (2004); in Vs-based methods, NCEER workshop (Youd et al., 2001) that is based on Andrus and Stokoe (2000) provides more conservative results than Kayen et al. (2013). For the case study under considerations, the best approximations emerge from the methods: Robertson-CPT, Cetin et al.-SPT, and Kayen et al.-Vs.

APPENDICE A

A.1 Case Study of Cavezzo (MO)

A.1.1 Overview

The second case study for the comparison between simplified triggering approaches and advanced numerical analysis is provided using the CPT profile and other geotechnical information for the Italian City of Cavezzo.

Cavezzo is used as one of the target sites for the European international research project LIQUEFACT-WP2: European Liquefaction Hazard Map and Methodology for Localized Assessment of Liquefaction Potential. Recently, a detailed microzonation study is completed based on significant amount of geotechnical, geophysical, and geological information collected and developed (Lai et al., 2018).

For brevity purposes, in this Appendix, the results of a single CPT profile and related laboratory tests of this extensive dataset is considered. In Figure 6-1, cone tip resistance, cone sleeve resistance and pore pressure and Figure 6-2 SBT-Ic site classification of the CPT profile is provided.

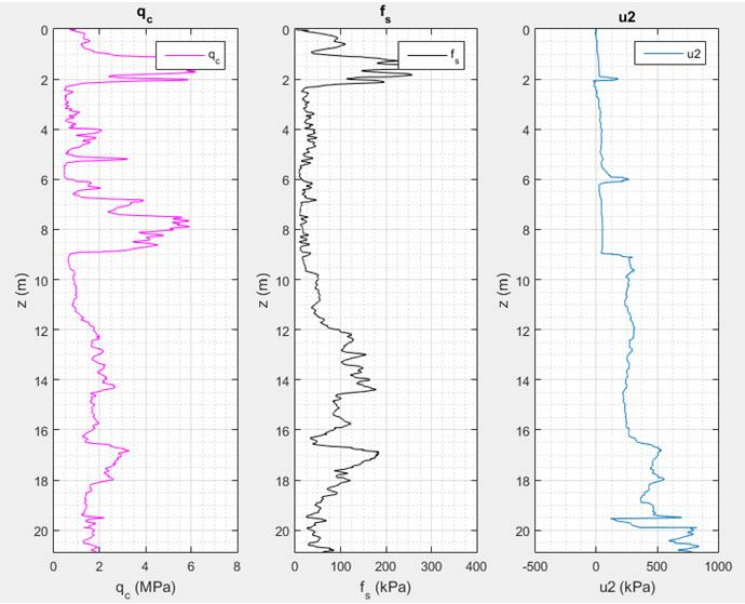

Figure 6-1 Con tip resistance, cone sleeve resistance and pore pressure

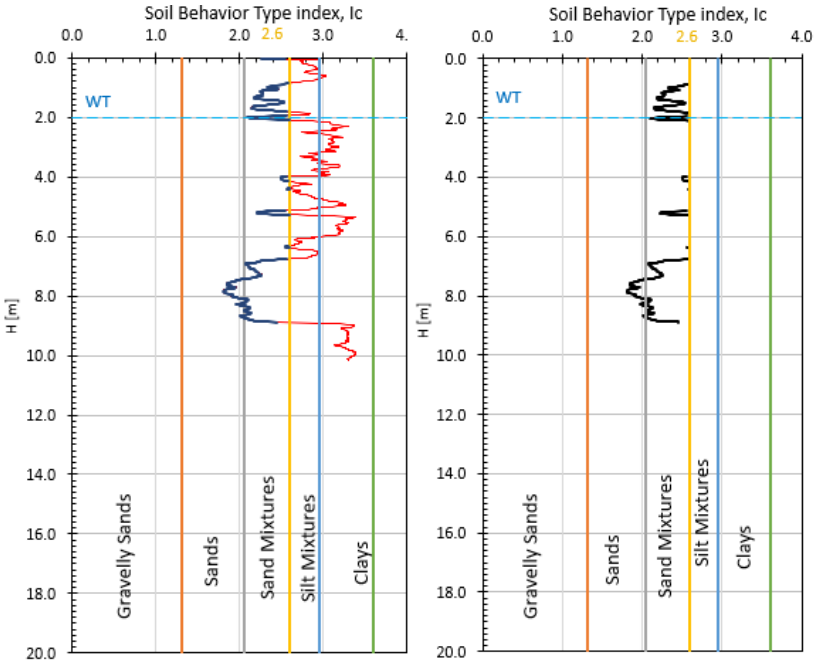

Figure 6-2 SBT-Ic site classification of the CPT profile

Geotechnical model of the relevant profile is obtained from macroscale model that University of Pavia and EUCENTRE research group developed and it is only refined based on the local setting and available geotechnical information. Finalized geotechnical model is presented in Table 6-1

Finalized geotechnical model, the water table is at 2 meters depth from surface and shear wave velocity of the viscoelastic-halfspace below Layer 12 is 800 m/s. For modulus degradation and damping curves, the unified framework proposed by Darendeli (2001) is adopted.

Table 6-1 Finalized geotechnical model

	depth (m)			Plasticity index (%)	Effective stress				Rel. Dens	Friction angle	
	from	to	middle	PI	σ'v0 (kPa)	σ'h0 (kPa)	σ'0 (kPa)	σ'0 (atm)	D_r (%)	ϕ'	Vs (m/s)
1	0	2	1	10	16.00	8.00	10.67	0.11	-	31	115
2	2	4.5	3.25	10	44.50	22.25	29.67	0.30	-		115
3	4.5	5	4.75	10	59.50	29.75	39.67	0.40	-	-	115
4	5	5.5	5.25	30	64.50	32.25	43.00	0.43	-	-	115
5	5.5	7	6.25	10	74.50	37.25	49.67	0.50	-	-	205
6	7	9	8	0	92.00	46.00	61.33	0.61	28 to 48	33 to 37	205
7	9	15	12	55	132.00	66.00	88.00	0.88	-	-	205
8	15	16	15.5	30	167.00	83.50	111.33	1.11	-	-	205
9	16	36	26	30	272.00	136.00	181.33	1.81	-	-	215
10	36	56	46	30	472.00	236.00	314.67	3.15	-	-	340
11	56	90	73	30	742.00	371.00	494.67	4.95	-	-	355
12	90	200	145	30	1462.00	731.00	974.67	9.75	-	-	455

It should be noted that relative density and friction angle estimates for the sandy zone between 7 to 9 meters are estimated from CPT-relations of Zhang et al. (2002) and Kulhawy and Mayne (1990), respectively. More detailed definitions of relative density and friction angle for the saturated sand zone is provided in Figure 6-3.

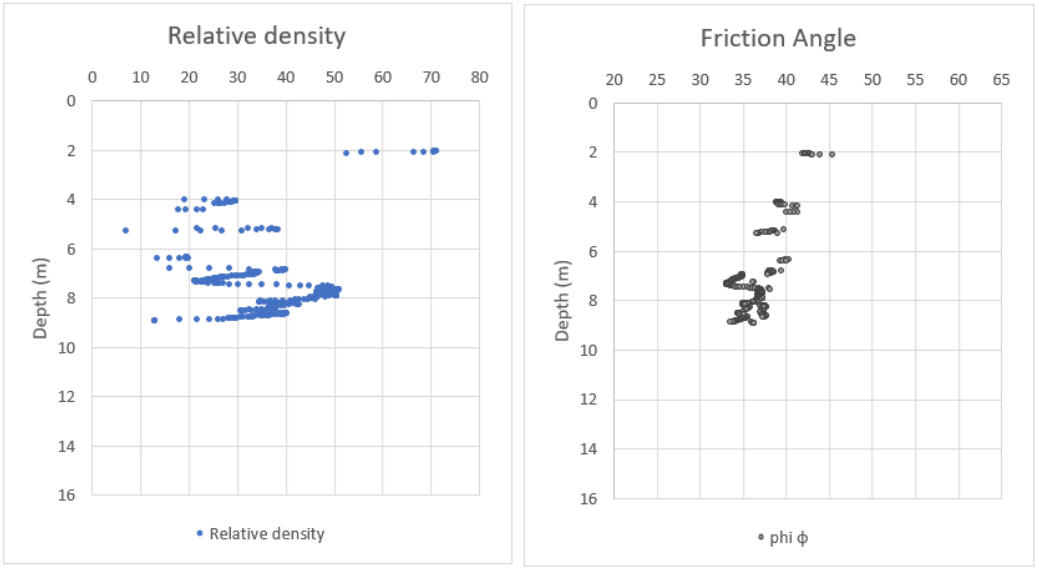

Figure 6-3 Profiles of relative density and friction angle

Compatible with one branch of the LIQUEFACT project, 7 scaled rock outcrop ground motions are used according to uniform hazard spectrum corresponding to 10% exceedence in 50 years. Target magnitude is $Mw = 6.0$.

Using the finalized geotechnical model, three groups of analyses are carried out in the comparisons:

Computations of factor of safety and probability of liquefaction profiles by using the methods of Robertson (2010), Boulanger and Idriss (2015), Moss et al. (2006) by completely respecting the CRR and CSR definitions;

Repeating the former step by replacing the CSR profile obtained as the median value from 7 local site response analyses carried out by using STRATA Kottke and Rathje, (2010) using the ground motions. Details are provided in A.1.2;

Carrying out loosely-coupled effective stress analyses by using FLAC2D (Itasca, 2016) and Bryne (1991) model. It is noted that at this step, help from UNIPV-EUCENTRE research group has been provided and only three analyses are carried out using the motions presented in Figure 6-6 and further details are provided in A.1.3;

A.1.2 Equivalent Linear Site Response Analyses

In the determination of surface acceleration and local CSR profile, the approach of equivalent linear analysis is adopted. In this approach, as first proposed by Seed and Idriss (1969), all soil layers of the soil profile are modelled with a linear viscoelastic constitutive model with a representative pair of shear modulus (G) and damping ratio (DR) that "equivalently" represent the level of nonlinearity present in the layers. Given the fact that all the layers are still linear, this approach can still adopt the analytical closed-form functions of transfer functions.

For small strains, the use of maximum shear modulus ($Gmax$) and minimum damping ratio ($Dmin$) may be adequate, however, starting from moderate strains, there is a need of an iterative procedure to define the pair of strain compatible G and DR. The iteration is as explained:

1. First run is completed with initial properties for each layer ($G_{max,i}$ and $D_{min,i}$),
2. Maximum strains are obtained at each layer ($\gamma_{max,i}$) and they are reduced to effective values ($\gamma_{eff,i}=n \times \gamma_{max,i}$) where $n=0.65$ or $n=(M-1)/10$ could be adopted,
3. New values of G and DR are obtained from material curves for each layer,
4. New run is executed, and strains are computed,

5. New values of G and DR are obtained.

Steps 3 to 5 are repeated until previous (3) and current (5) values of G and DR are sufficiently close to each other (error < 2-5%).

Moreover, as input information we have the curves of the materials that are summarized in the Figure 6-4 and Figure 6-5.

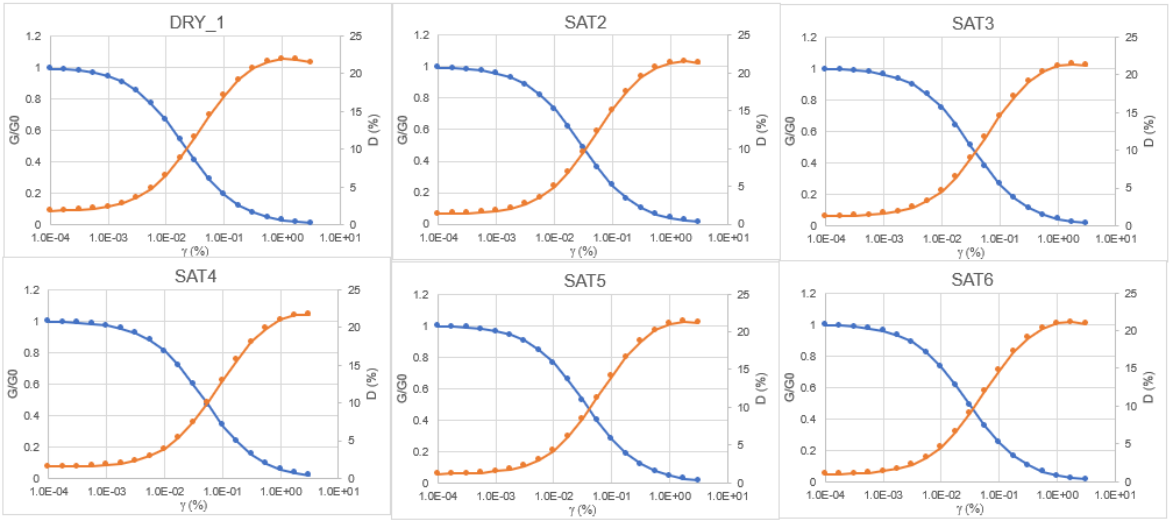

Figure 6-4 Soil Types 1 Cavezzo, modulus degradation and damping curves

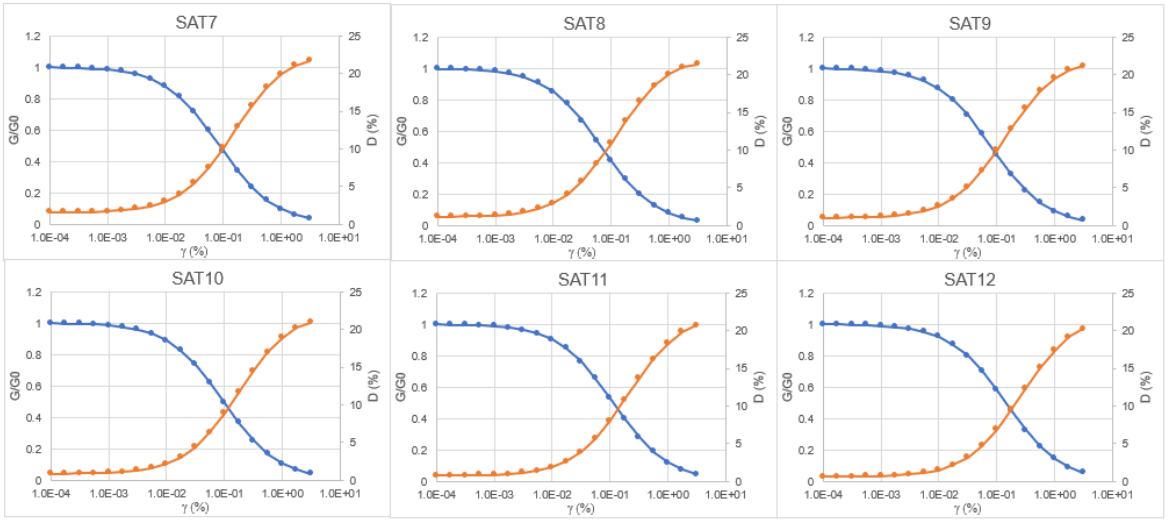

Figure 6-5 Soil Types 2 Cavezzo, modulus degradation and damping curves

A.1.3 loosely-Coupled Effective Stress Analysis

Either loosely-coupled or fully-coupled, nonlinear analyses define the generation of excess pore water pressure during the propagation of seismic waves. In loosely coupled models, the volumetric deformation of the soil skeleton is defined as an external relation. If the matrix is partially or fully undrained, then soil skeleton cannot get compressed and excess pore water pressures develop.

In case of Bryne (1991), the relation between shear strain and volumetric strain is as follows:

$$\frac{\Delta\epsilon_{vd}}{\gamma} = C_1 exp\left(-C_2 \frac{\epsilon_{vd}}{\gamma}\right)$$

Where, $\Delta\epsilon_{vd}$: irreversible volumetric strain increment, γ: current shear strain, ϵ_{vd}: irreversible cumulative volumetric strain. $C1=7600(Dr)^{-2.5}$ and $C_2=0.4/C_1$

In addition to the relation of shear strain-volumetric strain, any nonlinear model must consider the soil plasticity and energy dissipation in a reliable manner. In this case, Bryne (1991) model is mounted on Mohr-Coulomb model and hysteretic damping relation (calibrated according to Darendeli curves used in A.1.2) for small to moderate strains. It should be also noted that small amount of Rayleigh damping (0.25% at 1Hz) is also provided to damp out the high frequencies and to represent the small strain damping ratio at very low strains at which the hysteretic mechanism is not reliably activated.

For the zones, other than liquefiable layer, a total stress model is adopted by assigning S_u values that are compatible with the backbone curves.

Excess pore water pressure ratios computed through numerical model is presented in Table 6-2.

Table 6-2 Excess pore water pressures computed through numerical means

		u_f(kPa)						
depth (m)	u_0 (kPa)	EQ1	EQ2	EQ3	max	Δu (kPa)	σ'_{v0} (kPa)	r_u (-)
5.5								0.00
6.5	44	62	54	67	67	23	76	0.30
7.25	52	112	94	116	116	64	83	0.78
7.75	56	138	129	124	138	82	88	0.93
8.25	61	118	131	105	131	70	93	0.75
8.75	66	87	104	89	104	38	98	0.39
9.25	71	75	81	78	81	10	103	0.10
9.75								0.00

A.1.4 Comparison between the results of loosely-coupled effective stress analysis and simplified assessment of liquefaction triggering

In Figure 6-6, the comparison of the maxima of excess pore water pressure ratio, as the ratio of excess pore water pressure to the initial vertical effective stress ($\Delta u/\sigma'_{v0}$), obtained from three dynamic simulations compared with the factor of safety profiles obtained from simplified CPT-based procedures.

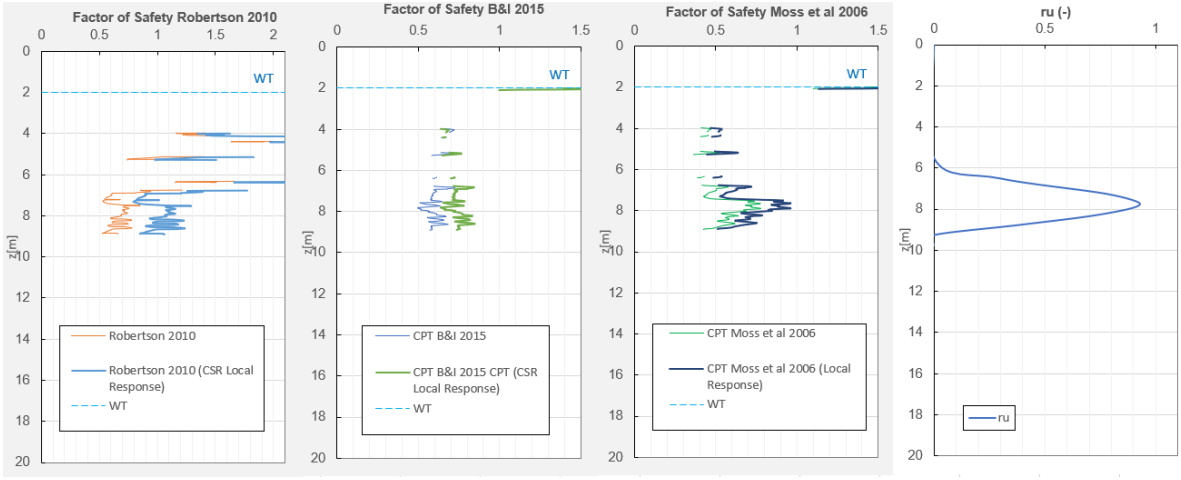

Figure 6-6 Comparison of the maxima of excess pore water pressure ratio with the factor of safety profiles obtained from simplified CPT-based procedures

It could be observed that almost for all of the cases CSR obtained from local site response analyses provide a closer agreement with the results of numerical model, whereas the best match for this particular case is obtained with the method of Robertson (2010).

Bibliography

Andrus, R. D., and Stokoe, K. H., II. (1997). "Liquefaction resistance based on shear wave velocity." Proc., NCEER Workshop on Evaluation of Liquefaction Resistance of Soils, Nat. Ctr. for Earthquake Engrg. Res., State Univ. of New York at Buffalo, 89–128.

Andrus, R. D., and Stokoe, K. H., II. (2000). "Liquefaction resistance of soils from shear-wave velocity." J. Geotech. and Geoenvir. Engrg., ASCE, 126(11), 1015–1025

ASTM D1586, (1999), Standard Test Method for Penetration Test and Split-Barrel Sampling of Soils

Been, K. and Jefferies, M. G. (1985). "A state parameter for sands", Géotechnique, 35: pp.99-112.

Been, K., Crooks, J. H. A., Becker, D. E. and Jefferies, M. G. (1986). "The cone penetration test in sands: Part I, state parameter interpretation". Géotechnique, 36: pp.239-249.

Been, K., Jefferies M. G., Crooks J. H. A., and Rothenberg, L. (1987a). "The cone penetration test in sands: Part II, general inference of state". Géotechnique, 37: pp.285-299.

Boulanger, R. W. and Idriss, I. M. (2014). "CPT and SPT based liquefaction triggering procedures." Rep. No. UCD/CGM-14/01, Univ. of California, Davis, CA.

Boulanger, R. W. and Idriss, I. M. (2015). "CPT-based liquefaction triggering procedure." J. Geotech. Geoenviron. Eng., 10.1061/(ASCE)GT .1943-5606.0001388, 04015065.

Boulanger, R.W. (2010). A Sand Plasticity Model for Earthquake Engineering Applications. Report No. UCD/CGM-10-01. Center for Geotechnical Modeling, Department of Civil and Environmental Engineering, University of California, Davis. 77 pp.

Bozorgnia, Y. and Bertero, V. V. (2004). "Earthquake Engineering: From Engineering Seismology to Performance-Based Engineering," Ch. 4: Geotechnical Aspects of Seismic Hazards, by S. L. Kramer and J. Stewart, CRC Press, 976 pages

Bryne P.M. (1991). A cyclic shear-volume coupling and pore-pressure model for sand, in Proceedings: Second International Conference on Recent Advances in Geotechnical Earthquake Engineering and Soil Dynamics (St. Louis, Missouri). Paper no. 1.24,47-55.

Cetin, K. O. (2000). "Reliability-based assessment of seismic soil liquefaction initiation hazard." Ph.D. dissertation, Univ. of California, Berkeley, California.

Cetin, K. O., Seed, R. B., Der Kiureghian, A., Tokimatsu, K., Harder, L. F., Jr., Kayen, R. E., and Moss, R. E. S. (2004)). "Standard penetration test-based probabilistic and deterministic assessment of seismic soil liquefaction potential." J. Geotech. Geoenviron. Eng., 130(12), 1314–1340.

Chiaradonna, A., Ozcebe, A.G., Bozzoni, F., Famà, A., Zuccolo, E., Lai, C.G., Flora, A., Cosentini, R.M., d'Onofrio, A., Bilotta, E. and Silvestri, F., (2018), June. Numerical simulation of soil liquefaction during the 20 May 2012 M6. 1 Emilia Earthquake in Northern Italy: the case study of Pieve di Cento. In Proceedings, 16th European Conference on Earthquake Engineering, 16ECEE, Thessaloniki, Greece (pp. 18-21).

Cubrinovski and Ishihara, (2002) Maximum and minimum void ratio characteristics of sands Soils Found., Jpn. Geotech. Soc., 42 (6) (2002), pp. 65-78.

Dafalias, Y.F., and M.T. Manzari. (2004). Simple plasticity sand model accounting for fabric change effects. Journal of Engineering Mechanics 130(6):622–634.

Darendeli, M. B. (2001). Development of a New Family of Normalized Modulus Reduction and Material Damping Curves, Department of Civil, Architectural and Environmental Engineering, The University of Texas, Austin, Texas.

Golesorkhi, R. (1989). Factors influencing the computational determination of earthquake-induced shear stresses in sandy soils. Ph.D. thesis, University of California, Berkeley, 395 pp. 1989.

Idriss, I. M. (1999). "An update to the Seed–Idriss simplified procedure for evaluating liquefaction potential." Presentation Notes, Proc. Workshop, New Approaches to Liquefaction Analysis, Transportation Research Board, Washington, D.C.

Idriss, I. M. and Boulanger, R. W. (2004). “Semi-empirical procedures for evaluating liquefaction potential during earthquakes.” Proc., 11th Int. Conf. Soil Dynamics and Earthquake Engineering and 3rd Int. Conf. Earthquake Geotechnical Engineering, Berkeley, Calif., 32–56.

Idriss, I.M. and Boulanger, R.W. (2008). Soil Liquefaction during Earthquakes, EERI Publication (2008), 235 pp.

Ishihara, K. (1985). Stability of Natural Deposits During Earthquakes Proceedings of the 11th International Conference on Soil Mechanics and Foundation Engineering, San Francisco, 1:321-376

ITASCA (2016) FLAC, Itasca Consulting Group

Jefferies, M.G. & Been, K. (2015). Soil Liquefaction: A Critical State Approach, Second Edition, CRC Press, 2015

Kayen, R. E., Mitchell, J. K., Seed, R. B., Lodge, A., Nishio, S., and Coutinho, R. (1992). “Evaluation of SPT-, CPT-, and shear wave-based methods for liquefaction potential assessment using Loma Prieta Data.” Proc., 4th U.S.-Japan Workshop on Earthquake Resistant Design of Lifeline Facilities and Countermeasures Against Soil Liquefaction, Honolulu, HI NCEER

Kayen, R., et al. (2013). “Shear-wave velocity–based probabilistic and deterministic assessment of seismic soil liquefaction potential.” J. Geotech. Geoenviron. Eng., 10.1061/(ASCE)GT.1943-5606.0000743, 407–419

Kramer, S. L. (1996). Geotechnical earthquake engineering. Prentice Hall, Upper Saddle River, N.J

Kulhawy, F.H., and Mayne, P.H., (1990). Manual on estimating soil properties for foundation design, Report EL-6800 Electric Power Research Institute, EPRI, August 1990.

Lai, C.G., Bozzoni, F., Poggi, V., Zuccolo, E., Meisina, C., Famà, A., Conca, D., Bonì, R., Cosentini, R., Martelli, L. and Özcebe, A.G. (2018) Microzonazione Sismica per il Rischio Liquefazione.

Liao, S. S. C. and Whitman, R. V. (1986). “Overburden correction factors for SPT in sand.” J. Geotech. Eng., 112(3), 373–377.

Liu A.H., Stewart J.P., Abrahamson N.A. and Moriwaki, Y. (2001). Equivalent number of uniform stress cycles for soil liquefaction analysis, J. Geotech. & Geoenv. Engrg., ASCE, 127 (12), 1017-1026.

Marcuson WF (1978) Definition of terms related to liquefaction. J Geotech Eng Div ASCE 104(9):1197–1200.

Martin, et. al (1975). “Fundamentals of Liquefaction Under Cyclic Loading,”J. Geotech., Div. ASCE, 101(GT5), pp., 423- 438.

MATLAB and Statistics Toolbox Release (2015a), The MathWorks, Inc., Natick, Massachusetts, United States.

Mogami, T., and Kubo, K. (1953). “The behavior of soil during vibration. “, Proceedings, 3rd International Conference on Soil Mechanics and Foundation Engineering, Zurich, Vol. 1, pp. 152-155.

Moss, R. E. S., Seed, R. B., and Olsen, R. S. (2006). “Normalizing the CPT for overburden stress.” J. Geotech. Geoenviron. Eng., 132(3), 378–387.

National Academies of Sciences, Engineering, and Medicine, (2016). State of the Art and Practice in the Assessment of Earthquake-Induced Soil Liquefaction and Its Consequences. Washington, DC: The National Academies Press. doi: 1017226/23474.

NCEER/NSF, Youd et al. (2001). “Liquefaction resistance of soils: Summary report from the 1996 NCEER and 1998 NCEER/NSF workshops on evaluation of liquefaction resistance of soils.” J. Geotech. Geoenviron. Eng., 127 (10), 817–833.

Plewes et al. (1992) “CPT based screening procedure for evaluating liquefaction susceptibility”. Proceedings of the 45th Canadian Geotechnical Conference, Toronto.

Robert W. Day (2002) Geotechnical Earthquake Engineering Handbook. Earthquake Structural Damage, Chapter (McGraw-Hill Professional, 2002).

Robertson, P. K. and Wride, C. E. (1998). “Evaluating cyclic liquefaction potential using the cone penetration test.” Can. Geotech. J., 35(3), 442–459.

Robertson, P. K. (1990). “Soil classification using the cone penetration test.” Can. Geotech. J., 27(1), 151–158.

Robertson, P. K. (2009a). “Discussion of ‘CPT-based probabilistic soil characterization and classification’ by K. Onder Cetin and Cem Ozan.” J. Geotech. Geoenviron. Eng., 135 1 , 84–107.

Robertson, P. K. (2009b) . “Interpretation of cone penetration tests—A unified approach.” Can. Geotech. J., 46, 1337–1355

Robertson, P.K. and Wride, C.E. (1997). Cyclic liquefaction and its evaluation based on SPT, CPT@, Final contribution to the proceedings of the 1996 NCEER workshop on evaluation of liquefaction resistance.

Seed, H. B., and Idriss, I. M. (1969). "Influence of soil conditions on ground motions during earthquakes." ASCE J Soil Mech Found Div, 95, 99-137.

Seed HB. and Idriss IM (1971). "A simplified procedure for evaluating soil liquefaction potential." Journal of Soil Mechanics and Foundation Engineering, ASCE, 97, 9, 1249-1274, 1971.

Seed, H. B., Makdisi, F., Idriss, I. M., and Lee, K. L. (1975). The slides in the San Fernando Dams during the earthquake of February, 9, 1971. J. Geotech. Eng. Div. 101:7, 651-688.

Seed, H. B., and Idriss, I. M. (1982). Ground motion and soil liquefaction during earthquakes, Monograph, Earthquake Engineering Research Institute, Oakland, Calif.

Seed, H. B., Idriss, I. M., and Arango, I. (1983). “Evaluation of liquefaction potential using field performance data.” J. Geotech. Eng., 109(3), 458–482

Seed, H. B., Tokimatsu, K., Harder, L. F., and Chung, R. M. (1984). The influence of SPT procedures in soil liquefaction resistance evaluations. Earthquake Engineering Research Center Rep. No. UCB/EERC-84/15, Univ. of California, Berkeley, Calif.

Seed, H. B., Tokimatsu, K., Harder, L. F. and Chung, R. F. (1985), "Influence of SPT Procedures in Soil Liquefaction Resistance Evaluations," Journal of Geotechnical Engineering, Vol. 111, No. 12, December 1985.

Skempton, A. W. (1986), "Standard Penetration Test Procedures and the Effects in Sands of Overburden Pressure, Relative Density, Particle Size, Ageing and Over Consolidation", Geotechnique 36: 3, September, 1986

Suzuki, Y., Sanematsu, T., and Tokimatsu, K. (1998). "Correlation between SPT and seismic CPT." Proc., Conf. on Geotechnical Site Characterization, Balkema, Rotterdam, Netherlands, 1375–1380

Stokoe, K. H., II, Lee, S. H. H., and Knox, D. P. (1985). "Shear moduli measurements under true triaxial stresses." Advances in the art of testing under cyclic conditions, ASCE, New York, 166–185

STRATA (Software, version 0.5.9), NU Public License (GPL) version 3, Developed by Albert Kottke and Ellen Rathje.

Terzaghi, K. & Peck, R.B. (1948). Soil Mechanics in Engineering Practice. Wiley, New York, 566 p.

Tonni L., et al. (2015). Interpreting the deformation phenomena triggered by the 2012 Emilia seismic sequence on the Canale Diversivo di Burana banks. Italian Geotechnical Journal, 2: 28 - 58 (in Italian).

Youd, T. L. (1984) "Geologic Effects - Liquefaction and Associated Ground Failure," Proceedings of the Geologic and Hydrologic Hazards Training Program, Open-File Report 84-760, U.S. Geological Survey, Menlo Park, California, 1984.

Zhang, G., Robertson, P.K., and Brachman, R.W.I. (2002). Estimating liquefaction-induced ground settlements from CPT for level ground. Canadian Geotechnical J. 39, 1168-1180.

Zhang, G., Robertson, P.K. and Brachman, R.W.I. (2004). Estimating Liquefaction induced Lateral Deformations from SPT and CPT, ASCE, Journal of Geotechnical and Geoenvironmental Engineering, Vol. 130, No. 8, pp 861-871.